

**UNIVERSITY OF GAZİANTEP
GRADUATE SCHOOL OF
NATURAL & APPLIED SCIENCES**

**INVESTIGATION OF OPTICAL,
STRUCTURAL, AND ELECTRICAL
PROPERTIES OF SEMICONDUCTING
FILMS PRODUCED BY DIFFERENT
CHEMICAL TECHNIQUES**

**Ph.D THESIS
IN
ENGINEERING OF PHYSICS**

**BY
SERAP SÜR ÇELİK
NOVEMBER 2011**

**Investigation of Optical, Structural, and Electrical
Properties of Semiconducting Films Produced by Different
Chemical Techniques**

**PhD Thesis
in
Engineering of Physics
University of Gaziantep**

**Supervisor
Prof. Dr. Zihni ÖZTÜRK**

**by
Serap SÜR ÇELİK
November 2011**

T.C.
UNIVERSITY OF GAZİANTEP
GRADUATE SCHOOL OF
NATURAL & APPLIED SCIENCES
ENGINEERING OF PHYSICS

Name of the thesis: Investigation of Optical, Structural, and Electrical Properties of
Semiconducting Films Produced by Different Chemical Techniques


Name of the student: Serap Sür Çelik

Exam date: 18.11.2011


Approval of the Graduate School of Natural and Applied Sciences


(Prof. Dr. Ramazan KOÇ)
Director

I certify that this thesis satisfies all the requirements as a thesis for the degree of Doctor of
Philosophy.


(Prof. Dr. A. Necmeddin YAZICI)
Head of Department

This is to certify that we have read this thesis and that in our consensus/majority opinion it is
fully adequate, in scope and quality, as a thesis for the degree of Doctor of Philosophy.



(Prof. Dr. Zihni ÖZTÜRK)
Supervisor

Examining Committee Members

Title and Name-surname

signature

Prof. Dr. Ramazan ESEN



Prof. Dr. Zihni ÖZTÜRK



Prof. Dr. A. Necmeddin YAZICI



Doç. Dr. Mustafa ÖZTAŞ



Doç. Dr. Metin BEDİR



Anneme.....

ABSTRACT

INVESTIGATING OF THE OPTICAL, STRUCTURAL, AND ELECTRICAL PROPERTIES OF SEMICONDUCTING FILMS PRODUCED BY DIFFERENT CHEMICAL TECHNIQUES

SÜR ÇELİK, Serap

Ph.D in Engineering of Physics

Supervisor: Prof. Dr. Zihni ÖZTÜRK

November 2011, 117 pages

In this study, the semiconducting CdS and ZnS thin films were obtained by the two methods: chemical bath deposition and spray pyrolysis under different deposition conditions. The influence of the preparation technique on the structural, electrical and optical properties of the polycrystalline CdS and ZnS films were investigated by using X-ray diffraction (XRD), Van der Pauw method and optical transmission. The optical properties of the films were investigated from optical absorption coefficient and transmittance spectra data using double beam visible spectrophotometer. By using these data the band gap energies of all films were determined. In addition, the crystal structures of all films were studied by x-ray diffraction peaks.

$Cd_xZn_{1-x}S$ films were obtained with incorporation of Cd element into ZnS at different concentrations ($0 \leq x \leq 1$) by spray pyrolysis technique using aqueous solutions of $CdCl_2$, $ZnCl_2$ and $(CS(NH)_2)_2$, which were atomized with compressed air as carrier gas. The $Cd_xZn_{1-x}S$ films were obtained on glass substrates at different substrate temperatures. The influence of x composition on structural, optical, thermoluminescence and electrical properties of sprayed and chemical bath deposited cadmium zinc sulfide (CdZnS) films were investigated. The structural properties were determined by XRD and a hexagonal wurtzite phase was present in all as-grown samples. The films have a direct band gap which varies from 3.50 eV for zinc sulphide to 2.40 for cadmium sulphide. It was seen that the crystallinity level of the films increased with increasing x composition and grain size.

Keywords: Spray Pyrolysis, Chemical Bath Deposition, Structural Properties, Optical Properties, Electrical Properties, CdS films, ZnS films, CdZnS films

ÖZET

DEĞİŞİK KİMYASAL TEKNİKLERLE ÜRETİLEN YARIİLETKEN FİMLERİN OPTİKSEL, YAPISAL VE ELEKTRİKSEL ÖZELLİKLERİNİN İNCELENMESİ

SÜR ÇELİK, Serap
Doktora Tezi, Fizik Müh. Bölümü
Tez Yöneticisi: Prof. Dr. Zihni ÖZTÜRK
Kasım 2011, 117 sayfa

Bu çalışmada, değişik depolama şartları altında kimyasal depolama ve spray pyrolysis methodu ile yarıiletken kadmiyum sülfür (CdS) ve çinko sülfür (ZnS) filmleri elde edilmiştir. Değişik hazırlama tekniklerinin polikristal CdS ve ZnS filmlerin yapısal, optiksel, ve elektriksel özelliklerine etkisi X-ışını kırınımı (XRD), optik geçirgenlik ve Van der Pauw metotları kullanılarak incelenmiştir. Çift ışınlı görünür spektrometreyle elde edilen optik absorbanans katsayısı ve geçirgenlik spektrumu datalarıyla filmlerin optiksel özellikleri incelendi. Bu datalarla tüm filmlerin yasak band enerjileri hesaplanmıştır. Bunlara ek olarak tüm filmlerin kristal yapı özellikleri x-ışınımı desenleri yardımıyla çalışılmıştır.

$Cd_xZn_{1-x}S$ ($0 < x < 1$) filmleri, $CdCl_2$, $ZnCl_2$ and $(CS(NH)_2)_2$, çözeltileri kullanılarak ZnS'e değişik konsantrasyonlarda Cd elementi katılarak ve taşıyıcı gaz olarak havanın kullanıldığı spray pyrolysis methoduyla elde edilmiştir. $Cd_xZn_{1-x}S$ filmleri değişik taban sıcaklıklarında cam altlıklara çöktürülmüştür. X bileşenin değişiminin spray pyrolysisle ve kimyasal depolama yöntemiyle elde edilen kadmiyum çinko sülfür (CdZnS) filmlerin yapısal, optiksel, elektriksel ve termolüminisans özelliklerine etkisi incelenmiştir. XRD kullanılarak yapısal özellikleri incelenerek büyütülen tüm filmlerin hexagonal yapıya sahip olduğu bulunmuştur. Filmler ZnS'ün 3.5 eV CdS'ün 2.4 eV olan enerji bant aralığında değişen direk bant aralığı değerlerine sahiptir. X bileşenin ve grain boyutunun artmasıyla filmlerin kristal yapılarında gelişme gözlenmiştir.

Anahtar Kelimeler: Spray Pyrolysis, Kimyasal Depolama, Yapısal Özellikler, Optiksel Özellikler, Elektriksel Özellikler, CdS Film, ZnS Film, CdZnS Film

ACKNOWLEDGEMENTS

First and foremost, my utmost gratitude to all my teachers from primary school to university. Special thanks should be given to Ayşe Kalyenciođlu who is my primary school teacher, I will never forget her.

I wish to express my deepest gratitude to my supervisor Prof. Dr. Zihni Öztürk for their valuable advice, caring, patience and guidance of this work.

Special thanks and gratitude to Doç. Dr. Mustafa Öztaş for his genuine support, valuable advice and sincere comments which helped me a lot to finish this study and providing me with an excellent atmosphere for doing research. I also want to express my thanks to Doç. Dr. Metin Bedir for his valuable comments and criticism during the preparation of this study.

I would like to thank Gültekin Şahinođlu, who as a good friend, was always willing to help, give his best suggestions and supporting documents.

I would like to thank my colleague, Derya Korkmaz, for helping and assisting me in all the experimental stages of this work. It would have been a lonely lab without her.

Words alone cannot express the thanks I owe to Gülten Sür, my mother, and my sisters, Sibel and Songül, for their patience, best wishes and all kinds of support during all of my studies.

Finally, I would like to thank my husband, Eyup Çelik. He was always there cheering me up and stood by me through the good times and bad. And thanks to my daughter, Bilge, for happily times with her.

CONTENTS

	page
ABSTRACT	i
ÖZETii
ACKNOWLEDGEMENTSiii
CONTENTSiv
LIST OF FIGURES	vii
LIST OF TABLES	xi
LIST OF SYMBOLS	xv
CHAPTER 1: INTRODUCTION AND LITERATURE SURVEY	1
1.1. Introduction	1
1.2. Historical perspective of CdS films	3
1.3. Historical perspective of ZnS films	11
1.4. Historical perspective of CdZnS films	17
CHAPTER 2: THEORY	20
2.1. Introduction20
2.2. Periodic Structures of Solids	21
2.3. Crystalline Properties of Solids	22
2.3.1 Cubic Lattice	23
2.3.2 The Diamond and Zinc-Blende Lattice	24
2.4. Semiconductor Materials26
2.5. Energy Band Structures27
2.5.1 Direct and Indirect Band gap29
2.6. Intrinsic and Extrinsic Semiconductor30
2.7. Defects in Solids	32
2.7.1 Grains and Grain Boundaries	33
2.8. Optical Properties of Semiconductors	34
2.9. Electrical Properties of Semiconductors36
2.10. Mechanical Properties of Semiconductors	38

2.11. Thermoluminescence Properties of Semiconductors.	39
CHAPTER 3: EXPERIMENTAL STUDIES.	40
3.1. Introduction.	40
3.2. Thin Film Production Methods.	40
3.2.1. Spray Pyrolysis Method.	41
3.2.2. Chemical Bath Deposition.	43
3.3. Substrate Preparation	43
3.3.1 Cleaning Process of The Glass Substrate.	44
3.4. Development of Thin films by Spray Pyrolysis.	45
3.4.1 Development of CdS Thin Films by Spray Pyrolysis.	45
3.4.2 Development of ZnS Thin Films by Spray Pyrolysis.	46
3.4.3 Development of Cd _x Zn _{1-x} S Thin Films by Spray Pyrolysis.	46
3.5. Development of Thin Films by Chemical Bath Deposition.	47
3.5.1 Development of CdS Thin Films by Chemical Bath Deposition.	47
3.5.2 Development of ZnS Thin Films by Chemical Bath Deposition.	48
3.5.3 Development of Cd _x Zn _{1-x} S Thin Films by Chemical Bath Deposition.	48
3.6. Measurements Techniques.	49
3.6.1 The Structural Properties Measurements	49
3.6.2 The Optical Properties Measurements.	51
3.6.3 The SEM Analysis.	52
3.6.4 The Electrical Properties Measurements.	53
3.6.4.1 The Resistivity and Conductivity Measurements.	54
3.6.4.2 Hall Mobility Measurements.	55
CHAPTER 4 : RESULTS AND DISCUSSIONS.	57
4.1. Introduction	57
4.2. Growth CdS Films.	57
4.2.1 Structural Studies of the CdS films.	58
4.2.2 Surface Morphology Studies of the CdS films.	60
4.2.3 Optical Studies of the CdS films.	61
4.2.4 Electrical Studies of the CdS films.	64
4.3. Growth ZnS Films	66
4.3.1 Analysis of the CBD ZnS Films.	67
4.3.1.1 Structural Studies of the CBD ZnS films.	67

4.3.1.2 Optical Properties of the CBD ZnS films.	68
4.3.1.2 Electrical Properties of the CBD ZnS films.	69
4.3.2 Analysis of the SP ZnS Films.	71
4.3.2.1 Structural Properties of the SP ZnS Films.	71
4.3.2.2 Optical Properties of the SP ZnS Films.	73
4.3.2.3 Electrical Properties of the SP ZnS Films.	73
4.4. Growth $Cd_xZn_{1-x}S$ Films.	75
4.4.1 Analysis of the CBD $Cd_xZn_{1-x}S$ Films.	75
4.4.1.1 Structural Properties of the CBD $Cd_xZn_{1-x}S$ Films.	76
4.4.1.2 Optical Properties of the CBD $Cd_xZn_{1-x}S$ Films.	78
4.4.1.3 Electrical Properties of the CBD $Cd_xZn_{1-x}S$ Films.	80
4.4.2 Analysis of the Sprayed $Cd_xZn_{1-x}S$ Films.	82
4.4.2.1 Structural Properties of the Sprayed $Cd_xZn_{1-x}S$ Films.	82
4.4.2.2 Optical Properties of the Sprayed $Cd_xZn_{1-x}S$ Films.	85
4.4.2.3 Electrical Properties of the Sprayed $Cd_xZn_{1-x}S$ Films.	86
4.4.2.4 Thermoluminescence Properties.	87
4.4.3 Analysis of Effect of Water Concentration on the Sprayed $Cd_{0.5}Zn_{0.5}S$ Films.	90
4.4.3.1 Structural Properties of the Sprayed $Cd_{0.5}Zn_{0.5}S$ Films. . . .	90
4.4.3.2 Electrical Properties of the Sprayed $Cd_{0.5}Zn_{0.5}S$ Films.	93
4.4.3.3 Optical Properties of the Sprayed $Cd_{0.5}Zn_{0.5}S$ Films.	95
CHAPTER 5 : CONCLUSIONS.	96
REFERENCES	101
CURRICULUM VITAE	

LIST OF FIGURES

	page
Figure 2.1. a) Amorphous b) Polycrystals c) Crystal.....	21
Figure 2.2 Three lattice types: a) simple cubic b) body-centered cubic c) face-centered cubic.....	24
Figure 2.3 The Diamond structure.....	25
Figure 2.4 The Zinc-blende structure.....	25
Figure 2.5. Possible energy band diagrams of a crystal: a) a half filled band, b) two overlapping bands, c) an almost full band separated by a small band gap from an almost empty band and d) a full band and an empty band separated by a large band gap.....	28
Figure 2.6 a) The scheme of the direct band gap, b) The scheme of indirect band gap.....	30
Figure 2.7 Grains and Grain Boundaries a) Microscopic b) Atomic.....	33
Figure 2.8 Semiconductors band gaps and wavelengths.....	35
Figure 2.9 Optical Absorption Experiment.....	36
Figure 2.10 Room-temperature conductivity of various materials.....	37
Figure 3.1 Schematic diagram of the spray pyrolysis system.....	42
Figure 3.2 Schematic diagram of the chemical bath deposition system.....	43
Figure 3.3 The cleaning process of the glass substrate.....	44
Figure 3.4 The Indium-ohmic contacts prepared on the thin film samples.....	54
Figure 3.5 The experimental set-up of the resistivity measurement.....	54
Figure 3.6 The Standard Configuration of Hall Effect Measurements.....	55
Figure 4.1 X-ray diffraction patterns of the CdS films deposited by a) spray pyrolysis, b) CBD.....	59
Figure 4.2 Scanning electron micrographs of the surface of CdS films prepared by a) spray pyrolysis, b) CBD.....	61

Figure 4.3 Plots and linear fits of $(\alpha hv)^2$ versus hv for the CdS films a) spray pyrolysis, b) CBD	63
Figure 4.4 X-ray diffraction spectra for ZnS films deposited by CBD at different bath temperatures.....	67
Figure 4.5 Plots and linear fits of $(\alpha hv)^2$ versus hv for the ZnS films deposited by chemical bath method.....	69
Figure 4.6 X-ray diffraction spectra for ZnS films deposited by SP at different substrate temperatures.....	72
Figure 4.7 Variation of substrate temperature in the polycrystalline films with grain size and lattice strain of ZnS films deposited by spray pyrolysis method.....	74
Figure 4.8 The transformation of preferred orientation in Cd addition to ZnS films, with increasing dopant content, (a) 0 %, (b) 5 %, (c) 10 %, (d) 15 %, (e) 20 %.....	76
Figure 4.9 X-ray diffraction patterns of $Cd_xZn_{1-x}S$ films with various x at $T_s=400^{\circ}C$	82
Figure 4.10 Variation of x composition in the polycrystalline films with grain size and lattice strain of $Cd_xZn_{1-x}S$ films deposited by SP method at $400^{\circ}C$..	84
Figure 4.11 Variation of grain size in the polycrystalline films with energy band gap of $Cd_xZn_{1-x}S$ films deposited by SP at $400^{\circ}C$	85
Figure 4.12 Variation of grain size in the polycrystalline films with resistivity and carrier density of $Cd_xZn_{1-x}S$ films deposited by SP at $400^{\circ}C$	86
Figure 4.13 Selected glow curves of $Cd_xZn_{1-x}S$ films produced by spray pyrolysis method at $400^{\circ}C$ substrate temperature.....	89
Figure 4.14 X-ray diffraction patterns of $Cd_{0.5}Zn_{0.5}S$ films with various substrate temperatures: (a) $300^{\circ}C$, (b) $350^{\circ}C$, (c) $400^{\circ}C$ and (d) $450^{\circ}C$	91
Figure 4.15 X-ray diffraction patterns of the $Cd_{0.5}Zn_{0.5}S$ film prepared by adding different concentrations of H_2O : (a) 0%, (b) 0.5%, (c) 1.0%, (d) 1.5%.....	92

LIST OF TABLES

	page
Table 2.1 Conditions for lengths and angles for the 7 crystal classes.....	23
Table 2.2 Variations of compound semiconductors.....	26
Table 4.1 Structural, optical and electrical properties of CdS films.....	62
Table 4.2 Structural and electrical properties of ZnS films deposited by CBD.....	70
Table 4.3 Structural and electrical properties of ZnS films deposited by SP.....	74
Table 4.4 Structural and electrical properties of $Cd_xZn_{(1-x)}S$ films with various x composition deposited by CBD.....	80
Table 4.5 Structural and electrical properties of Sprayed $Cd_xZn_{1-x}S$ Films with various x at different substrate temperature.....	87
Table 4.6 Electrical and optical properties of $Cd_{0.5}Zn_{0.5}S$ films with different H_2O concentrations.....	93

CHAPTER ONE

INTRODUCTION AND LITERATURE SURVEY

1.1 Introduction

Thin films are thin material layers ranging from fractions of a nanometer to several micrometers in thickness. In recent years, thin film science has become one of the most important and exciting forefront fields in physics, chemistry and engineering research area. The importance of coatings and the synthesis of new materials for industry have resulted in a tremendous increase in innovative thin film processing technologies. Currently, this development goes hand-in-hand with the explosion of scientific and technological breakthroughs in microelectronics, optics and nanotechnology. For this reason, there are always growing and urgent needs to find new, economical and simple techniques to prepare thin films. A second major field comprises process technologies for films with thicknesses ranging from one to several microns. These films are essential for a multitude of production areas, such as thermal barrier coatings and wear protections, enhancing service life of tools and to protect materials against thermal and atmospheric influences. Presently, rapidly changing needs for thin film materials and devices are creating new opportunities for the development of new processes, materials and technologies [1]. To respond to this need, several research groups have worked in recent years on the preparation and characterization of the thin films.

There are various reports in the literature on preparation, characterization and applications of II–VI materials, for example Zn(S, Se, Te), Cd(S, Se, Te) and their alloys in which high quality epitaxial films were mostly desirable. Recent research focused on new materials which are in the form of solid solutions of the II–VI materials [2]. CdS and ZnS crystals are II -VI semiconductors having the direct band gaps and they are most promising materials due to their remarkable size-dependent optical properties. Since the wavelength corresponding to the band-gap of CdS is

green 500 nm that is very sensitive for human eyes, the CdS thin film is useful for the photovoltaic cells, photoconductive cells, photosensors, transducers, optical detectors, and the light source. On the other hand, ZnS has been used for the fluorescence materials with the various doped elements. The band-gap of ZnS is so large (3.6 eV) that has been applied for the quantum well [3], blue light emitting diodes [4], electroluminescent devices, photovoltaic cells [5] and the optical waveguide [6]. Both CdS and ZnS are widely used as a window material in thin film solar cells. The ternary compound which combines these properties in a controlled way may allow the optimization of the window layer. $Cd_{1-x}Zn_xS$ film is applicable to short-wavelength optical devices from visible to UV region because of various band gap that depend on the composition x . The films have been prepared by different deposition methods such as vapour evaporation, spray pyrolysis, electrodeposition, chemical bath deposition, SILAR deposition, sputtering, sol-gel, and aerosol jet deposition. Chemical bath deposition (CBD) has been recognized as an important route for the manufacture of these materials, since it is a fast, simple and low cost method that enables to obtain good quality films that can compete with films obtained by other more sophisticated methods. Also, spray pyrolysis method is an effective production method to lead to short production time, homogeneous particle composition, and one step production. And it is widely used to obtain semiconductor films because of the low production cost and simplicity of operation and is a process well-suited to large scale production. Also, experimental parameters can be changed to produce high-quality samples.

In this study, a certain number of CdS, ZnS and $Cd_{1-x}Zn_xS$ films, having different concentrations of cadmium chloride ($CdCl_2$), zinc chloride ($ZnCl_2$) and thiourea ($(CS(NH)_2)_2$), have been deposited by spray pyrolysis and chemical bath deposition methods at different deposition parameters. The structural, electrical, optical and thermoluminescence properties of the films have been investigated by using X-ray diffraction (XRD), Van der Pauw method, optical transmission, and thermoluminescence dosimetry (TLD). These studies are presented in the chapters as follows: In chapter one a general introduction about CdS, ZnS and $Cd_{1-x}Zn_xS$ films and deposition methods spray pyrolysis and chemical bath deposition is given and experimental and theoretical studies done by other researchers are reviewed. In chapter 2 some basic semiconductor physics information is given. In the third chapter

the information about spray pyrolysis and chemical bath deposition methods, substrate preparation, measurement techniques and the deposited films are explained. The semiconducting cadmium sulphide (CdS), zinc sulphide (ZnS) and cadmium zinc sulphide ($Cd_xZn_{1-x}S$) films were deposited by the two methods: chemical bath deposition and spray pyrolysis under different deposition conditions. The influence of the deposition parameters on the structural, electrical, optical and thermoluminescence properties of the deposited films was investigated by using X-ray diffraction (XRD), Van der Pauw method, and optical transmission. In fourth chapter, the results of structural, optical and electrical analysis of the films is explained. The conclusions about all studies are mentioned in chapter 5.

1.2 Historical perspective of CdS films

Cadmium sulphide (CdS) is an important chalcogenide II–VI group semiconductor with a wide band gap of 2.42 eV at room temperature. Extensive research has been done in the last two decades on CdS thin films, mainly due to their interesting electrical, optical and photoconductive properties. These films offer a large number of applications in solid state technologies as the solar cells, thin films transistors for flat panel displays, piezo-electronic and semiconducting devices. A large number of studies on the synthesis and characterization of CdS films have been published in recent years.

The CdS thin films have been prepared by various methods; Khan et al. [7] deposited CdS films on silicon (100) wafer by thermal evaporation technique in vacuum. CdS thin films are found to be polycrystalline in nature with hexagonal structure. The optical properties of the polycrystalline thin films are investigated systematically by spectroscopic ellipsometry (SE) and a blue shift compared with bulk cadmium sulphide is observed. The optical band gap of the thin film is estimated to be 2.50 eV. The structural and optical properties of the films fabricated by the thermal evaporation technique are found to be desirable for optoelectronic devices. Das et al. [8] at the Jadavpur University (India) have dealt with the effect of film thickness on the energy band gap of nanocrystalline CdS thin films analyzed by spectroscopic ellipsometry. Nanocrystalline cadmium sulfide thin films were deposited by the radio frequency magnetron sputtering technique on Si and glass substrates with different

particle sizes and thicknesses by varying deposition time. The optical band gaps of the films were also measured by spectrophotometric studies. It was found that the energy band gap decreased from 3.28 to 2.54 eV when the film thickness increased from 153 to 205 nm. Pulsed-laser deposition is a versatility and straightforwardness method to form operative devices based on hetero-pairing. Thin-film CdS (300–400 nm) was deposited onto p-GaAs with low-temperature pulsed-laser deposition. The deposited CdS films are closely stoichiometric and the film texture is of polycrystalline nature embedded in an amorphous matrix [9]. Praveen and et al. [10] have described an rf-sputtering technique for the synthesis of nanocrystalline CdS thin films. They have reported a simple and viable technique for the long-term chemical passivation of such CdS films. The passivated nanocrystalline CdS films have shown strong, blue-shifted luminescence excitation and emission peaks at room temperature. A high-efficiency deposition technique, electrostatic assisted aerosol jet deposition (EAAJD), has been used to prepare CdS, CdSe and ZnS thin films in an open atmosphere [11]. Thin amorphous nanostructured CdS films were photochemically obtained via direct UV radiation ($1 \frac{1}{4}$ 254 nm) of complex $\text{Cd}[(\text{CH}_3)_2\text{CHCH}_2\text{CH}_2\text{OCS}_2]_2$ on Si(100) and ITO- covered glass substrate by spin coating. CdS was synthesized using a direct, fast, simple, quick and inexpensive photochemical method. These films contain sulfur impurities and cadmium oxide as sub- products. This method is a good alternative for deposition of the amorphous metal sulfides by thin films. Tejos and his co-workers [12] have found that the reduction in particles size, impurities, and the amorphous nature of the films increase the optical band.

Comparison of different deposition methods used by some researchers, such as Morales-Acevedo et al. [13]. They reported a comparative study of the properties of the CdS thin films grown by Laser Ablation (LA), Close Space Vapour Transport (CSVT), Sputtering (SP) and Chemical Bath Deposition (CBD), taking into account that the physical properties of CdS thin films depend upon the growth technique, and the optimization of the growth conditions for each technique. LA-CdS thin films showed the best structural properties. Therefore, although CBD films have poor crystalline quality, they may give excellent results for photovoltaic applications because of their better morphological properties (roughness and pinhole density) than films grown by other techniques. The same results were found about poor crystalline

quality of CBD CdS films by researchers in National Renewable Energy Laboratory, CO 80401. Close-spaced Sublimation and Chemical Bath Deposition methods are compared by them [14] and Oliva et al from Mexico [15]. Ravichandran and his co-workers [15] reported another comparative study on structural and optical properties of CdS films fabricated by the conventional spray pyrolysis using carrier gas and CBD methods. The structural and optical properties of the films fabricated by the simplified spray are found to be desirable for opto-electronic applications.

Chemical bath deposition (CBD) is known to be a simple, low temperature, and inexpensive large-area deposition technique. Deposition of CdS using CBD is based on the slow release of Cd^{2+} ions and S^{2-} ions in an aqueous alkaline bath and the subsequent condensation of these ions on substrates suitably mounted in the bath. It is also possible to control effects of using different cadmium sources for deposition by using the CBD technique. Also some reports are found in literature deals with this phenomenon. The first report was presented at University of Mohamed, Morocco dealt with the effect of the cadmium ion sources on the structural and optical properties of CBD-CdS films [17]. CBD has been used to deposit cadmium sulphide from cadmium chloride and cadmium acetate as the cadmium ion source. Another study was reported by Khallaf et al. [18] about the characterization of CdS thin films grown by chemical bath deposition using four different cadmium sources: cadmium sulfate, cadmium chloride, cadmium iodide, and cadmium acetate. The effect of cadmium sources on film optical/electrical properties as well as film thickness, composition, crystal structure, and surface morphology was studied. Film growth rate and band gap were found to be sensitive to the Cd source used. Films were found to be highly stoichiometric when cadmium chloride and cadmium iodide were used. Another important parameter is baths of pH values. Cadmium sulphide (CdS) thin films of different thicknesses were prepared by the chemical bath deposition technique (CBD) onto well-cleaned glass substrates at 80°C from two chemical baths of different pH values 10 and 11. The thickness of the deposited films has been determined by gravimetry technique. The structural characterization was carried out by X-ray diffraction (XRD) and scanning electron microscopic (SEM) studies. It has been found that the films prepared from chemical bath of pH value 10 have better structural and optical properties than the films from bath of pH value 11 [19].

For all thin films, crystallite size is observed to be a function of thickness. Crystallite size is also depends on deposition parameters such as substrate temperature, evaporation rate, and annealing. Also enourmous number of study have reported in literature dealt with temperature and annealing effects on optical and crystallographic properties of grown films. CdS thin films were deposited onto glass substrates by the chemical bath deposition (CBD). The influence of the deposition temperature varied from 55⁰C to 85⁰C in a step of 5⁰C on the crystallographic structure, morphology as well as optical and electrical properties was investigated in detail. The band gaps are found to decrease from 2.56 eV to 2.38 eV with an increase in deposition temperature. Increasing deposition temperature can promote phase transformation from cubic to hexagonal and improvement of crystallinity in CdS films [20]. The same phase transition from cubic to hexagonal occured by increasing the substrate temperature was found by Ikhmayies and Ahmad-Bitar [21]. They have produced CdS films by the spray pyrolysis technique at different substrate temperatures ranging from 350 to 490⁰C on glass substrate. Also thermal annealing process produces a gradual structural transition from cubic for as-grown CdS film to hexagonal for the annealed at 400⁰C [22]. Despite these results, Maliki and his co-workers [23] have shown that, even after annealing at 623 K, the CdS films are poorly crystallized. More precisely the films are neither cubic nor hexagonal but they crystallize in polytype structure. Chavez et al. [24] have deposited CdS by vacuum evaporation, solution growth and spray pyrolysis. Regardless of deposition technique, all films had similiar grain size before annealing. The thicker evaporated and sprayed films showed significant grain growth after annealing at 550⁰C. Dipping in CdCl₂ solution followed by annealing at 550⁰C tended to destroy preferred orientations and promoted grain growth. Increasing bath temperature for CBD and increasing substrate temperature for SP and also annealing for both CBD and SP results a reduction in the energy band gap [20,22,25,26,27]. The electrical properties of CdS films can be improved by annealing at a certain temperature range if these films are used as optical windows for solar cell. The resistivity of CdS films can be decreased by annealing at some suitable temperature [28]. Ramaiah and his co-workers [29] have been carried out similiar investigations with the study related preparing CdS films by using CBD, the resistivity of the films was decreased from 3×10⁶ to 1×10³Ωcm. In 2003, Metin and Esen reported two studies about annealing effects on optical and crystallographic properties of CBD grown CdS films. The

crystallite sizes were found to increase, and the X-ray diffraction patterns were seen to sharpen by annealing. The optical properties of the films were seen to be dependent on the film thicknesses. The band edge sharpness of the optical absorption was seen to oscillate by thermal annealing [29,30]. Another study of Metin and his co-workers reported in 2010 [31] is related with annealing effect on CdS/SnO₂ films grown by CBD. The extensive investigation of the annealing effect in nitrogen atmosphere on the structural optical and electrical properties of chemically deposited CdS films on SnO₂ has been performed. The as-deposited film shows 2.45 eV band gap (E_g) and decreases with increasing annealing temperature. The film annealed at 623K having pure hexagonal phase and E_g = 2.36 eV shows 10 times higher conductivity for all temperature range. The same year they have reported a new study [32] investigating the thermoluminescence properties of CdS films under nitrogen atmosphere. The optical band gap of the as-deposited film (2.44 eV) decreases with an increase in annealing temperature due to an increase in crystallite size, which also results a decrease in TL efficiency of the film. The film annealed at 423 K shows highest electrical conductivity and also highest TL efficiency. Therefore, it might be suggested that 423 K is the best annealing temperature for these CdS films for the application.

The spray pyrolysis method is basically a chemical deposition technique in which fine droplets of the desired material are sprayed onto preheated substrates. Continuous films are formed onto the hot substrate by thermal decomposition of the material droplets. Spray pyrolysis is a rather simple and inexpensive technique which enables the production of large area uniform and transparent films with good adherence and reproducibility. CdS thin films were prepared by chemical spray pyrolysis technique by Ashour in 2003 [33]. Films characterized by X-ray diffraction showed hexagonal phase. The resistivity of the as-deposited films was found to vary in the range 10³-10⁵Ω.cm, depending on the substrate temperature. Direct band gap values of 2,39-2,42 eV were obtained from optical absorption measurements. Raji and his co-workers have used photo acoustic technique for measuring the thermal properties of CdS thin films grown by spray pyrolysis [34]. In 2010, CdS thin films were deposited onto glass substrates by spray pyrolysis method at 275, 300, 325 and 350⁰C substrate temperatures by Yadav and his workers [35]. Compositional analysis reveals that the material formed is stoichiometric at the optimized substrate

temperature. The optical band gap energy is found to be 2.44 eV with direct allowed band-to-band transition for film deposited at 300⁰C. The electrical resistivity measurement shows that the films are semiconducting with a minimum resistivity for film deposited at 300⁰C. The thermoelectric power measurement shows that films exhibit n-type of conductivity.

Chemical bath deposition (CBD) is one of the most promising techniques for film synthesis since it allows for a continuous coverage of rough surfaces with minimum thickness and at low costs. In CBD, the structure of the film is influenced by composition of the bath, temperature and pH of the solution. So, there are lots of studies in literature investigating these relations. The influence of cadmium salt and thiourea concentrations and deposition time on morphological and structural properties of chemical bath deposited CdS thin films has been studied by Martinez and his co-workers [36]. Another important deposition parameter is the substrate type; a related study was done to investigate the growth states of CdS thin films on ITO/glass substrates by chemical bath deposition. The time, the chemistry, and morphology of the different stages that form the growth process by CBD were identified through the results taken from the analysis techniques -Xray photoelectron spectroscopy (XPS), Rutherford backscattering spectrometry (RBS), and atomic force microscopy (AFM)- furthermore, clear evidence was obtained by the formation of Cd(OH)₂ as the first chemical species adhered to the substrate surface which forms the first nucleation centers for a good CdS formation and growth. On the other hand, the ITO coating caused growth stages to occur earlier than in just glass substrates, with which they can obtain a determined thickness in a shorter deposition time [37]. Kim et al. [38] dealt with the physical properties of the CdS thin films depending on the various substrates such as ITO, CIGS, sodalime glass and the stirring speed. As the stirrer speed is increased, the thickness of the film is increased due to the weak molecule interaction between CdS cluster and the grown CdS film can be easily broken by the fast motion of solution. Therefore, the CdS large cluster cannot have a chance to contribute to the CdS growth by not being adhered to the grown CdS film. The structural property of the CdS film depends on the substrate crystal structure even if all experimental parameter are identical. It can be investigated what CdS grain's orientation is favorable on the specific orientation of ITO grain. The film thicknesses is an important parameter that effects the film quality. The band gap of

the film decreases as the films grows in thickness and the grain size increases with the thickness of the film [39,40]. The influence of cadmium salt and thiourea concentrations and deposition time on the optical and electrical properties of chemical bath deposited CdS thin films has been studied by Gullien and his co-workers [41]. In order to obtain high transparent CdS films with adequate growth rates and thickness control, it is needed to maintain low cadmium salt concentration and a high thiourea in the bath. Dark electrical behaviour has been found to be independent on the deposition parameters by them. The films properties have been investigated as a function of bath temperature and deposition time by Moualkia et al. [42]. The results suggested that increasing the deposition time yields a cubic phase structure and a preferred orientation in the (111) plane. Orthorhombic phase is present in samples deposited with 90 min. Films grown at different bath temperatures 55 °C to 65 °C show good transmittance. The crystallite sizes of CdS thin films are found to decrease with the solution temperature. Khomane investigated the morphological and opto-electronic characterization of chemically deposited cadmium sulphide films [43]. The X-ray diffraction analysis showed that the film samples are in cubic modification. The optical band gap energy (E_g) of film sample was found to be 2.4 eV. The electrical conductivity of the film sample was found to be in the order of $10^{-7} (\Omega\text{cm})^{-1}$.

CdS films are often grown by the chemical bath deposition (CBD) technique and spray pyrolysis and have shown good properties for device fabrication. CdS films are commonly used as a window or buffer layer material for solar cells of the type CdS/CdTe and CdS/CIGS but the CdS films generally exhibits high resistivities. When the thermal treatments in CdCl_2 ambient is performed in order to decrease the resistivity, the films can show cracks and the problems in the reproducibility of the devices. Some researchers solve this problem by adding dopants such as Cu, Ni, In and some metal-organic salts. Petre and his co-workers [44] have doped CdS films with copper using the direct method consisting in the addition of a copper salt (CuCl_2) in the deposition bath of CdS. They showed that the copper content in the deposition bath is increased, the dark resistance and the photosensitivity of CdS films increase and the optical bandgap energy of undoped CdS film changes from 2.48 eV to 2.3 eV after Cu doping. The lifetime of photocarriers decreases from 8 ms to 1.3 ms. The concentration of trapped carriers increases when the Cu content increased.

The modification of trapped carriers concentrations influences the lifetime of photocarriers, the spectral distribution of photoconductivity and photosensitivity. A similar study was done by Paulraj and his co-workers. They fabricated CdS homojunction by Cu deposition on spray pyrolysed CdS thin film for improved performance of solar cell [45]. CdS thin films with low In doping concentration in starting solution have deposited using the spray pyrolysis technique by Acosta et al. [46]. CdS thin films doped with metal-organic salts were grown on glass substrates at 90 °C by the chemical bath deposition technique by Cruz et al. [47]. Metal-organic salts such as zinc acetate, chromium acetylacetonate, ammonium fluoride, aluminum nitrate, tin acetate and indium acetate were used. Undoped CdS films with an S/Cd ratio equals to 2 have the best optical, structural and electric properties. In the case of doped CdS thin films, the lowest resistivity of 9.7 Ω cm was obtained for the films doped with Zn (1at.%). Chandramohan et al. [48] have studied the modifications in structural, optical, and morphological properties of CdS thin films due to Ni doping (up to ~10.2 at.%) by implantation with different fluences at room temperature. They didn't observe any structural phase transformation or formation of any secondary phase or metallic clustering. Optical absorption studies show a reduction in the band gap of CdS due to Ni-doping.

CdS thin film has good quantities for window film and attractive for thin film solar cell. Also CdS nanorods-structure is promising for organic-inorganic hybrid solar cells. Some researcher to fabricate CdS films for using photovoltaic studies such as Chun and his co-workers, have grown CdS thin film and nanostructure on transparent ITO electrode for solar cells [49]. Ochoa-Landin et al. [50] have deposited CdS on two different transparent conductive substrates, namely indium tin oxide and fluorine doped tin oxide and the influence of their properties on CdS/CdTe solar cell performance was determined; the window layers deposited with the sodium citrate-based CBD processes have a reasonable performance. The efficiency of the solar cells was between 5.7% and 8.7% depending on the conductive transparent substrate and on the CdS window layer. A similar study was done by Herrero and his co-workers; the understanding of the chemical deposition processes of CdS and other alternative materials that can be used as window layers in polycrystalline thin film solar cell devices were investigated [50]. The field of printed electronics is receiving increasing attention from researchers in both industrial and academical studies.

Printed thin film transistors (TFTs) would enable production of low cost drivers for displays, radio frequency identification (RFID) tags, etc. Cadmium sulfide (CdS) is a candidate semiconducting material for printed electronics. Meth et al. [51] have fabricated thin film transistors incorporating patterned cadmium sulfide as the active layer.

Complexing agent is another important deposition parameter that effects the film quality Patil et al. [52] have investigated the performance of bath deposited CdS films based on complexing agents i.e. ammonia and triethanolamine (TEA). Triethanolamine complex led to better crystallinity and marigold flower-like morphology. The films deposited using triethanolamine complex showed good stability under photoelectrochemical cell conditions. CdS films have been deposited using succinic acid [53], nitrilotriacetic acid [54], and tartaric acid [55].

1.3 Historical perspective of ZnS films

Zinc sulfide (ZnS) films with a wide direct band gap and n-type conductivity are promising for optoelectronic device applications, such as electroluminescent devices and photovoltaic cells. In optoelectronics, it can be used as light emitting diode in the blue to ultraviolet spectral region due to its wide band gap of 3.7 eV at room temperature, which is the largest value of all II-IV compound semiconductors. In the area of optics, ZnS can be used as a reflector and dielectric filter because of its high refractive index (2.35) and high transmittance in the visible range, respectively.

Several techniques such as ultrasonic spray pyrolysis, chemical vapour deposition (SS-CVD), pulsed-laser deposition, MOVPE and liquid phase techniques such as solution growth technique (SGT), electrochemical deposition, chemical bath deposition (CBD) have been used to produce ZnS films. A large number of studies on the synthesis and characterization of ZnS films have been published in recent years. Thin films of zinc sulfide were prepared by ultrasonic spray pyrolysis method onto silicon, sapphire and gallium arsenide substrate at 460-520⁰ C by Pike and his co-workers [56]. The films prepared on silicon or sapphire were found to have a highly oriented hexagonal structure, while those deposited onto gallium arsenide showed highly oriented cubic structure. Zinc sulphide thin films were grown on

silicon (100) substrates at all growth temperatures (250 to 500⁰ C) by single source chemical vapour deposition (SS-CVD) by Tran et al. [57]. The total amount of residual carbon and nitrogen contamination found in the films was ≤ 16 at %. Although the total amount of the contamination found in film bulk was relatively high, highly crystalline ZnS films were produced at substrate temperature as low as 300⁰ C. The ZnS films could be considered cubic with 36-50 nm size of crystallites and with a preferred (111) orientation. Lee and his co-workers [58] have grown the nanosized ZnS thin films that can be used for fabrication of blue light-emitting diodes, electro-optic modulators, and n-window layers of solar cells by the solution growth technique (SGT). ZnS films grown by them have cubic structure and the most uniform film was obtained with the growth temperature of 75⁰ C. From UV spectrophotometer measurement the energy band gap of ZnS film are 3.69-3.91 eV. The absorption and photocurrent properties of thin film ZnS on quartz glass formed by pulsed-laser deposition have been studied experimentally and theoretically at room temperature by Yano and his co-workers [59]. ZnS thin film have been deposited on a glass substrate by photochemical deposition (PCD) technique from an aqueous solution with varying pH (2.5-7.0) and stirring speed of the solution by Gunesakaran and his co-workers [60]. The optimized value of pH of the solution for good deposition was between 3.0 and 3.5 and the optimum stirring speed for good deposition was found to be 300 rpm for their system. The annealing effects was researched and it was observed that the crystallinity and the surface morphology of the films were improved by annealing. Zhang et al. [61] have produced nanocrystalline ZnS films by sulfidation of the as-deposited ZnO films of various sputtering time. The structural, electrical and optical properties of ZnS films deposited by close-spaced evaporation was studied by Subbaiah and his co-workers [62]. Their studies showed that the optimum substrate temperature for the growth of ZnS layers was 300⁰ C. The films grown at these temperatures exhibited cubic structure and had nano-sized grain size of ~ 40 nm. The optical studies exhibited direct allowed transition with an energy band gap of 3.61 eV.

The spray pyrolysis technique for the preparation of thin films is very attractive because it is inexpensive, simple and capable of depositing optically smooth, uniform and homogenous layers. So there are lots of studies in literature about ZnS films deposited by spray pyrolysis. Lopez and his co-workers [63] have prepared ZnS

films by spray pyrolysis using two mixed aqueous solutions: (a) dehydrated zinc acetate and thiourea in bidistilled water; (b) zinc chloride and thiourea in bidistilled water. It was found that films prepared from solution A, have largest crystal size, smoothest surface and high optical transmittance, as determined by XPS. A similar study was done by Nasrallah and his co-workers; ZnS films have been prepared on pyrex substrates by the spray pyrolysis technique using zinc chloride and thiourea. The depositions were carried out on substrates heated at 450⁰ C and annealed at 450 or 500⁰ C. After deposition the presence of the (111) plane of the cubic structure of ZnS in the XRD spectra attested to the growth of ZnS. The presence ZnO peaks showed that the films are contaminated with oxygen [64]. The structure, surface morphology, chemical composition and optical properties of ZnS films were investigated as a function of substrate temperatures, deposition time and solution spray rate by Elidrissi et al. [65]. It was found the films prepared at substrate temperature of 500⁰ C, deposition time of 35 min and solution rate of 5 ml min⁻¹ had good adherence to the glass substrates and exhibited a mixture of hexagonal (α) and cubic (β) phases, with a preferential orientation along the (111) $_{\beta}$ direction. Öztaş and his co-workers investigated the role of growth parameters on structural, morphology and optical properties of sprayed ZnS thin films. The ZnS films could be considered to be the hexagonal structure and with a preferred (002) orientation [66]. Structural, morphological and optical properties of ZnS films studied by many researchers and thermoluminescence properties have been studied by Yazıcı and his co-workers [67]. They investigated the effect of thin film production conditions (substrate temperature and ratio starting material) on the intensity of thermoluminescence (TL) and TL emission spectrum of ZnS samples that were grown by spray pyrolysis. It was observed that the intensity of TL signal increases with increasing the substrate temperature (T_s) and reaches a maximum point at the substrate temperature of 500⁰C with a high ratio of ZnCl₂ salt solutions. Secondly, it was observed that the energy level of trap present in ZnS samples is not single-level but instead has a distribution of energy levels.

Chemical bath deposition (sometimes, called the “solution growth technique” or “electroless deposition”) method is most commonly used because it is a very simple, cost effective and economically reproducible technique that can be applied in large area deposition at low temperature. In addition, this method is free of many

inherent problems associated with high-temperature techniques; these problems include increased point defect concentrations, evaporation and decomposition of ZnS thin films. ZnS thin films had been successfully deposited by chemical bath deposition technique using tartaric acid as a complexing agent at 85 °C by Roy et al. [68]. XRD studies showed formation of pure ZnS films with a wurtzite structure. The crystallinity of the films increased with increasing annealing temperature from 200 to 500 °C. The film shows better optical transmission (80–100%) in the visible region and the band gap value is found to be 3.69 eV. PL spectrum has also been investigated for both as-deposited as well as annealed films. Highly transparent and adherent nanocrystalline large-area ZnS thin films were grown on the slide glass and the SnO₂-coated glass substrate by chemical deposition using an aqueous solution containing zinc sulfate and thioacetamide by Lee et al. [69]. The films were highly transparent from the near ultraviolet to the near infrared with a transmittance of more than 80%. The cut-off wavelengths at about 315 nm and 325 nm correspond to the value of 3.9 eV and 3.8 eV, respectively, which is considerably larger than the optical band gap of bulk ZnS (3.67 eV), caused by the quantum size effect. ZnS/glass/ZnS heterostructures with optical homogeneous chalcogenide films with thickness within 40–300 nm were prepared by CBD technique, using mono- and multi-layer deposition technique [70]. Nasr and his co-workers have investigated the effect of pH on the properties of ZnS thin films grown by chemical bath deposition. The deposition was carried out in the pH range of 10 to 11.5. It is particularly observed that the best crystallinity of the ZnS thin films is obtained at pH=10. The decreasing in the pH value from 10.99 to 10 is related with the increasing in the (111) diffraction peak intensity. The optical transmission coefficient is found to increase when the pH increases from 10 to 11.5. This may be interpreted by the decrease in the film thickness. ZnS film prepared with pH 11.5 shows a high transmission coefficient (70%) and a wide band gap of 3.67 eV [71]. A similar study was done to investigate the physical properties of the polycrystalline ZnS thin films by CBD. Transparent and polycrystalline zinc sulfide (ZnS) thin films were prepared by the chemical bath deposition (CBD) technique onto glass substrates deposited at 80 °C using aqueous solution of zinc acetate, thiourea, triethanolamine and tri-sodium citrate at a pH of about 10.55 by Göde and his co-workers [72]. The thickness of the films varied from 403 to 934nm in the visible range. UV–visible spectrophotometric measurement showed transparency from 66% to 87% of the films

with a direct allowed energy band gap in the range of 3.79–3.93 eV. Transmission measurement on the study of Liu et al. [73] shows that an optical transmittance is about 90% when the wavelength over 500 nm. The band gap value of deposited film is about 3.51 eV. ZnS thin films that are used as buffer layers in thin film solar cells are usually deposited by chemical bath deposition using hydrazine hydrate as a complementary complexing agent. This material is, however, highly hazardous and its replacement by a less-hazardous material is desirable. So Johnston et al. [74] dealt with chemically bath deposited ZnS based buffer layers using low toxicity materials. ZnS thin films have been deposited using sodium citrate as a novel complementary complexing agent. The layers deposited were found to consist of Zn and S but with a small concentration of O present.

The literature survey shows that ZnS thin films have been prepared using suitable source compounds that can release cations and anions which reacts to form the compound. The ZnS thin films get precipitated due to low solubility and they have a rough topology with low transmittance. To overcome these problems, a complexing agent is used which forms complex ions with the metal ions. The most widely used agents are ammonia and hydrazine hydrate. These agents changes the pH value of deposition bath solution. Also the structural, morphological, and optical properties of ZnS films are effected with varying pH values. Kang and his co-workers studied the effect of pH on the characteristics of nanocrystalline ZnS thin films prepared by CBD method in acidic medium [75]. The effect of the pH ranging from 5 to 6.5 on quality of ZnS thin films is investigated. Irrespective of the pH values used for the deposition all films are polycrystalline with a wurtzite (hexagonal) structure. The absorption coefficient depends on the pH values of the solution used and are responsible to the changes observed in absorption edges. The band gap energy values of ZnS thin films decreased from 3.91 to 3.78 eV with increasing pH values of the solution. Antony et al. [76] also investigated the effect of the pH value on the growth and properties of chemical bath deposited ZnS films. The resistivity of the films was found to decrease with the increase in pH of the reaction mixture and was $\sim 10^4 \Omega \text{ cm}$ for pH 10.6. A similiar study; composition and properties of ZnS thin films prepared by chemical bath deposition from acidic and basic solutions was done by Makhova and his co-workers. Films deposited using the acidic bath showed a smaller concentration of Zn-O bonds and much closer to ZnS stoichiometry and X-ray

diffraction patterns prove crystallinity of as deposited films from acidic bath, which crystallize in the cubic modification [77]. Dhanam et al. [78] had reported a paper than presents the preparation of ZnS thin films from different chemical baths having TEA as complexing agent with various pH values.

ZnS films can be deposited by conversion of ZnO to ZnS and vice versa. The formation of photoconducting ZnO films from chemically deposited films by air annealing is reported by Fernandez and Sebastian [79]. As-deposited films exhibited very little dark conductivity and no photoconductivity. Air annealing of the films at about 400⁰ C for at least 15 min. converted them to ZnO films with higher dark conductivity and photoconductivity. A similiar study named a new approach to fabrication of ZnO ultra thin films from annealing ZnS nanoparticulate was reported by Mu et al. [80]. ZnO films prepared by the thermal oxidation of the ZnS films through thermal evaporation are reported by Wang et al. [81], and Zhang and his co-workers [82,83]. Zhang and his co-workers have also studied the conversation of ZnO to ZnS films. They have prepared nanocrystalline ZnS films by sulfidation of the reactive magnetron sputtered ZnO films. They have studied the effects of the sulfidation temperature [84] and influence of sulfidation ambience [85] on the structure, composition and optical properties of ZnS films prepared by sulfurizing ZnO films.

ZnS crystals are known as a material having high photoluminescence and thermoluminescence properties above room temperature and are widely used in opto-electronic devices for their photoluminescence properties. The thermoluminescence (TL) glow curves of ZnS thin films developed using chemical spraying technique were carefully investigated and its kinetic parameters were determined with a specially developed computer program by Yazıcı and his co-workers [86,87]. Wei et al. [88] have also studied thermoluminescence of ZnS nanoparticles and and reported that the TL intensity increases as the particle size decreased. Neumark dealt with electroluminescence and thermoluminescence of ZnS single crystals [89]. Öztaş and his co-workers have deposited ZnS thin films on a glass substrate by the spray pyrolysis technique and have doped films with copper using the direct method [90]. The effect of the spraying time on the electrical and optical properties of the films has been studied. Optical studies of the Cu-doped thin films show a decrease in the

transmission and also show that copper doping of the ZnS thin films results in a significant increase in resistivity and a slight decrease in the band gap of the ZnS thin films.

1.4 Historical perspective of CdZnS films

CdS and ZnS crystals are II -VI semiconductors having the direct band gaps and they are most promising materials due to their remarkable size-dependent optical properties. Since the wavelength corresponding to the band-gap of CdS is green 500 nm that is very sensitive for human eyes, the CdS thin film is useful for the photovoltaic cells, photoconductive cells, photosensors, transducers, optical detectors, and the light source. On the other hand, ZnS has been used for the fluorescence materials with the various doped elements. The band-gap of ZnS is so large (3.6 eV) that has been applied for the quantum well, blue light emitting diodes, electroluminescent devices, photovoltaic cells and the optical waveguide. Both CdS and ZnS are widely used as a window material in thin film solar cells. The ternary compound which combines these properties in a controlled way may allow the optimization of the window layer.

$Cd_{1-x}Zn_xS$ film is applicable to short-wavelength optical devices from visible to UV region because of various band gap that depend on the composition x . Different deposition of $Cd_{1-x}Zn_xS$ methods has been reported such as chemical bath deposition, spray pyrolysis, solvothermal method, ultrasonic spray pyrolysis, precipitable-hydrothermal process, pulsed laser deposition and SILAR. Each technique produces films with different properties, which should be optimized for the particular application of the film. Generally, in each of these methods, polycrystalline, stable, uniform, adherent and hard films are obtained and their electrical properties are very sensitive to the method of preparation.

Optical characterization of pyrolytically deposited $Zn_xCd_{1-x}S$ thin films has been studied by Eleruja and his co-workers. A direct optical band gap of 2.63 eV was obtained from the analysis of the absorption spectrum [91]. $Cd_xZn_{1-x}S$ solid solution thin films were grown by successive ionic layer adsorption and reaction (SILAR) technique on soda lime glass, ITO-covered glass and polymer substrates by

Valkonen et al. [92]. Using the pulsed laser deposition (PLD) method, Sakai and his co-workers first produced the $Zn_xCd_{1-x}S$ mixed crystal thin films. The surface morphology, the composition x and the crystal structure of the thin films were observed with SEM, EDAX and XRD respectively. The lattice constant corresponding to (002) plane of hexagonal crystal linearly depends on x following the Vegard's law. The crystal grains of the $Zn_xCd_{1-x}S$ thin films have the c -axis perpendicular to the film surface and good crystallinity. The optical transmittance was measured at room temperature so that the optical band gaps of direct transition continuously increase from 2.43 eV (510 nm) to 3.63 eV (340 nm) with x [93]. Also Shi et al. [94] have dealt with composition-dependent optical properties of $Zn_xCd_{1-x}S$ synthesized by precipitable-hydrothermal process. A new method, solvothermal method was used by Song and his co-workers for synthesizing of a series of ternary $Zn_{0.2}Cd_{0.8}S$ photocatalysts [95]. CdS , $Cd_{0.9}Zn_{0.1}S$ and $Cd_{0.8}Zn_{0.2}S$ films were deposited onto glass substrates at $300^{\circ}C$ substrate temperature by using ultrasonic spray pyrolysis technique (USP) by Özer and his co-workers [96]. XRD patterns showed that films have polycrystalline nature with a hexagonal structure. The grain size of the films decreased with increasing x values. The optical band gap values of the films were found to be between 2.44 and 2.45 eV. The variations of conductivity of $Cd_{1-x}Zn_xS$ ($0 \leq x \leq 0.2$) films have been investigated depending on applied voltage in dark and under illumination. The resistivity significantly decreased with increasing tin concentration and under illumination. The ternary semiconductor $CdZnS$ films were prepared by chemical bath deposition and growth characterization of films was investigated by the optical transmission spectra [97].

The spray pyrolysis technique is particularly attractive because of its simplicity in comparison with methods as explained previously. It is fast, inexpensive and is suitable for mass production. In particular, spray pyrolysis has proved well suited for producing semiconductor films of the desired stoichiometry on large and non-planar areas. Although the spray deposition technique was employed earlier for the preparation of $Cd_xZn_{1-x}S$ thin films, cadmium chloride and zinc chloride were used as source for the cadmium and zinc in the deposits. The electronic and optical properties of $Zn_xCd_{(1-x)}S$ thin films ($0.0 \leq x \leq 0.7$) fabricated using the chemical spray method have been investigated in nitrogen atmosphere by Bedir and his co-workers [98]. The crystallite size and degree of preferential orientation were found to

decrease with the increase in x . The transmission edge shifted towards shorter wavelengths with increase in x in agreement with the expected shift in energy band gap. The films were found to exhibit room temperature resistivity variation in the range 100-1000 Ωcm with composition. Öztaş and Bedir have reported another study dealt with the some properties of $\text{Zn}_x\text{Cd}_{(1-x)}\text{S}$ and $\text{Zn}_x\text{Cd}_{(1-x)}\text{S}(\text{In})$ thin films prepared by spray pyrolysis [99]. Baykul et al. [100] have investigated the band alignment of $\text{Cd}_x\text{Zn}_{1-x}\text{S}$ films produced by spray pyrolysis. Energy band gaps of the $\text{Cd}_x\text{Zn}_{1-x}\text{S}$ samples obtained using optical absorption spectra vary between 2.445 and 3.75 eV and the energy band gap of $\text{Cd}_x\text{Zn}_{1-x}\text{S}$ thin films increases quadratically with increasing zinc content. XRD results have shown that in the deposition conditions used, the $\text{Cd}_x\text{Zn}_{1-x}\text{S}$ thin films on glass substrates are in the polycrystalline form. The grains of these thin films have a hexagonal structure. Raviprakash and his co-workers reported two papers dealing with preparation and characterization of $\text{Cd}_x\text{Zn}_{1-x}\text{S}$ thin films deposited using spray pyrolysis technique [101,102]. The XRD study showed that the compounds have hexagonal phase. It was observed that crystallinity of film increased with the composition. The lattice parameters are modified with the composition and optical band gap varies from 3.32 to 2.41 eV.

CHAPTER TWO

THEORY

2.1 Introduction

One of the remarkable and dramatic developments in recent years has been the application of solid state science to technical developments in electrical devices made from semiconductor materials such as the transistor, many kinds of diodes including the light-emitting diode, the silicon controlled rectifier, and digital and analog integrated circuits. Solar photovoltaic panels are large semiconductor devices that directly convert light energy into electrical energy. Semiconductor devices now influence our lives on a daily basis. Although insulators and conductors are useful in their own right, semiconductors such as silicon and gallium arsenide have dramatically changed the way in which billions of people live. Their intermediate ability to conduct electricity at room temperature makes them very useful for electronic applications. The rapid growth of the semiconductor industry has stimulated the demands for better material understanding and material quality. So some basic semiconductors physics information is given in this chapter.

The semiconductor is in general a single-crystal material. The electrical properties of a single-crystal material are determined not only by the chemical composition but also by the arrangement of atoms in the solid. Another particular interest is knowing how many fixed and mobile charges are present in the material and understanding the transport of the mobile carriers through the semiconductor; this being true, a brief study of the crystal structure of solids is warranted. Crystalline properties of solids, the concepts of energy bands, energy band gaps and the direct and indirect band gap are explained in this chapter. The semiconductor materials is also discussed. A short discussion of the types of semiconductors according to their purity: intrinsic and extrinsic semiconductor is included in this chapter to provide the information about charge carrier of semiconductors. The understanding of structural, optical, electrical,

mechanical and thermoluminescence (TL) properties of films is important, hence some basic information about defects, mobility, strain, TL properties and the transitions of the electrons between energy bands is also discussed in this chapter.

2.2 Periodic Structures of Solids

Classification of solids can be based on atomic arrangement, binding energy, physical and chemical properties, energy bands or the geometrical aspects of the crystalline structure.

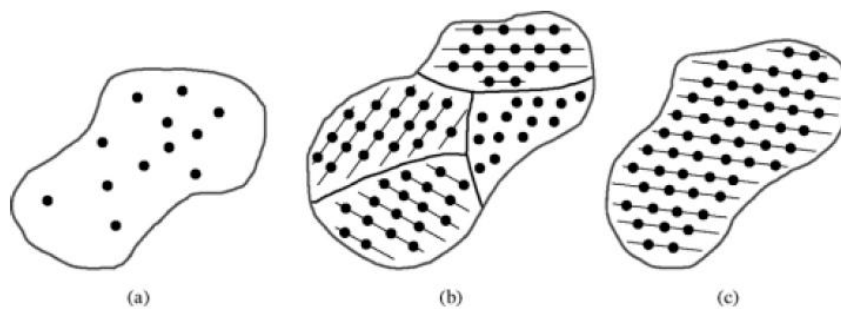


Figure 2.1 a) Amorphous b) Polycrystals c) Crystal

A solid substance with its atoms held apart at equilibrium spacing, but with no long-range periodicity in atom location in its structure is an amorphous solid as shown in Figure 2.1. Examples of amorphous solids are glass and some types of plastic. Amorphous solids do not show a sharp phase change from solid to liquid at a definite melting point, but rather soften gradually when they are heated. In another type, the atoms or group of atoms in the solid are arranged in a regular manner. These solids are referred to as the crystalline solids (Fig. 2.1). They have characteristic geometrical shape. When crystalline solids are rotated about an axis, their appearance does not change. This shows that they are symmetrical. Such crystalline solids typically have flat surfaces, with unique angles between faces and unique 3-dimensional shape. Examples of crystalline solids include diamonds, and quartz crystals. The crystalline solids can be further divided into two categories: the single-crystalline and the polycrystalline solids. In a single-crystalline solid, the regular manner extends over the entire crystal. In a polycrystalline solid, however, the regular manner exists only over a small region of the crystal, with grain size ranging

from a few hundred angstroms to a few centimeters. A polycrystalline solid contains many of these small single-crystalline regions surrounded by the grain boundaries. Distinction between these two classes of solids —amorphous and crystalline— can be made through the use of X-ray or electron diffraction techniques [103].

2.3 Crystalline Properties of Solids

Some of the properties of crystalline solids depend on the crystal structure of the material, the manner in which atoms, ions, or molecules are spatially arranged. Crystal structures may be conveniently specified by describing the arrangement within the solid of a small representative group of atoms or molecules, called the unit cell. Unit cells for most crystal structures are parallelepipeds or prisms having three sets of parallel faces; one is drawn within the aggregate of spheres, which in this case happens to be a cube. A unit cell is chosen to represent the symmetry of the crystal structure, wherein all the atom positions in the crystal may be generated by translations of the unit cell integral distances along each of its edges [104]. In other words, the unit cell defines the basic building blocks of the crystal, and the entire crystal is made up of repeatedly translated unit cells. By multiplying identical unit cells in three directions, the location of all the particles in the crystal is determined. Also a crystal can be defined as a solid consisting of a pattern that repeats itself periodically in all three dimensions. This pattern can be consisting of a single group of atom, a group of atoms or other compounds. The crystal can be consisting of two separate parts: the lattice and the basis. The periodic arrangement of such patterns in a crystal is represented by a lattice. A lattice is a mathematical object which consists of a periodic arrangement of points in all directions of space. One pattern is located at each lattice point [105]. Crystals are categorized by their crystal structure and the underlying lattice. While some crystals have a single atom placed at each lattice point, most crystals have a combination of atoms associated with each lattice point. This combination of atoms is also called the basis.

A crystal structure is formed by associating with a lattice a regular arrangement of atoms or molecules. Since there are many different possible crystal structures, it is sometimes convenient to divide them into groups according to unit cell

configurations and/or atomic arrangements. The unit cell geometry is completely defined in terms of six parameters: the three edge lengths a , b , and c , and the three interaxial angles, α , β , and γ . On this basis there are seven different possible combinations of a , b , and c , and, α , β , and γ each of which represents a distinct crystal system. These seven crystal systems are cubic, tetragonal, hexagonal, orthorhombic, rhombohedral, monoclinic, and triclinic. Conditions for lengths and angles for the 7 crystal classes are tabulated in Table 2.1.

Table 2.1 Conditions for lengths and angles for the 7 crystal classes

System	#	Lattice symbol	conditions for the usual unit cell
triclinic	1		
monoclinic	2	s, c	$\alpha = \gamma = 90^\circ$ or $\alpha = \beta = 90^\circ$
Orthorhombic	4	s, c, bc, fc	$\alpha = \beta = \gamma = 90^\circ$
tetragonal	2	s, bc	$a = b$, $\alpha = \beta = \gamma = 90^\circ$
cubic	3	s, bc, fc	$a = b = c$, $\alpha = \beta = \gamma = 90^\circ$
trigonal	1		$a = b$, $\alpha = \beta = 90^\circ$, $\gamma = 120^\circ$
rhombohedral	1		$a = b = c$, $\alpha = \beta = \gamma$
hexagonal	1		$a = b$, $\alpha = \beta = 90^\circ$, $\gamma = 120^\circ$

2.3.1 Cubic Lattice

The cubic lattice is the most symmetrical of the systems. All the angles are equal to 90° , and all the sides are of the same length ($a = b = c$). Only the length of one of the sides (a) is required to describe this system completely. There is one atom wholly inside the cube ($Z = 1$). Unit cells in which there are host atoms (or lattice points) only at the eight corners are called primitive. In addition to simple cubic, the cubic lattice also includes body-centered cubic and face-centered cubic (Figure 2.2). Body-centered cubic results from the presence of an atom (or ion) in the center of a cube, in addition to the atoms positioned at the corners of the cube. Each atom touches eight other host atoms along the body diagonal of the cube ($a = 2.3094r$, $Z = 2$).

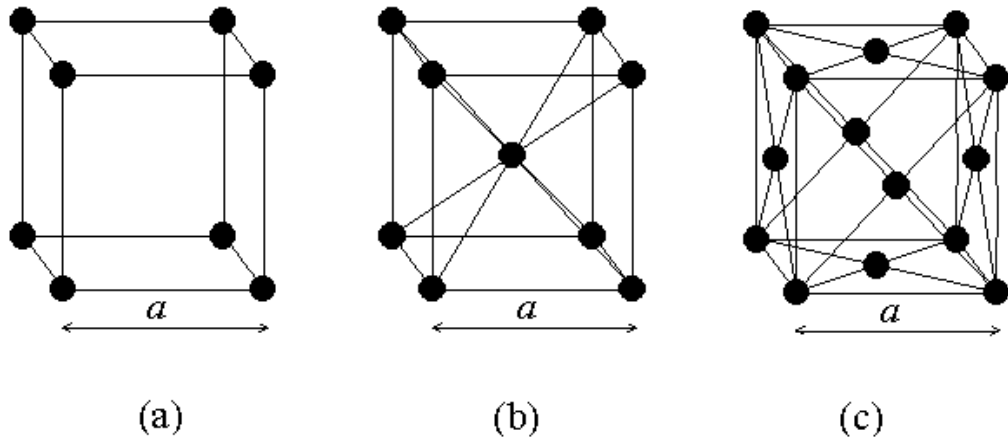


Figure 2.2 Three lattice types: a) simple cubic b) body-centered cubic c) face-centered cubic

In a similar manner, a face-centered cubic requires, in addition to the host atoms (ions) positioned at the corners of the cube, the presence of atoms (ions) in the center of each of the cubes face and the host atoms touch along the face diagonal ($a = 2.8284r$, $Z = 4$). There is one host atom at each corner, one host atom in each face, and the host atoms touch along the face diagonal ($a = 2.8284r$, $Z = 4$).

2.3.2 The Diamond and Zinc-Blende Lattice

The diamond structure refers to the particular lattice in which all atoms are of the same species, such as silicon or germanium. A unit cell of the diamond structure is more complicated than the simple cubic structures. The diamond cubic structure consists of two interpenetrating face-centered cubic lattices, with one offset $1/4$ of a cube along the cube diagonal. It may also be described as face centered cubic lattice in which half of the tetrahedral sites are filled while all the octahedral sites remain vacant. The diamond cubic unit cell is shown in Figure 2.3. Each of the atoms (e.g., C) is four coordinate, and the shortest inter-atomic distance (C-C) may be determined from the unit cell parameter (a).

$$C - C = a \frac{\sqrt{3}}{4} \approx 0.422a \quad (2.1)$$

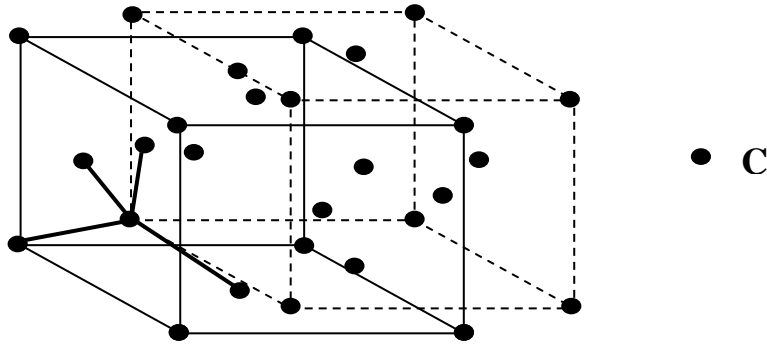


Figure 2.3 The Diamond structure

Zinc-blende is a binary phase (ME) and is named after its archetype, a common mineral form of zinc sulfide (ZnS). As with the diamond lattice, zinc-blende consists of the two interpenetrating fcc lattices. However, in zinc-blende one lattice consists of one of the types of atoms (Zn in ZnS), and the other lattice is of the second type of atom (S in ZnS). It may also be described as face centered cubic lattice of S atoms in which half of the tetrahedral sites are filled with Zn atoms. All the atoms in a zinc blende structure are 4-coordinate. The important feature of both the diamond and the zinc-blende structures is that the atoms are joined together to form a tetrahedron. The zinc-blende unit cell is shown in Figure 2.4. A number of inter-atomic distances may be calculated for any material with a zinc-blende unit cell using the lattice parameter (a).

$$ZnS = a \frac{\sqrt{3}}{4} \approx 0.422a \quad (2.2)$$

$$Zn - Zn = S - S = \frac{a}{\sqrt{2}} \approx 0.707a \quad (2.3)$$

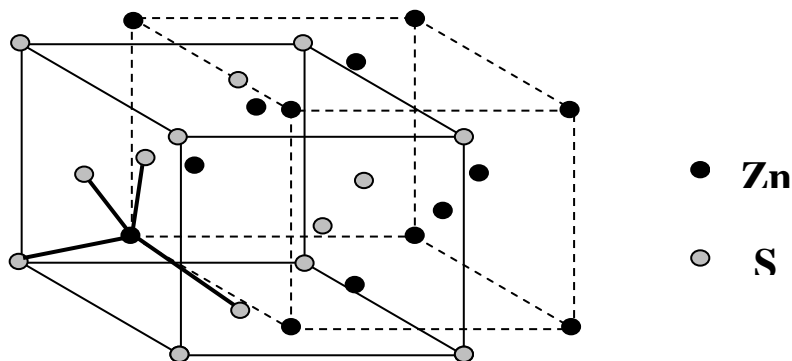


Figure 2.4 The Zinc-blende structure

Both the diamond lattice and the zinc-blende lattice are cubic lattices. A third common crystal structure is the hexagonal structure also referred to as the wurzite crystal structure, which is the hexagonal form of zinc sulfide (ZnS).

Many semiconductor materials can have more than one crystal structure. A large number of compound semiconductors including GaAs, GaN and ZnS can be either cubic or hexagonal. SiC can be cubic or one of several different hexagonal crystal structures. CdS exists in two crystalline modifications: the hexagonal (wurtzite) phase and cubic (zinc-blende) structure [106].

2.4 Semiconductor Materials

The semiconductors are covalent solids. That is, the atoms form covalent bonds with themselves, the most important being silicon and germanium in Group IV of the periodic table. Others may form semiconductor compounds where two or more elements form covalent bonds, such as gallium (Group III) and arsenic (Group V), which combine to form gallium arsenide. Semiconductors are classified into the two groups; elemental and compound semiconductors. Elemental semiconductors are semiconductors where each atom is of the same type such as Ge, Si. These atoms are bound together by covalent bonds, so that each atom shares an electron with its nearest neighbor, forming strong bonds.

Table 2.2 Variations of compound semiconductors

II-VI compound	CdS, CdSe, CdTe, ZnS, ZnSe, ZnTe
III-V compound	GaP, GaAs, GaSb, InP, InAs, InSb
IV-VI compound	PbS, PbSe, PbTe
IV-IV compound	SiC
V-VI compound	Bi ₂ Te ₃
III-VI compound	AlN, GaN, InN, AlP, AlAs, InSe, InS

Compound semiconductors are made of two or more elements. Common examples are CdS or ZnS. These compound semiconductors belong to the II-VI

semiconductors so called because first and second elements can be found in group II and group VI of the periodic table respectively. These compound semiconductors are tabulated in Table 2.2.

In compound semiconductors, the difference in electro-negativity leads to a combination of covalent and ionic bonding. Ternary semiconductors are formed by the addition of a small quantity of a third element to the mixture, for example $\text{Cd}_x\text{Zn}_{1-x}\text{S}$. The subscript x refers to the alloy content of the material, what proportion of the material is added and what proportion is replaced by the alloy material. Alloying semiconductors in this way allows the energy gap and lattice spacing of the crystal to be chosen to suit the application [107].

2.5 Energy Band Structures

Materials can be categorized into conductors, semiconductors or insulators by their ability to conduct electricity. It is a common belief that insulators do not conduct electricity, conductors conduct electricity easily and semiconductors are materials having electrical conductivities between conductors and insulators. When a solid is formed the energy levels of the atoms broaden and form bands with forbidden gaps between them. The electrons have energy values that exist within one of the bands, but cannot have energies corresponding to values in the gaps between the bands. The lower energy bands due to the inner atomic levels are narrower and are full of electrons, so they do not contribute to the electronic properties of a material. The outer or valence electrons that bond the crystals together are called valence band. An insulator is a material in which the highest occupied band, the valence band, is full of electrons that cannot move since they are fixed in position in chemical bonds. There are no delocalized electrons to carry current; hence the material is an insulator. The next available band, the conduction band, is far above the valence band in energy, usually greater than 3 eV, so it is not thermally accessible, and remains essentially empty. In other words, the heat content of the insulating material at room temperature $T=300\text{ K}$ is not sufficient to raise an appreciable number of electrons from the valence band to the conduction band; hence the number in the conduction band is negligible [108]. The distinction between semiconductors and insulators is a

matter of convention. One approach is to consider semiconductors a type of insulator with a low band gap. Conversely, a metal is highly conductive material. Metals are solids in which the conduction band is only partly filled. The conduction band consists then of many electrons and many empty states. A large current can be supported within a metal since most of the electrons within the conduction band can contribute to the current conduction since there exist many vacancies into which the electrons can move under the action of a driving field. Consequently, metals have a very high electrical conductivity. The conductivity of semiconductors is more complicated than that of metals because, besides the electron scattering processes being temperature dependent as in a metal, the actual number of current carriers N and their energy distribution also varies with temperature. The resistivity of a material is a measure of how difficult it is for a current flow. Semiconductors have a resistivity between $10^{-4} < \rho < 10^{-8} \Omega\text{m}$.

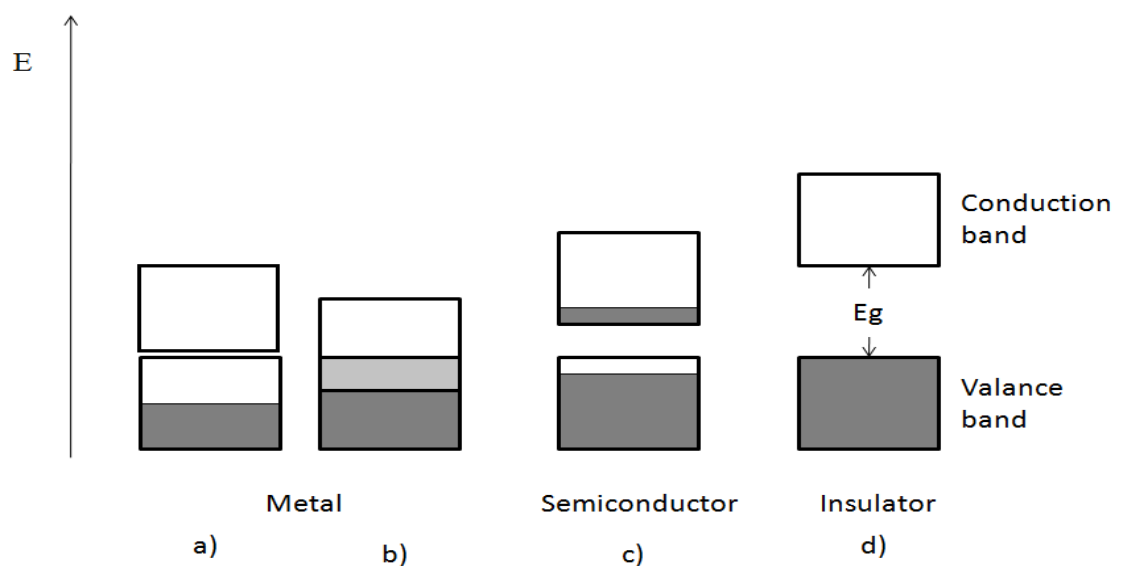


Figure 2.5. Possible energy band diagrams of a crystal: a) a half filled band, b) two overlapping bands, c) an almost full band separated by a small band gap from an almost empty band and d) a full band and an empty band separated by a large band gap

A half-filled band is shown in Figure 2.5 a. This situation occurs in materials consisting of atoms, which contain only one valence electron per atom. Most highly

conducting metals including copper, gold and silver satisfy this condition. Two overlapping bands are shown in Figure 2.5 b. Materials consisting of atoms that contain two valence electrons can still be highly conducting if the resulting filled band overlaps with an empty band. No conduction is expected for Figure 2.5 d, where a completely filled band is separated from the next higher empty band by a larger energy gap. Such materials behave as insulators. Finally, Figure 2.5 c, shows the situation in a semiconductor. The completely filled band is now close enough to the next higher empty band that electrons can jump to the next higher band. This yields an almost full band below an almost empty band.

2.5.1 Direct and Indirect Band gap

The band gap represents the minimum energy difference between the top of the valence band and the bottom of the conduction band. However, the top of the valence band and the bottom of the conduction band are not generally at the same value of the electron momentum. In a typical quantitative calculation of band structures, the wave function of a single electron traveling through a perfectly periodic lattice is assumed to be in the form of a plane wave moving in the x -direction with propagation constant k , also called a wave vector. A direct band gap means that the minima of the conduction band and the maxima of the valence band occur at the same value of k therefore an electron making the smallest energy transition from the conduction band to the valence band can do so without a change in k (and, the momentum). The energy of the recombination across the band gap will be emitted in the form of a photon of light. This is radiative recombination, also called spontaneous emission. In an indirect band gap semiconductor: the minima of the conduction band and the maxima of the valence band occur for different values of k , thus, the smallest energy transition for an electron requires a change in momentum, so a direct transition across the band gap does not conserve momentum and is forbidden (Fig.2.6).

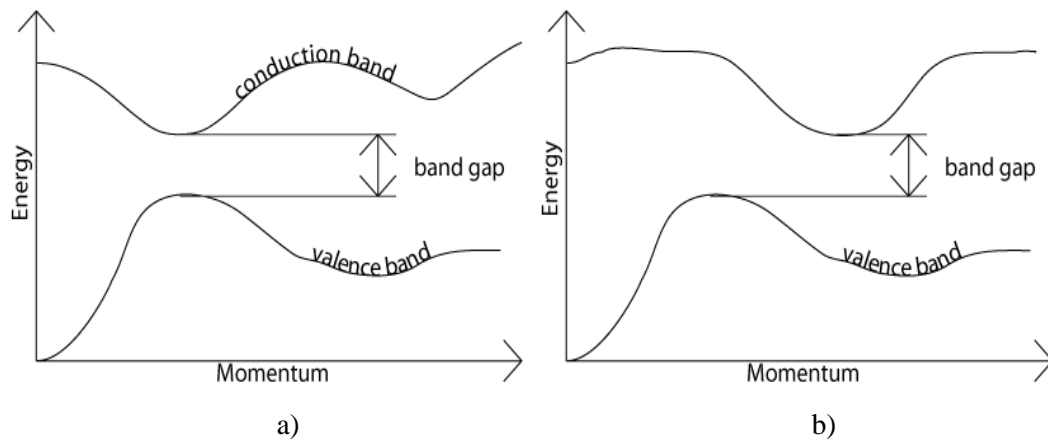


Figure 2.6 a) The scheme of the direct band gap, b) The scheme of indirect band gap

Recombination occurs with the mediation of a third body, such as a phonon or a crystallographic defect, which allows for conservation of momentum. This recombination will often release the band gap energy as phonons, instead of photons, and thus do not emit light. As such, light emission from indirect semiconductors is very inefficient and weak. The absorption of an indirect band gap material usually depends more on temperature than that of a direct material, because at low temperatures (e.g. 4K) phonons are not available for a combined process. In some materials with an indirect gap the value of the gap is negative, i.e. the top of the valence band is higher than the bottom of the conduction band in energy. Such materials are known as semimetals.

2.6 Intrinsic and Extrinsic Semiconductor

Semiconductors can be also divided into two groups according to their purity: intrinsic and extrinsic semiconductor. The pure (intrinsic) semiconductor mentioned earlier is basically neutral. In an intrinsic semiconductor, the charge carriers are solely the holes and electrons created in pairs by thermal energy. Electrons in the valence band gain thermal energy and are promoted into the conduction band as temperature increases, leaving behind corresponding holes in the valence band. As such, there is a one-to-one correspondence between the electrons in the conduction band and the holes in the valence band in an intrinsic semiconductor [109]. This is

why in an intrinsic semiconductor, $n=p$, where n and p are the intrinsic concentrations of the electrons and holes, respectively. Even with the application of thermal energy, only a few covalent bonds are broken, yielding a relatively small current flow. A much more efficient method of increasing current flow in semiconductors is by adding very small amounts of selected additives to them, generally no more than a few parts per million. These additives are called impurities and the process of adding them to crystals is referred to as doping. The purpose of semiconductor doping is to increase the number of free charges that can be moved by an external applied voltage. Electrical properties can also be changed by doping (adding impurities to the semiconductor material). The conductivity of semiconductors can be drastically increased by the controlled addition of impurities to the intrinsic semiconductor material. The mobility of both electrons and holes decreases linearly with an increase in temperature, but the number of mobile charge carriers increases exponentially with an increase in temperature. With increasing temperature, the exponential increase in the number of carriers is a more dominating factor than the linear decrease in carrier mobility, so the conductivity of an intrinsic semiconductor always increases as temperature increases. More specifically, the plot of $\ln \sigma$ of an intrinsic semiconductor versus $1/T$ is a straight line whose slope is $-E_g/2k$.

The doping process increases the number of carriers (electrons or holes) and thus increasing the conductivity of the semiconductor. Furthermore, the conductivity behavior of an extrinsic semiconductor depends on the type of impurity atoms that it has been doped with.

Energy bands develop to comply with Pauli's Exclusion Principle, such that the electrons in the solid's atoms can only occupy discrete energy levels within the permissible energy bands. If an impurity atom is introduced into a solid, however, its electrons will not be restricted to the energy levels allowed for the host atoms. The electrons of the impurity atom can, in fact, reside in energy levels forbidden to the electrons of the host atoms. In effect, adding impurity atoms to an intrinsic semiconductor to form an extrinsic semiconductor basically creates new energy levels within the band gap of the semiconductor [110]. Depending on the type of impurities added, these new energy levels in the band gap can be occupied by extra

electrons or extra holes from the impurity atoms. There are two types of dopants, n-type dopants and p-type dopants. N-type dopants are called donors while p-type dopants are called acceptors.

2.7 Defects in Solids

The picture of a perfect crystal structure repeating a particular geometric pattern of atoms without interruption or mistake is somewhat exaggerated. Although there are materials that have virtually perfect crystallographic structures extending over macroscopic dimensions, however, real crystals are not perfect. They always have imperfections such as extra/missing atoms or impurities, which are called defects. In thin crystalline films the presence of defects not only serves to disrupt the geometric regularity of the lattice on a microscopic level, it also significantly influences many film properties, such as chemical reactivity, electrical conduction, and mechanical behavior. There are three basic classes of defects in crystals:

- A point defect is a defect that occurs at a specific lattice point. There are many types of point defects such as *lattice vacancies*, *substitutional and interstitial impurities*, *self-interstitials*. The existence of point defects is thermodynamically predictable, and they influence the electronic properties of the crystal. There is *strain* in the crystal in the immediate vicinity of the point defect. This particularly can affect the electrical properties of the crystal.
- Line defects are defects that extend through the crystal along a one-dimensional boundary, such as a line or a curve. These defects, called *dislocations*, are created when planes of atoms are out of place. The crystal is divided in two by line defects, such that on each side of the defect the lattice planes are lined up perfectly, but the two sides are offset from each other. Thus it appears that there is an extra plane of atoms on one side. There are two types of dislocations: edge dislocations and screw dislocations. Edge dislocations can be thought of as an extra plane of atoms above or below the dislocation line. A screw dislocation winds through the dislocation like the thread of a screw.

- Planar (interfacial) defects occur wherever the crystalline structure of the material is not continuous across a plane. Some examples are *surfaces*, *grain boundaries*, and *interfaces* between different layers of materials [111].

2.7.1 Grains and Grain Boundaries

Most metallic materials are polycrystalline. Although the material has the same composition and structure on either side of a crystal boundary, the crystalline structure does not match up perfectly with the crystalline structure in a neighboring area. Each separate crystalline area is called a grain, and the boundaries between two small grains or crystals having different crystallographic orientations in polycrystalline materials are called grain boundaries [104].

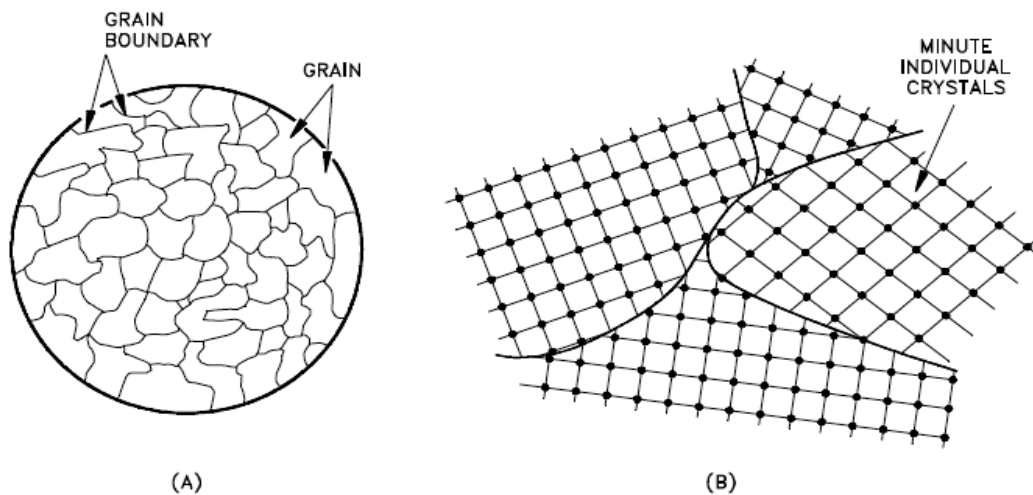


Figure 2.7 Grains and Grain Boundaries a) Microscopic b) Atomic

Grain boundaries are important in several ways. They present paths for atoms to diffuse into the material and scatter light passing through transparent materials to make them opaque. They also affect mechanical properties. The boundaries limit the lengths and motions of dislocations that can move. This means that smaller grains strengthens materials.

2.8 Optical Properties of Semiconductors

By “optical property” is meant a material’s response to exposure to electromagnetic radiation and, in particular, to visible light. The visible light wave consists of a continuous range of wavelengths or frequencies. When a light wave with a single frequency strikes an object, a number of things could happen. The light wave could be absorbed by the object, in which case its energy is converted to heat. The light wave could be reflected by the object. And the light wave could be transmitted by the object. Rarely however does just a single frequency of light strikes an object. While it does happen, it is more usual that visible light of many frequencies or even all frequencies are incident towards the surface of objects. When this occurs, objects have a tendency to selectively absorb, reflect or transmit light certain frequencies. The manner in which visible light interacts with an object is dependent upon the frequency of the light and the nature of the atoms of the object.

Transparent materials appear colored as a consequence of specific wavelength ranges of light that are selectively absorbed; the color discerned is a result of the combination of wavelengths that are transmitted. If absorption is uniform for all visible wavelengths, the material appears colorless; examples include high-purity inorganic glasses and high-purity and single-crystal diamonds and sapphire. For example, cadmium sulfide (CdS) has a band gap of about 2.4 eV; hence, it absorbs photons having energies greater than about 2.4 eV, which correspond to the blue and violet portions of the visible spectrum; some of this energy is reradiated as light having other wavelengths. Non-absorbed visible light consists of photons having energies between about 1.8 and 2.4 eV. Cadmium sulfide takes on a yellow-orange color because of the composition of the transmitted beam [112].

Optical properties of films are also important for band gap calculations. Band gaps and wavelengths of some common semiconductors relative to the optical spectrum is shown in Figure 2.8. Reflection or absorption spectra provide rich information on the energy levels of the material, such as inner or valence electrons, vibrations or rotations of molecules or defects in condensed matters, a variety of energy gaps and elementary excitations, e.g. phonons and excitons [113].

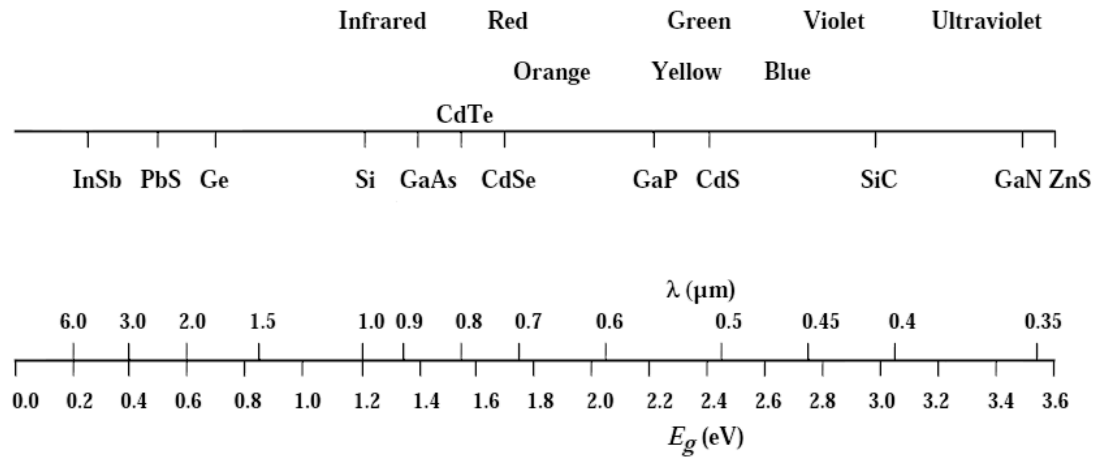


Figure 2.8 Semiconductors band gaps and wavelengths

Absorption of a photon of light can occur by the promotion or excitation of an electron from the nearly filled valence band, across the band gap, and into an empty state within the conduction band and a free electron in the conduction band and a hole in the valence band are created. These excitations with the accompanying absorption can take place only if the energy of the photons is larger than the band gap, i.e. $E_{\text{ph}} \geq E_g$. In other words: the wavelength of the light must be smaller than the wavelength. Each photon carries a certain amount of energy which is proportional to the frequency, ν , of the electromagnetic wave and is given by

$$E_{\text{ph}} = h\nu = hc/\lambda \quad (2.4)$$

where h is Planck's constant, c is the velocity of light and λ is the wavelength.

If a beam of photons with $h\nu > E_g$ falls on a semiconductor, there will be some predictable amount of absorption, determined by the properties of the material. It would be expected that the ratio of transmitted to incident light intensity depend on the photon wavelength and the thickness of the sample.

$$I(x) = I_0 e^{-\alpha x} \quad (2.5)$$

where I_0 is the intensity of the non-reflected incident radiation and α the *absorption coefficient* (in mm^{-1}), is characteristic of the particular material; furthermore, α varies

with wavelength of the incident radiation. The distance parameter t is measured from the incident surface into the material. Materials that have large α values are considered to be highly absorptive. To calculate this dependence, let us assume that a photon beam of intensity I_0 (photons/cm²-sec) is directed at a sample of thickness t (Fig.2.9).

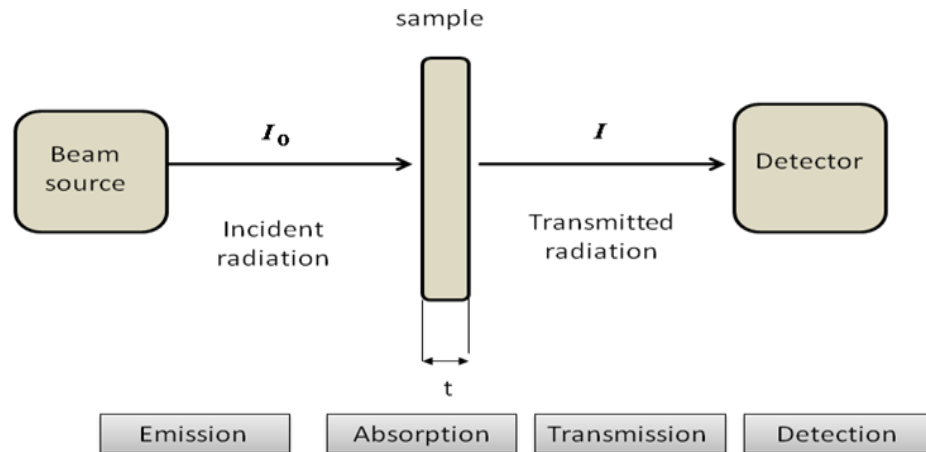


Figure 2.9 Optical Absorption Experiment

2.9 Electrical Properties of Semiconductors

Consideration of the electrical properties of materials is often important when materials selection and processing decisions are being made during the design of a component or structure. Sometimes, electrical conductivity σ is used to specify the electrical character of a material. Solid materials exhibit an amazing range of electrical conductivities, extending over 27 orders of magnitude as depicted in Figure 2.10; probably no other physical property experiences this breadth of variation [112]. In fact, one way of classifying solid materials is according to the ease with which they conduct an electric current; within this classification scheme there are three groupings: *conductors*, *semiconductors*, and *insulators*. Metals are good conductors, typically having conductivities on the order of 10^7 (Ωm)⁻¹. At the other extreme are materials with very low conductivities, ranging between 10^{-10} and 10^{-20} (Ωm)⁻¹; these are electrical insulators. Materials with intermediate conductivities, generally from 10^{-6} to 10^4 (Ωm)⁻¹, are termed semiconductors.

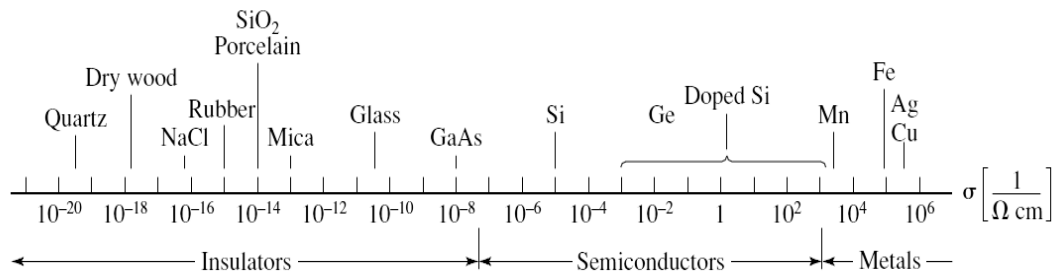


Figure 2.10 Room-temperature conductivity of various materials

One of the principal characteristics of materials is their ability (or lack of ability) to conduct electrical current. According to their conductivity σ they are divided into conductors, semiconductors, and insulators (dielectrics). The inverse of the conductivity is called resistivity ρ that is $\rho = 1/\sigma$. The resistance R of a piece of conducting material is proportional to its resistivity and to its length L and is inversely proportional to its cross-sectional area A .

Semiconductors or insulators which have only a small number of free electrons (or often none at all) display only very small conductivities. The small number of electrons results from the strong binding forces between electrons and atoms that are common for insulators and semiconductors. Conversely, metals which contain a large number of free electrons have a large conductivity. In all conductors, semiconductors, and many insulating materials, only electronic conduction exists, and the magnitude of the electrical conductivity is strongly dependent on the number of electrons available to participate in the conduction process. However, not all electrons in every atom will accelerate in the presence of an electric field [113]. The number of electrons available for electrical conduction in a particular material is related to the arrangement of electron states or levels with respect to energy, and then the manner in which these states are occupied by electrons. The electrical properties of a solid material are a consequence of its electron band structure, that is, the arrangement of the outermost electron bands and the way in which they are filled with electrons.

2.10 Mechanical Properties of Semiconductors

The mechanical behavior of a material reflects the relationship between its response or deformation to an applied load or force. If the load is static or changes relatively slowly with time and is applied uniformly over a cross section or surface of a member, the mechanical behavior may be ascertained by a simple stress–strain test [112]. Stress is the internal resistance, or counterforce, of a material to the distorting effects of an external force or load. These counterforces tend to return the atoms to their normal positions. The total resistance developed is equal to the external load. This resistance is known as stress. Strains are determined by the relative displacements of points within a body that has been subjected to external forces. The degree to which a structure deforms or strains depends on the magnitude of an imposed stress. In other words, Stress gives the intensity of the mechanical forces that pass through the body, whereas strain gives the relative displacement of points within the body.

Mechanical stress or strain is one of the complex parameter in semiconductors and the researchers at national Institute of Standards and Technology are able to measure the low levels of stress and strain as small as 10 nanometer distance between the two layers. This measurement will lead to many new developments in the area of new generation integrated circuits.

Although stress and strain is not always harmful, however the stress in light-emitting diodes (LEDs) and lasers can change the output colors as well as the stress can lower the life of the device. Similarly stress in microelectromechanical system can cause buckling and fracture and can also reduce the lifespan of the device.

Researchers deliberately increase the good stress as it plays an important role in the efficiency of the output of transistors by increasing the speed of the transistor without affecting its other properties, however device engineers feel that both good and bad stresses needs to be measured. With the advancement of microelectronics applications, the devices are becoming smaller and measuring stress is one of the most difficult tasks.

2.11 Thermoluminescence Properties of Semiconductors

Thermoluminescence is the emission of light from an insulator or semiconductor when it is heated. This is not to be confused with the light spontaneously emitted from a substance when it is heated to incandescence. Thermoluminescence is the thermally stimulated emission of light following the previous absorption of energy from radiation [114].

Thermoluminescence method is a relatively complex process since it involves a trap and a luminescence center. When an insulator or semiconductor is exposed to ionization radiation at room or at low temperature, electrons are released from the valance band to the conduction band. This leaves a hole in the valance band. Both types of carriers become mobile in their respective bands until they recombine or until they are trapped in lattice imperfections in the crystalline solids. These lattice imperfections play very important rule in thermoluminescence process. The trapped electrons may remain for a long period when the crystals are stored at room temperature. They can be released due to the sufficient energy given to the electron when the crystal is heated. These electrons may move in the crystalline solid until they recombine with the emission of thermoluminescence light.

In this statement can be found that the three essential ingredients are necessary for the production of thermoluminescence. Firstly, the material must be an insulator or a semiconductor -metals do not exhibit luminescent properties. Secondly, the material must have at some time absorbed energy during exposure to radiation. Thirdly, the luminescence emission is triggered by heating the material. In addition, there is one important property of thermoluminescence which cannot be inferred from this statement as it stands at present. It is a particular characteristic of thermoluminescence that, once heated to excite the light emission, the material cannot be made to emit thermoluminescence again by simply cooling the specimen and reheating. In order to re-exposed to radiation, whereupon raising the temperature will once again produce light emission [114].

CHAPTER THREE

EXPERIMENTAL STUDIES

3.1 Introduction

Thin film technology is the basis of developments in solid state electronics. Semiconducting photovoltaic cells convert solar radiation to electric power. The physical mechanisms and the solar cell design which maximizes the power output are well understood. So, in recent years there has been considerable interest in thin film semiconductors for use in solar cell devices and thin film transistors at panel displays [115-117]. CdS and ZnS are belonging to the II-VI group, and more promising materials. They are very important semiconducting compounds which are widely used in different fields due to their optical and electronic properties. The films of $Cd_{1-x}Zn_xS$ have extensive applications in various optical, electrical and optoelectronic devices [118]. Many authors have studied the optical properties of $Cd_{1-x}Zn_xS/Cd_xZn_{1-x}S$ thin films [119-120]. These thin films were obtained from various deposition techniques such as electrodeposition [31], chemical bath deposition [121,122], SILAR deposition [123], and spray pyrolysis [99]. Among various deposition techniques, spray pyrolysis and chemical bath deposition techniques were used during this study. In this chapter the information about these two methods, substrate preparation, measurement techniques and the deposited films is provided.

3.2 Thin Film Production Methods

The spray pyrolysis involves the spraying of a fine mist of very small droplets containing reactants onto hot substrate. This is also an attractive technique to grow semiconducting films because it is simple, inexpensive, and capable of depositing

uniform layers and it usually results in good mixing of materials to form alloys. This deposition method yields to control a lot of spray parameters such as substrate temperature, deposition time and the solution spray rate. The Chemical bath deposition (CBD) has been recognized as an important route for the manufacture of these materials, since it is a fast, simple and low cost method that enables to obtain good quality films that can compete with films obtained by other more sophisticated methods. Currently, there are many semiconductor materials that can be deposited by CBD films. CBD is a process rather complex due to the series of chemical reactions, precipitation phenomena and surface chemistry in the reaction system. The reaction solution for the synthesis of thin films, where the substrates will be immersed, is prepared by mixing aqueous solutions of the precursors.

3.2.1 Spray Pyrolysis Method

The spray pyrolysis is a method of spraying a suitable solution mixture onto a heated substrate, where the constituents react to form a chemical compound. The chemical reactants are selected such that the products other than the desired compound are volatile at the temperature of deposition.

In this study, the apparatus which is used for the development of film samples based on the spraying pyrolysis technique has been designed and developed in our laboratory. A schematic block diagram of an experimental apparatus used for spray pyrolysis is shown in Fig. 3.1. This system consists of a spraying system, heater, temperature control system, and timer. The system is enclosed by a glass chamber. **Spraying system:** It is used to produce the bubbles from the spraying solution. The bubbles can be in different sizes depending on the geometry of the nozzle, as seen in Fig. 3.1. In this study, air is used as carrier gas and the flow rate of the spraying solution is regulated by air.

Heater: It is used to heat the substrates. It is consisted of a steel plate with a resistance coil lying under it. The power of the heater is 2500 watts and it operates at 220 volts and 50 Hz (AC).

Temperature control system: A thermostat is used to keep the substrates at required temperatures. One of the most important factors which play a vital role for producing high quality film samples is to keep the substrates at required temperatures. The substrate temperature is controlled to within an accuracy of $\pm 5^{\circ}\text{C}$ by thermostat system.

Glass chamber: The spraying system and the heater are placed in a glass chamber and nitrogen gas is passed through during the growth of the thin film.

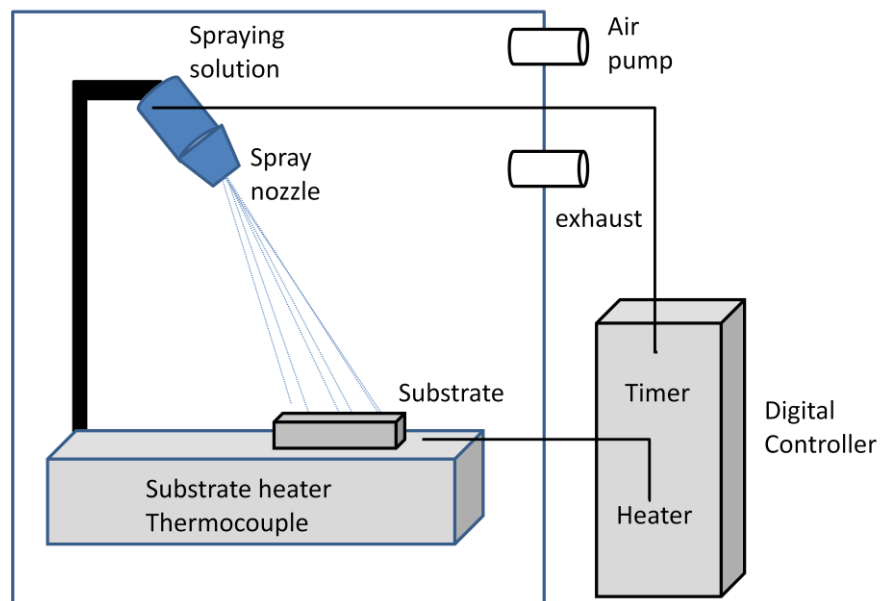


Figure 3.1 Schematic diagram of the spray pyrolysis system

3.2.2 Chemical Bath Deposition

When it is stated that CBD is a simple and low cost method, this essentially refers to the fact that it does not require high purity raw materials and the equipment where the synthesis of the films takes place is very simple. For example, the reactor can be a glass beaker and the substrates can be any shape, size or material, provided the latter is insoluble in water, because the deposition process takes place in an aqueous solution. The reaction occurs in the range of temperature from 10 to 90 $^{\circ}\text{C}$.

Nevertheless, the deposition of thin films by CBD is a process rather complex due to the series of chemical reactions, precipitation phenomena and surface chemistry in the reaction system [124]. In this study, the apparatus which is used for the development of film samples based on the chemical bath deposition method include a digital pH-meter, heat controlled magnetic stirrer, beaker, substrate, chemical agents and also pure water. The heat controlled magnetic stirrer provides heating the chemical bath solution and stirring it at any suitable speed. It operates between 0 to 750 rpm. The heat controlled magnetic stirrer includes a thermocouple which is used to keep the chemical bath solution at required temperatures. One of the most important factors which play a vital role for producing high quality film samples is to keep the substrates at required temperatures. The substrate temperature is controlled to within an accuracy of $\pm 5^{\circ}\text{C}$ by thermostat system. The holder is used to hang the substrate immersed vertically into the chemical bath solution. A schematic diagram is shown in Figure 3.2.

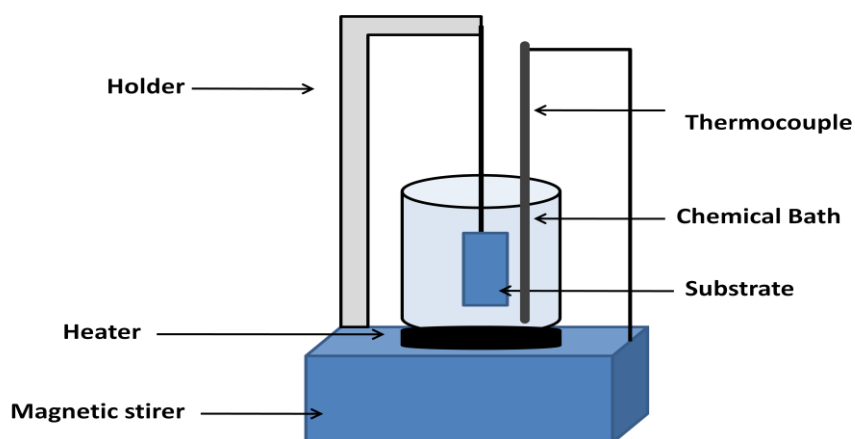


Figure 3.2 Schematic diagram of the chemical bath deposition system

3.3 Substrate Preparation

Cleanliness and preparation of substrates is essential for success in thin film work. The physical properties of substrates on which thin films is deposited, play a vital role in the growth of good quality thin film samples. The film properties are very strongly dependent on the crystal structure of substrate. Condensation rate and adhesion of the deposit are critically dependent of conditions on the surface. Even a

thin layer of grease can have such a gross effect on a molecular scale as to alter completely the characteristics of the layer. The crystalline films can be deposited on a non-crystalline material such as glass, ceramic and mica.

In this study, glass is used as substrate because of its cheapness when compared to other types of substrate. The preparation of glass substrate is as follows. Firstly, the glass substrates are cut into area of $0.5 \times 1.0 \text{ cm}^2$ in size. The following cleaning and surface preparation conditions must be followed immediately prior to application. The cleaning process with the solvent cloth can able remove any grease, oils, or dirt. The cleaning process of the glass substrate is carried out in four steps as seen in Figure 3.3.

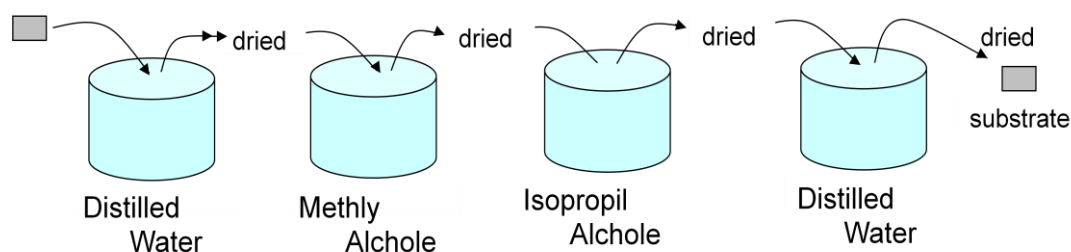


Figure 3.3 The cleaning process of the glass substrate

3.3.1 Cleaning Process of The Glass Substrate

The cleaning methods to ensure the substrate is completely clean and contaminant free included four combined steps as follows:

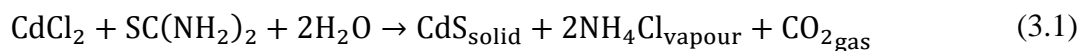
1. The glass substrate is firstly immersed into the distilled water to clean the dust on its surface for 15 minutes. Then it is taken out from the distilled water and dried.
2. The substrate which is taken from the first cup and dried, is immersed into the methyl alcohol and left there for 15 minutes to removal of the oil substance on the surface of the substrate, and then it is taken out from this liquid and dried in air.
3. The dried substrate is immersed into the third cup filled with isopropyl alcohol and it is treated again for 15 minutes to obtain a smooth surface.
4. Finally, the substrate is treated with the distilled water as in the first step to clean all the residues remaining on the surface of substrate during the other processes.

3.4 Development of Thin films by Spray Pyrolysis

In this study, the semiconducting cadmium sulphide (CdS), zinc sulphide (ZnS) and CdZnS thin films were obtained by the two methods: chemical bath deposition and spray pyrolysis under different deposition conditions.

3.4.1 Development of CdS Thin Films by Spray Pyrolysis

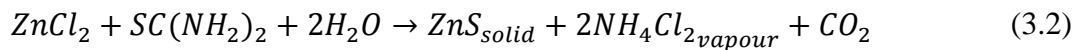
CdS films were deposited on highly clean glass substrates (about 0.5 cm² of geometric area) at substrate temperatures were kept at 250, 275 and 300 °C by using electronic temperature controller with an accuracy of ±10 °C., respectively, by using spray pyrolysis technique. The films were prepared using the aqueous solutions containing cadmium chloride (CdCl₂, Merck, purity 98%) and thiourea (SC(NH₂)₂, Merck, purity 98%). The spraying solution was prepared for the production of CdS thin film as follow; firstly, the molar ratio of Cd/S in the bath was kept as 1:1, 0.5 grams of CdCl₂ and SC(NH₂)₂ salts were weighted by high sensible electronic balance and stirred together into a cup containing the distilled water of 100 cm³ to form the solution. The atomization of the chemical solution into a spray of fine droplets is effected by the spray nozzle, with the help of compressed air by the air pump as carrier gas. The spray flow rate was adjusted to about 0.5 ml. per minute and the height of the nozzle was fixed to 20 cm form the substrate surface placed on the heater. During the spraying process the substrates were heated by an electrical heater. When the solution droplets reach to the heated glass substrate surface, following chemical reactions occurs,



As seen from this reaction, a CdS thin film is formed on the substrate surface while the NH₄Cl and CO₂ gases leave the system.

3.4.2 Development of ZnS Thin Films by Spray Pyrolysis

The same process followed for the production of CdS thin films is repeated for developing the ZnS thin film samples. ZnS films were deposited on highly clean glass substrates (about 0.5 cm² of geometric area) at substrate temperatures were kept at 450, 500 and 550 °C by using electronic temperature controller with an accuracy of ±10 °C., respectively. The films were prepared using the aqueous solutions containing zinc chloride (ZnCl₂, Merck, purity 98%) and thiourea (SC(NH₂)₂, Merck, purity 98%). The spraying solution was prepared for the production of CdS thin film as follow; firstly, the molar ratio of Zn/S in the bath was kept as 1:1 and 0.5 grams of ZnCl₂ and SC(NH₂)₂ salts were weighted by high sensible electronic balance and stirred together into a cup containing the distilled water of 100 cm³ to form the solution. The atomization of the chemical solution into a spray of fine droplets is effected by the spray nozzle, with the help of compressed air by the air pump as carrier gas. The spray flow rate was adjusted to about 0.5 ml. per minute and the height of the nozzle was fixed to 20 cm from the substrate surface placed on the heater. During the spraying process the substrates were heated by an electrical heater. When the solution droplets reach to the heated glass substrate surface, following chemical reactions occurs,



As seen from this reaction, a ZnS thin film is formed on the substrate surface while the NH₄Cl and CO₂ gases leave the system.

3.4.3 Development of Cd_xZn_{1-x}S Thin Films by Spray Pyrolysis

Cd_xZn_{1-x}S films were obtained by using spray pyrolysis method on the glass substrates at different temperatures of 350 °C, 400 °C and 450 °C. Cd_xZn_{1-x}S films were grown by using spray pyrolysis method on the glass substrates at different temperatures. Cd_xZn_{1-x}S films were produced with different Cd concentrations (for

x = 0, 0.2, 0.4, 0.6, 0.8 and 1.0) and different substrate temperatures. The initial solution were produced from cadmium chloride (CdCl_2), zinc chloride (ZnCl_2) and thiourea ($\text{CS}(\text{NH})_2$) as Cd, Zn and S sources, respectively. The substrate temperature was maintained at predetermined temperature using Eurotherm temperature controller with an accuracy of ± 5 °C. Chromel–Alumel thermocouple placed on glass substrate surface was used as a temperature sensor for the controller. The solution and carrier gas flow rates were $5 \text{ cm}^3 \text{ min}^{-1}$ and $5 \text{ dm}^3 \text{ min}^{-1}$, in all cases. The substrate to nozzle distance was maintained at 20 cm. The spray head was moved in the X–Y plane using a microprocessor controlled stepper motor system in order to get uniform films on the substrate. The precursor solution was sprayed onto the substrates at an interval of 1–1.5 min i.e., the spray process lasts for 3 s and was paused for 1–2 min, in order to overcome cooling effect caused by the mist of the precursor. After completion of the deposition process, the films were allowed to cool slowly to room temperature. Consistent conditions of flow rate of carrier gas were maintained during deposition of such films.

3.5 Development of Thin Films by Chemical Bath Deposition

Chemical bath deposition (CBD) has been recognized as an important route for the manufacture of thin films, since it is a fast, simple and low cost method that enables to obtain good quality binary, ternary and quaternary semiconducting films. Currently, there are many semiconductor materials that can be deposited by CBD films. CBD is a process rather complex due to the series of chemical reactions, precipitation phenomena and surface chemistry in the reaction system. In this study, the polycrystalline ZnS, CdS and $\text{Cd}_x\text{Zn}_{1-x}\text{S}$ films onto glass substrates are carried out from a chemical bath technique.

3.5.1 Development of CdS Thin Films by Chemical Bath Deposition

The CBD CdS films were deposited using the aqueous solution of CdCl_2 , NH_4Cl buffer, ammonia and thiocarbamide (thiourea) at low concentrations of cadmium salt

(0.003 M) and pH-9. The molar ratio of Cd/S in the bath was kept as 1:1. The glass substrates were vertically immersed into the chemical bath solution with the temperatures of 70, 75 and 80 °C, respectively. After growing for 90 minute, the film was ultrasonically cleaned in deionized water to remove any loosely adhered particles.

3.5.2 Development of ZnS Thin Films by Chemical Bath Deposition

The polycrystalline ZnS films onto glass substrates are carried out from a chemical bath technique. The deposition of zinc sulphide films by CBD technique in zinc chloride–ammonia–thiourea system consists of complexation of the zinc cations by the ammonia and the consecutive reaction with the sulphide ions provided by the hydrolysis of thiourea. The chemical bath solution was constituted of: 1,0 g of zinc chloride $ZnCl_2$, 1.0 g of thiourea $(CS(NH_2)_2)$, 10 ml of 30% ammonia solution (NH_4OH) , and 5.0 ml of hydrazine hydrate (N_2H_4) . The deposition is carried out in a 50 ml beaker at different bath temperatures of 70, 75 and 80 °C and for a deposition time of 1,5 h. The bath pH was optimised between $9 \pm 0,5$ by the addition of ammonia solution. After the deposition, the samples are taken out from the bath, washed in distilled water and dried at 80 °C for 15 min in a hot air oven.

3.5.3 Development of $Cd_xZn_{1-x}S$ Thin Films by Chemical Bath Deposition

The chemical bath deposition of ZnS onto glass substrates are carried out from a chemical bath technique. The deposition of zinc sulphide films by CBD technique in zinc chloride–ammonia–thiourea system consists of complexation of the zinc cations by the ammonia and the consecutive reaction with the sulphide ions provided by the hydrolysis of thiourea. The chemical bath solution was constituted of: 1.0.g of zinc chloride $ZnCl_2$, 1.0 g of thiourea $(CS(NH_2)_2)$, 10 ml of 30% ammonia solution (NH_4OH) , and 5.0 ml of hydrazine hydrate (N_2H_4) . The deposition is carried out in a 50 ml beaker at different bath temperatures of 70, 75 and 80 °C and for a deposition time of 1.5 h. The bath pH was optimized between 9 ± 0.5 by the addition of ammonia solution. And the Cd dopant is added to chemical bath solution in the form

of CdCl₂, yielding Cd concentration of about 5, 10, 15 and 20 mol% relative to Zn. The mixture was poured into a beaker and heated to 70, 75 and 80 °C with the same bath pH. After the deposition, the samples are taken out from the bath, washed in distilled water and dried at 80 °C for 15 min in a hot air oven.

3.6 Measurements Techniques

Structural properties of the deposited films were studied by X-ray diffraction (XRD) technique and SEM analysis. The optical properties of the films were investigated from optical absorption coefficient and transmittance spectra data using double beam visible spectrophotometer. By using these data the band gap energies of the deposited films were determined. The electrical resistivity of the films was measured with Van der Pauw method measurement system. The carrier density was determined by Hall effect measurements. For the thermoluminescence measurements the glow curves of the deposited films were measured by using a thermoluminescence dosimetry (TLD) reader that is interfaced to a PC where all glow curves were analyzed.

3.6.1 The Structural Properties Measurements

X-ray diffraction provides to find the geometry or shape of a molecule using X-rays. X-ray diffraction techniques are based on the elastic scattering of X-rays from structures that have long range order. Thin film diffraction and grazing incidence X-ray diffraction may be used to characterize the crystallographic structure and preferred orientation of substrate-anchored thin films. High-resolution X-ray diffraction is used to characterize thickness, crystallographic structure, and strain in thin films. The X-ray measurements were carried out by X-ray diffraction (XRD) technique on Braker AXS D5005 diffractometer (monochromatic CuK α radiation, $\lambda=1.54056$ A). The XRD patterns were recorded in 2θ interval from 20° up to 35° with the step 0.05°. The peaks (2θ) of the XRD patterns of the film samples were identified by using Bragg diffraction law equation (eq. 3.4) as given below. The Bragg equation establishes a relationship between the diffraction experiment and the

structural parameters. The measured value is the Bragg angle θ and the structural parameter is the lattice spacing d_{hkl} .

$$n\lambda = 2d \sin \theta \quad (3.4)$$

The planes are characterized by their (hkl) values and the d_{hkl} interplanar spacings. The d_{hkl} values are a geometric function of the size and shape of the unit cell. The relationship between d_{hkl} and the real unit cell is usually stated in a different form for each crystal system.

The lattice constant 'a' for the cubic phase structure is determined by the relation

$$a^2 = \frac{\lambda^2 (h^2 + k^2 + l^2)}{4 \sin^2 \theta} \quad (3.5)$$

where θ is the diffraction spectra (Bragg's angle), λ is the wavelength of the X-ray. The line profiles were measured by means of point by point cutting using a fix period 20s and 2θ increment of 0.02° . From the XRD profiles, the inter-planar spacing d_{hkl} was calculated for (hkl) plane using the Bragg's relation [103]

$$d_{hkl} = \frac{n\lambda}{2 \sin \theta} \quad (3.5)$$

where λ is the wavelength of the X-ray used, d is the lattice spacing, n is the order number and θ is the Bragg's angle. The factor d is related to (h k l) indices of the planes and the dimension of the unit cells.

The crystallite size (D) of the films was calculated from the Debye Scherer's formula from the full-width at half-maximum (FWHM) β of the peaks expressed in radians [125].

$$D = \frac{0.94\lambda}{\beta \cos \theta} \quad (3.6)$$

where β is the FWHM calculated from the (dkl) plane.

The strain value (ε) can be evaluated by using the following relation

$$\varepsilon = \frac{\beta \cos \theta}{4} \quad (3.7)$$

The lattice parameter 'a' can be calculated from the equation given below for cubic geometry.

$$\frac{1}{d^2} = \frac{(h^2 + k^2 + l^2)}{a^2} \quad (3.8)$$

where h, k, l represent the lattice planes

3.6.2 The Optical Properties Measurements

An important technique used for the determination of the band gap energy of a semiconductor is the absorption of incident photons by material. Optical absorption studies of the sprayed and chemically bath deposited films on the glass substrate have been carried out in the wavelength range of 300 nm to 900 nm employing a UV/VIS spectrophotometer (Jasco 7800 model). The absorption coefficients of the great majority of elements have been studied over at least some part of the X-ray spectrum. The principle is to determine absorption coefficients simple. The attenuator is interposed between source and detector, and the reduction in intensity is measured. It will be appreciated that this reduction in intensity may be caused either by absorption of the photon within the intervening matter or by scattering out of the collimated beam. To determine the energy band gap values of the samples, it is necessary to determine the value of the absorption coefficients of the samples corresponding to different wavelengths of the photons. For this purpose, a Jasco 7800 Model Spectrometer was used for the transmission and absorption measurements.

The absorption coefficient of sample corresponding to different wavelengths can be calculated from the following equation:

$$\frac{I}{I_0}(\text{transmission}) = e^{-\alpha} \quad (3.9)$$

where t is the thickness of the film sample, $T=I/I_0$ is the transmittance (I_0 is the incident light intensity and I is the transmitted light intensity).

By using α values, the optical band gap of the film sample can be determined by means of the following equation:

$$\alpha = \frac{A}{h\nu} (h\nu - E_g)^{1/2} \quad (3.10)$$

where A is a constant, E_g is the energy band gap of film, h is the Planck constant, $\nu=c/\lambda$, c is the speed of light and λ is the wavelength of light.

3.6.3 The SEM Analysis

The SEM instrument has many applications across different industry sectors. The extremely high magnification images together with localised chemical information enable the instrument to solve a great deal of common industrial issues such as particle analysis, defect identification materials and metallurgical problems. The Scanning Electron Microscope (SEM) is a microscope that uses electrons rather than light to form an image. Electron microscopes were developed due to the limitations of Light Microscopes which are limited by the physics of light. There are many advantages to using the SEM instead of a light microscope. The scanning electron microscope is a type of electron microscope that creates various images of the sample with the necessary sample preparation, cross-sections by focusing a high energy beam of electrons onto the surface of a sample and detecting signals from the interaction of the incident electrons with the sample's surface. The types of signals collected in a SEM alter and can comprise secondary electrons, characteristic X-rays, and back scattered electrons. In a SEM, these signals come not only from the primary beam infringing on the sample, but from other interactions within the sample near the surface. The SEM is capable of producing high resolution images of a sample surface in its primary use mode, secondary electron imaging. Due to the manner in which this image is created, SEM images have great depth of field yielding a characteristic three-dimensional appearance useful for understanding the surface structure of a sample. This great depth of field and the wide range of magnifications are the most

familiar imaging mode for specimens in the SEM [126]. The SEM generates a beam of incident electrons in an electron column above the sample chamber. The electrons are produced by a thermal emission source, such as a heated tungsten filament, or by a field emission cathode. The energy of the incident electrons can be as low as 100 eV or as high as 30 keV depending on the evaluation objectives. The electrons are focused into a small beam by a series of electromagnetic lenses in the SEM column. Scanning coils near the end of the column direct and position the focused beam onto the sample surface. The electron beam is scanned in a pattern over the surface for imaging. The beam can also be focused at a single point or scanned along a line for x-ray analysis.

3.6.4 The Electrical Properties Measurements

A number of techniques have been employed to measure electrical properties of thin films. Some are adaptations of well-known methods utilized in bulk materials. For insulating films, where current flows through the film thickness, electrodes are situated on opposite film surfaces. Small evaporated or sputtered circular electrodes frequently serve as a set of equivalent contacts; the substrate is usually the other contact. For more conductive metal and semiconductor films, it is common to place all electrodes on the same film surface. Such measurements employ four terminals—two to pass current and two to sense voltage. In this study, the Van Der Pauw method was used to measure the resistivity, conductivity and Hall coefficient of the thin film samples. Van der Pauw has devised a perfectly general method to determine the resistivity of a film using four probes located arbitrarily at points A, B, C, D on the surface of the sample. The precision of such a van der Pauw measurement depends on the flatness and parallelism of the surfaces of the sample and on the fact that the contacts are point contacts. Several contact configurations are suitable for this purpose.

To apply this method, four indium ohmic contacts A, B, C, and D were prepared on the semiconducting samples by the evaporation method as seen in Figure 3.4.

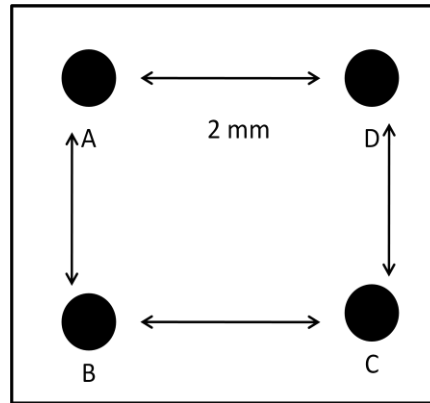


Figure 3.4 The Indium-ohmic contacts prepared on the thin film samples

3.6.4.1 The Resistivity and Conductivity Measurements

The Van der Pauw method requires two measurements for the resistivity measurement. Firstly an input potential V_{in} was applied across the contacts A and B, then the current is passed into contacts A and B and the voltage is measured at contacts C and D. $R_{AB,CD}$ denotes the ratio of the voltage V_{CD} measured between contacts C and D, to the current I_{AB} passed into contacts A and B, as seen in figure 3.5.(a). To determine the resistance $R_{BC,DA}$ at this time, the current I_{BC} is passed into contacts B and C and the voltage V_{DA} is measured at contacts D and A, as seen in figure 3.5.(b). These two voltage–current measurements together with the measurement of the thickness of the thin film allow for the determination of the conductivity.

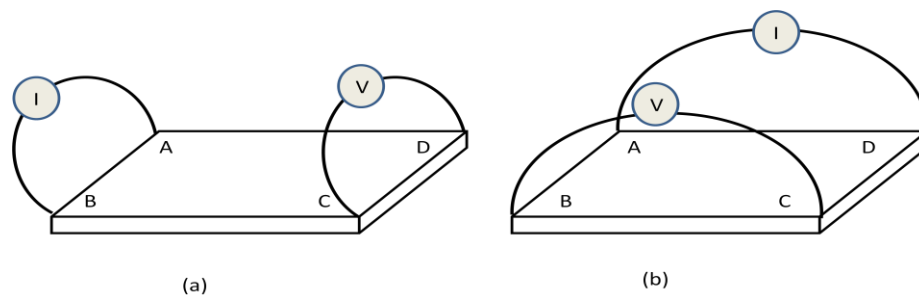


Figure 3.5 The experimental set-up of the resistivity measurement

The resistivity of sample is calculated by using the following equation:

$$\rho = \left(\frac{t}{\ln 2} \right) (R_{AB,CD} + R_{BC,DA}) F \left(\frac{R_{AB,CD}}{R_{BC,DA}} \right) \quad (3.11)$$

where t is the thickness of the thin film and F is a function. If $R_{AB,CD}$ and $R_{BC,DA}$ are nearly equal to each other, the approximate value of F can be obtained from following expression [127].

$$F = 1 - \left(\frac{R_{AB,CD} - R_{BC,DA}}{R_{AB,CD} + R_{BC,DA}} \right)^2 \left(\frac{\ln 2}{2} \right) - \left(\frac{R_{AB,CD} - R_{BC,DA}}{R_{AB,CD} + R_{BC,DA}} \right)^4 \left(\frac{(\ln 2)^2}{4} - \frac{(\ln 2)^3}{12} \right) \quad (3.12)$$

3.6.4.2 Hall Mobility Measurements

The experiment which is performed to determine the Hall Mobility is carried out into two steps. Firstly, the resistance $R_{AC,DB}$ of the sample is measured with the experimental set up as shown in Figure 3.6.a. following the procedure given in section 3.6.4.1. In the second step the same measurements were done. The sample was placed in a magnetic field perpendicular to the sample plane, Fig.3.6.b.

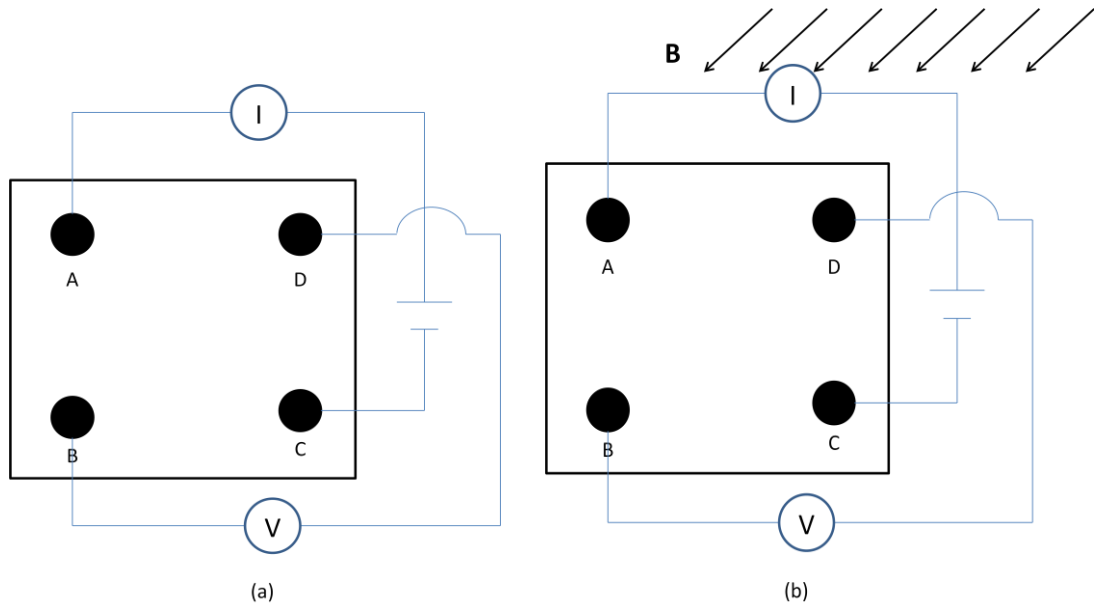


Figure 3.6 The Standard Configuration of Hall Effect Measurements

The hall mobility of the sample is calculated substituting the average values of the $R_{AC,DB}$ is taken from two different measurements, and the value of the resistivity found from equation (3.11), in the following expression,

$$\mu_H = \frac{t}{B} \frac{\Delta R_{AC,DB}}{\rho} \quad (3.13)$$

where B is the strength of the applied magnetic field and t is the thickness of the sample [127].

CHAPTER FOUR

RESULTS AND DISCUSSIONS

4.1 Introduction

In this study, the semiconducting cadmium sulphide (CdS), zinc sulphide (ZnS) and cadmium zinc sulphide ($\text{Cd}_x\text{Zn}_{1-x}\text{S}$) films were deposited by the two methods: chemical bath deposition and spray pyrolysis under different deposition conditions. The influence of the deposition parameters on the structural, electrical, optical and thermoluminescence properties of the deposited films was investigated using X-ray diffraction (XRD), Van der Pauw method, and optical transmission. In this chapter, the results of structural, optical and electrical analysis of the films are explained.

4.2 Growth CdS Films

CdS, belonging to the II-VI group is one of promising materials. CdS is a technologically useful material, as many devices based on CdS, including sensors have come up in the recent years. The thin film cadmium sulphide solar cell has been considered to be a promising alternative to the more widely used silicon devices. The deposition of CdS films has become increasingly important in recent years due to the widened industrial application with a large number of uses [128-130]. CdS is widely used as a window material in thin film solar cells. It has been used as a partner of several types of thin films solar cells, such as, Cu_2S , CuInSe_2 , and CdTe. Cadmium sulfide has been the subject of intensive research because of its intermediate band gap, high absorption coefficient, reasonable conversion efficiency, stability and low cost [131-132]. Knowledge of the optical, electrical, and structural properties of CdS films is important in many scientific, technological, and industrial applications in the field of optoelectronic devices, particularly solar cells. For solar cells applications, CdS films need to have a suitable conductivity ($>10^{16}$ carriers/cm³), and adequate thickness to

allow high transmission, low resistivity, and a semiconductor with optimum band gap [15,133]. In this part, a comparative study of the structural, electrical and optical properties of spray pyrolysis and chemical bath deposition CdS films has been made using X-ray diffraction, Van der Pauw method and optical transmission measurements.

4.2.1 Structural Studies of the CdS films

The crystal structure of CdS films obtained by CBD and spray pyrolysis were determined by X-ray diffractometry by using a Philips model X-ray diffractometer with CuK_α radiation ($\lambda=1.5405\text{\AA}$). The XRD patterns of all thin films were taken from 20° to 50° (2θ). The XRD pattern of the as-deposited sprayed and CBD-CdS thin films is shown in Fig. 4.1. CdS films exist in two crystalline modifications: the hexagonal (wurtzite) phase and cubic (zinc-blende) phase. CdS films deposited by the spray pyrolysis technique show very simple spectra, while CdS films deposited by chemical bath deposition technique show many diffraction peaks associated with both cubic and hexagonal phases. The XRD pattern of the deposited sprayed CdS film shows the presence of a strong sharp peak at $2\theta= 26.44^\circ$. This could be indexed as either (002) hexagonal or (111) cubic. It is quite difficult to conclude from the single peak appearing at $2\theta= 26.44^\circ$ in the diffraction pattern whether the film is purely hexagonal or purely cubic or a mixture of two phases as the d-spacings for (002) hexagonal and (111) cubic match well. However, Laukaitis et al. [134] and Mathew et al. [135] have been obtained a single phase of hexagonal phase of CdS thin films. Thus, the preparation methods affect the resulting of micro structural characteristics, such as crystallinity. The XRD pattern of the sprayed CdS film shows that the (002) peak height increases and peak width decreases indicating an improvement in the crystallinity of the film according to the CBD CdS film. The XRD pattern of the deposited CBD CdS film shows the presence of a strong sharp peak at $2\theta= 26,44^\circ$ and other peaks at $2\theta=24.81^\circ$ and 28.68° .

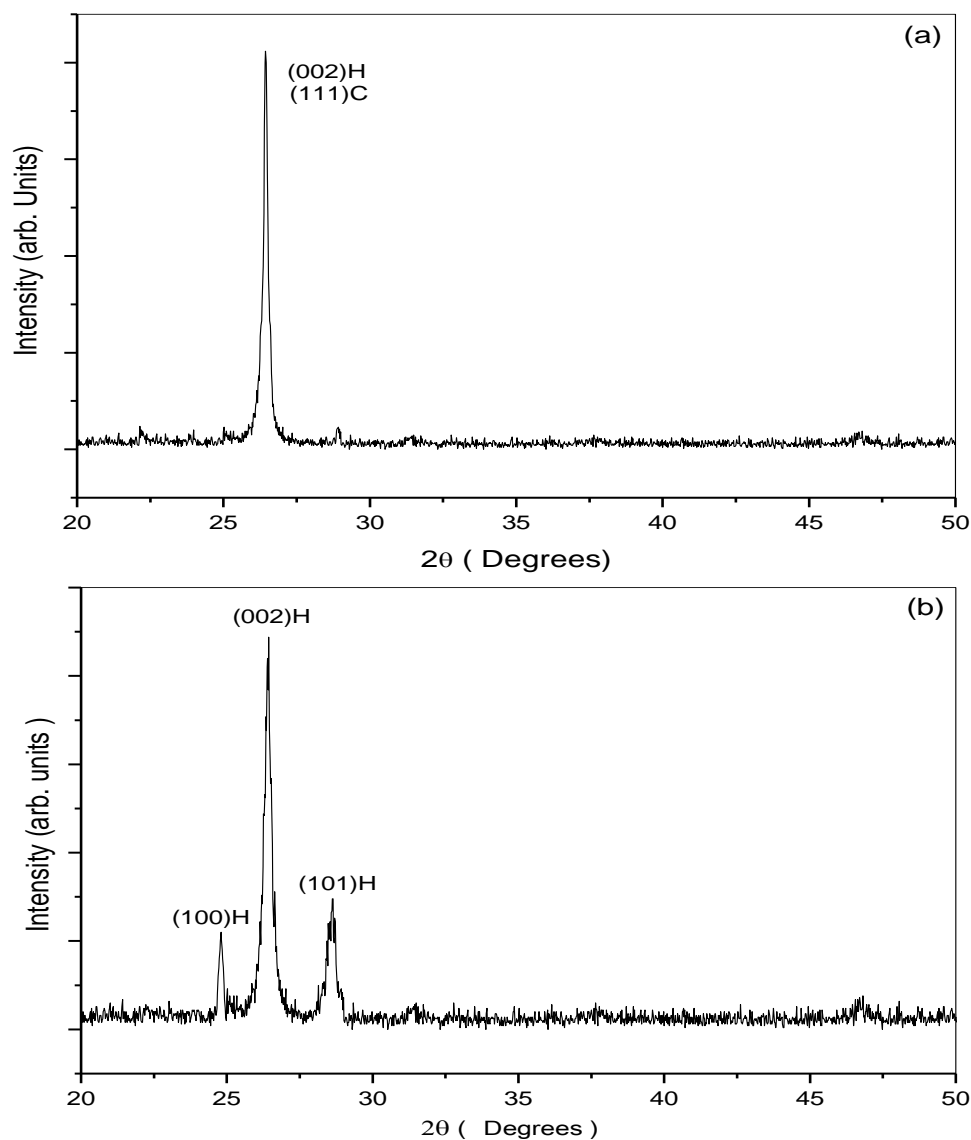


Figure 4.1 X-ray diffraction patterns of the CdS films deposited by a) spray pyrolysis, b) CBD

They are associated with the (100) and (101) reflections of the hexagonal modification CdS structure, indicating an increase in hexagonal phase is evident from the appearance of other well defined hexagonal reflections. The X-ray results were compared with the results; there are some differences in the preferred orientation of the crystallite. These differences were also attributed to the film preparation method. The XRD studies also show that the films that were deposited sprayed CdS has better crystallinity as compared to the films deposited CBD CdS films. The intensity of the (002) peak and its narrowing indicated an improvement in the degree of crystallinity of the films. Hence, it can be assumed that the substrate temperature of the sprayed

CdS films enables the atoms to move to the stable sites, which implies that thin films fabricated at these conditions are rather homogenous, and their crystalline state improves. This type of similar results was observed by Yazıcı [136] for ZnS thin films. Crystallite size of the two kinds of CdS films was calculated from the (002) reflection using the Scherer's formula neglecting peak broadening due to residual stresses in the films, $D=0.9\lambda/(\beta\cos\theta)$ where D is the size of crystallite, β is the broadening of diffraction line measured at half its maximum intensity in radians and λ is wavelength of X-rays (1.5405Å). The calculated values of crystallite size are given in Table 4.1. It is shown that the full width at the half maximum (FWHM) of the (002) reflection of the sprayed CdS films has narrower broadening than that of the CBD films. Narrow broadening reflects the decrease in the concentration of lattice imperfection due to the decrease in the internal micro strain within the film and/or increase in the crystallite size; crystallinity also increases [138]. Relatively, higher peak intensities have been observed for the sprayed CdS films. The decrease in XRD peak intensity deposited CBD-CdS films may be due to the sufficient increase in supply of thermal energy for recrystallization and the grain growth with temperature. Further decrease in crystallinity CBD-CdS films may be attributed to the non-uniformity of the films [139]. Therefore, the observed increase in the crystallite size may be interpreted in terms of a sample growth method.

4.2.2 Surface Morphology Studies of the CdS films

The surface morphology of CdS films was analyzed by using SEM. SEM images of CdS films are shown in Fig. 4.2. It is observed that the CdS film is homogenous, without cracks or pinholes and it well covers the glass substrate. CdS films grown by spray pyrolysis technique is larger-grained than films grown by CBD method. It can be seen that the crystallinity of the sprayed CdS films improves and the crystallite size become larger as compared to the CBD CdS films which is shown by XRD analysis. The average grain size of the samples is reported in Table 4.1. Therefore, there are two possibilities to improve the crystallinity of the layers: the increase in the grain size to decrease the number of grain boundaries and the decrease in the barrier height at the grain boundaries [140].

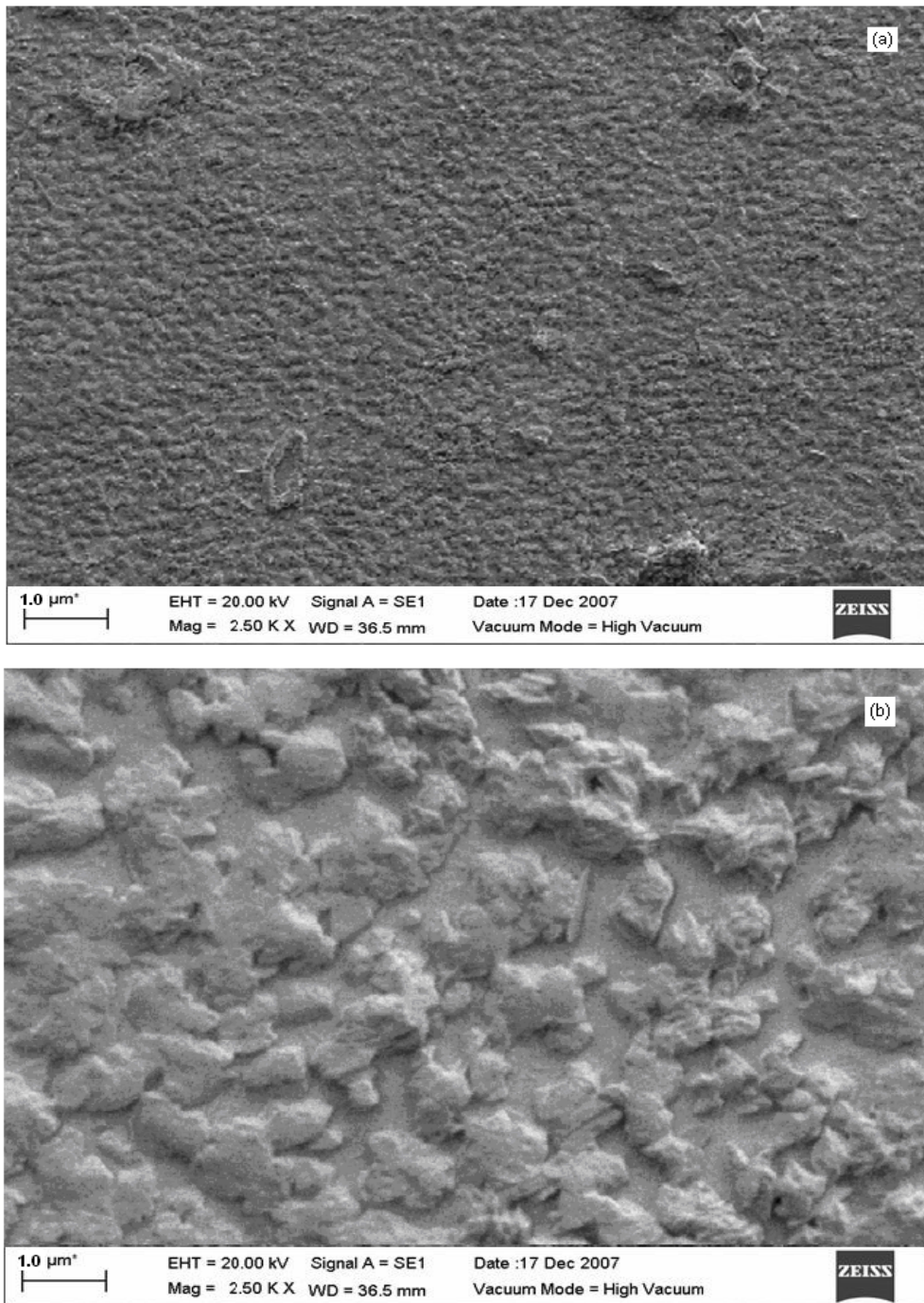


Figure 4.2 Scanning electron micrographs of the surface of CdS films prepared by a) CBD, b) spray pyrolysis

4.2.3 Optical Studies of the CdS films

The absolute transmittances of these films vary over the range 70–88% in the region 400–900 nm. This region is the transparent region of films. The variations in

transmission are due mainly to interference phenomena. The optical interferences in the transmittance can be only observed in very homogeneous films comparable to those obtained by growth techniques between the SP and CBD as shown in Table 4.1.

Table 4.1 Structural, optical and electrical properties of CdS films

Deposition methods	Substrate temperature (°C)	Grain Size (nm)	Band gap (eV)	Transmittance (%)	Carrier concentrations (cm ⁻³)	Resistivity (Ohm-cm)	Strain ϵ
Spray pyrolysis	300	177	2,42	88	5.5×10^{18}	255	4.3×10^{-3}
	275	171	2,51	80	1.2×10^{18}	775	4.9×10^{-3}
	250	163	2,60	71	7.5×10^{17}	1345	5.6×10^{-3}
Chemical bath deposition	Bath temperature (°C)	Grain Size (nm)	Band gap (eV)	Transmittance (%)	Carrier concentrations (cm ⁻³)	Resistivity (Ohm-cm)	Strain ϵ
	80	97	2,50	70	8.4×10^{16}	2575	7.7×10^{-3}
	75	91	2,58	65	2.5×10^{16}	2895	8.2×10^{-3}
	70	85	2,65	61	7.5×10^{15}	3255	8.7×10^{-3}

The samples deposited using by CBD-CdS films exhibit low transmittance as compared to the films deposited sprayed CdS films. This can be attributed to increasing grain size and roughening. This may also due to the rearrangement of crystallites or grains. It can easily be seen from the Table 4.1 that the transmission of the SP-CdS films improves as compared to the CBD-CdS films. This improvement can be attributed to perfection and stoichiometry of the films. The result shows that the decrease in band gap of the SP-CdS films can be explained by the fact that the grain size increases significantly with the increase in the transmittance as supported by XRD studies. Similar effect has been observed for CBD grown ZnS nanocrystalline [141]. Also, the increase in transmittance may be due to decreasing optical scattering caused by the densification of grains followed by grain growth and the reduction of grain boundary density [142].

The optical absorption coefficient of the CdS films as a function of photon energy was calculated and plotted for allowed direct transitions (neglecting exciton effects) by using the expression.

$$\alpha = \frac{A}{h\nu} (h\nu - E_g)^{1/2} \quad (4.1)$$

where $h\nu$ is the photon energy, E_g denotes the optical energy band gap, and A the characteristic parameter (independent of photon energy) for respective transitions.

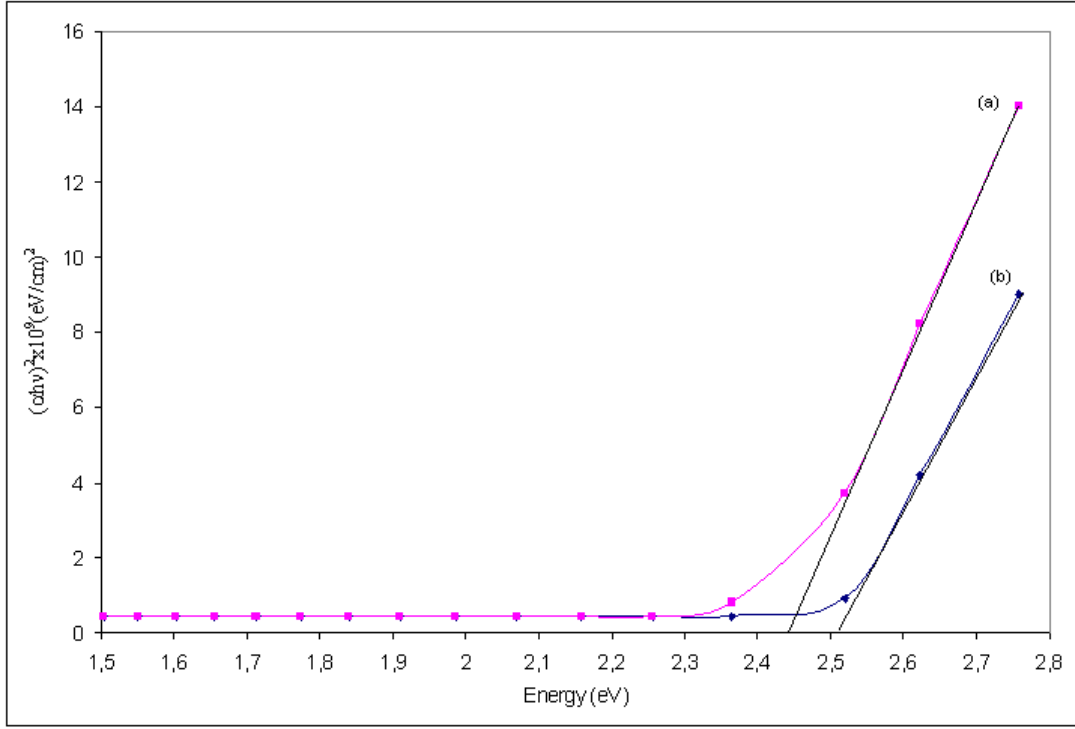


Figure 4.3 Plots and linear fits of $(\alpha h\nu)^2$ versus $h\nu$ for the CdS films a) spray pyrolysis, b) CBD

Figure 4.3 shows that the dependences of $(\alpha h\nu)^2$ as a function of photon energy $h\nu$ indicates the direct nature of band-to-band transitions for the studied samples. The values of optical band gap, E_g have been determined by extrapolating the linear portions of respective curves to $(\alpha h\nu)^2 \rightarrow 0$, for the two different samples which were deposited at different methods. The optical band gap for the sprayed and CBD CdS film is found to be 2.44 and 2.51 eV, respectively, as shown in Figure 4.3. The band gap value of sprayed CdS film is found to be low according to the CBD deposition CdS film. This decrease in band gap with deposition method may be based on possible increase in the grain size of the sprayed CdS films. The decrease in band gap of sprayed CdS film observed in the present study could also be attributed to the cubic-

hexagonal transformation based on XRD evidence. The lower values of band gap may be due to the presence of the cubic phase in the predominant hexagonal phase and the effect of strain and imperfections might have some influence on it.

As a result, this indicates that crystallization would cause the E_g narrowing. It could be explained by crystalline state improvement. Also, the shift observed at absorption edge toward lower photon energies for the films deposited on heated substrates could be attributed to the increase in crystallite size and is in good agreement with the results reported by others [143-144]. This is explained by the fact that the free electrons are trapped at grain boundaries. When the grain size increases, the density of grain boundaries decreases [140] and as a result fewer carriers are trapped in the space charge region, leading to a higher amount of free carriers.

4.2.4 Electrical Studies of the CdS films

The resistivity and carrier concentrations of CBD and sprayed CdS films measured at room temperature are presented in Table 4.1. The electrical resistivity of sprayed films is found to be about one hundredth of the resistivity of a CBD film. It is clear that the resistivity of sprayed films is smaller than that of the CBD film. The result seems to be related to the crystal structure of CBD CdS film as shown in Table 4.1. It can be inferred from structural data that the value of the carrier concentration of the sprayed CdS films has higher value as compared to CBD CdS films. The increase in the carrier concentration causes shrinkage in the gap, known as the band gap narrowing. This increase in carrier concentration may be due to the decrease in resistivity [145]. This signifies that the dislocations and density of grain boundaries decrease [146]. Therefore, it could be related to an improvement of the crystallinity leading to a decrease in donor sites trapped at the dislocations and grain boundaries [147]. Grain boundaries are known to locate defects, impurities and more traps than within a grain. The increase in carrier concentration can also be explained by the fact that the grain size increases and thus reducing grain boundary scattering. It can be deduced that if the grain size of the films increases, which induces a decrease in resistivity; there is

also an increase in the number of faults at the grain boundary. The quality of the crystallites, improved the sprayed films, indicating that impurities and defaults migrate toward the grain boundaries where they accumulate, which induces barrier height inhomogeneities. Also, it could be related to an improvement of the crystallinity leading to a decrease in donor sites trapped at the dislocations and grain boundaries [146]. These results are coherent with the SEM and X-ray measurements, since large (002) oriented grains are observed. The density of grain boundaries and dislocations therefore decreases, leading to the improvement of the quality of the CdS films. A similar behavior was observed by Oztas [148].

Electrical resistivity, optical properties and other relevant parameters of the prepared samples are presented in Table 4.1. It can be seen that the substrate temperature and bath temperature affect the resistivity of the films and other properties. The table demonstrates that, as the substrate temperature and bath temperature increases, the resistivity decreases. This behavior may be due to increase in crystallite size and carrier concentration. Thus it can be said that the films had poor crystallinity and the resistivity markedly increased, which was primarily due to the decrease in carrier concentration. The films had poor crystallinity, which indicated that the films consisted of a few atomic layers of disordered atoms. The poor crystallinity resulted in lower carrier concentration in this study. Therefore, the resistivity was affected by carrier concentration and temperature. It can be seen from Table 4.1, the substrate temperature and bath temperature are both of the most important factors influencing the film property. The decrease in resistivity with increase in substrate and bath temperature can also be explained by the fact that the grain size increases significantly with the increase in deposition temperature, thus reducing grain boundary scattering.

4.3 Growth ZnS Films

Zinc sulphide (ZnS) is another important II–VI semiconducting material with a wide direct band gap of 3.7 eV in the bulk which is the highest among all II–VI compound semiconductors and n-type conductivity are promising for optoelectronic device applications, such as electroluminescent devices and photovoltaic cells. ZnS is highly suitable as a window layer in heterojunction photovoltaic solar cells, because the wide band gap decreases the window absorption losses and improves the short circuit current of the cell. In optoelectronics, it can be used as a light emitting diode in the blue to ultraviolet spectral region due to its wide band gap. However, deposition of a high quality ZnS thin film over a large area is required if it is to be used effectively in electroluminescent devices and solar cells [149]. In the area of optics, ZnS can be used as a reflector and dielectric filter because of its high refractive index (2.35) and high transmittance in the visible range, respectively [150,151]. Zinc sulphide (ZnS) is less toxic, efficient, cost effective material, and has good transparency. In this part, the analysis of the structural, electrical and optical properties of sprayed and chemical bath deposited ZnS films has been made by using X-ray diffraction, Van der Pauw method and optical transmission measurements.

4.3.1 Analysis of the CBD ZnS Films

The CBD process uses a controlled chemical reaction to effect the deposition of ZnS film by precipitation. In the most typical experimental approach, substrates are immersed in an alkaline solution containing the chalcogenide source, the metal ion, added base and a complexing agent. The deposition of ZnS by CBD is a more difficult proposition than that of CdS. It is evident that there is a much wider range of conditions in which the concurrent deposition of zinc sulfide and zinc oxide can occur [152]. The literature survey shows that ZnS thin films have been prepared using suitable source compounds that can release cations and anions which reacts to form the compound. To overcome these problems, a complexing agent is used which forms complex ions with the metal ions. The most widely used agents are ammonia and

hydrazine hydrate [72,77]. The addition of hydrazine hydrate and ammonia improves the growth rate and crystal quality of the ZnS films.

4.3.1.1 Structural Studies of the CBD ZnS films

The structural characterization of chemical bath deposited films was carried out by X-ray diffraction (XRD) technique on Braker AXS D5005 diffractometer (monochromatic CuK_α radiation, $\lambda=1.54056 \text{ \AA}$). The XRD patterns were recorded in 2θ interval from 20° up to 35° with the step 0.051. Fig. 1 shows X-ray spectra made for ZnS films with different deposition bath temperatures such as 70, 75 and 80°C . It is observed that, the XRD of CBD ZnS film (Fig. 4.4) is found to be polycrystalline with preferential orientation along the (0 0 2) plane, the other secondary peaks visible are (1 0 0) and (1 0 1). These peaks are of much lower intensity than the (0 0 2) peak. All the peaks are associated with hexagonal ZnS and no major zinc or sulfide peaks are found.

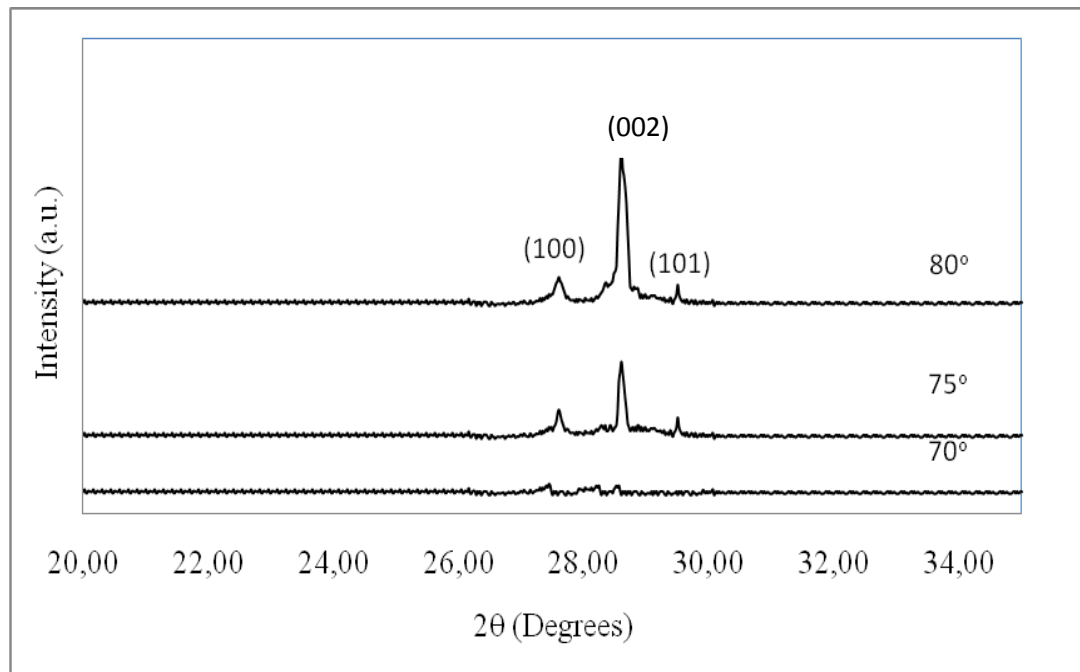


Figure 4.4 X-ray diffraction spectra for ZnS films deposited by CBD at different bath temperatures

XRD results obtained at 80 °C for 4.5 h using tri-sodium citrate agree well with that reported for ZnS [153] obtained on glass substrates at 80 °C for 4 h using tri-sodium citrate as complexing agent by the CBD technique. Fig. 4.4 shows the XRD patterns for CBD ZnS films at different deposition temperatures. The films that were prepared at different deposition temperatures have not revealed diffraction peaks, which are indicative of amorphous materials. Then, as the deposition temperature increases the intensity of ZnS (0 0 2) peak increases and this peak becomes narrower indicating an improvement of the crystallinity. It is observed that the crystallinity is enhanced as shown from the increase in the diffraction peak intensities and their narrowness. This indicates that the grain size of the films increases with increase in the deposition temperature. Consequently, It is obtained that the best diffraction peak at 80 °C for 1.5 h and this is indicating a good crystallinity of the samples. Moreover, the full width at half maximum (FWHM) in the XRD diffraction peak decreases with the deposition temperature which indicates an enhancement in the crystallinity.

In general ZnS films would crystallize in both cubic (sphalerite or β -ZnS) and/or hexagonal (wurtzite, or α -ZnS) structure, depending on the synthesis conditions such as the temperature and precursors concentrations. More recently, Lee et al. [155] and Hichou et al. [154] reported cubic and a combination of cubic and hexagonal phases, respectively, for ZnS films grown by the different deposition techniques. A comparison between our data with standard data from JCPDS shows that ZnS films obtained in this study have the hexagonal structure [156].

4.3.1.2 Optical Properties of the CBD ZnS films

Band gap information was obtained from transmission spectra which were recorded in the wavelength range of 300–900 nm in the transmission mode using unpolarised light at normal incidence by a Perkin-Elmer double beam spectrophotometer.

The optical properties of the film are shown in Figure 4.5. All films exhibit a sharp edge in absorption in the wave length range of 300 to 900 nm. Figure 4.5 shows the

$(\alpha h\nu)^2$ versus $h\nu$ for the ZnS films deposited by chemical bath deposition with different deposition temperatures such as 70, 75 and 80 °C.

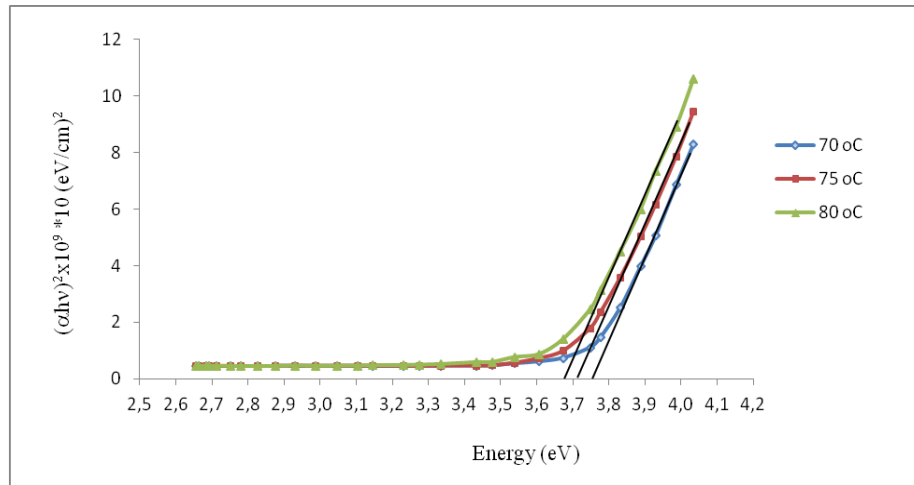


Figure 4.5 Plots and linear fits of $(\alpha h\nu)^2$ versus $h\nu$ for the ZnS films deposited by chemical bath method

The presence of a single slope in the curves suggests that films from all deposition temperatures are of single phase in nature and the type of transition is direct and allowed. The intercept with the x axis gives the value of the direct band gap. The calculated direct band gaps of the films deposited at deposition temperatures 70, 75 and 80 °C are 3.75, 3.71 and 3.68 eV respectively. Band gaps of the films are decreased with increasing deposition bath temperatures.

4.3.1.2 Electrical Properties of the CBD ZnS Films

The resistivity of the ZnS films was found to vary considerably with the bath temperature. The resistivity of the films reduced from 385×10^4 to 95×10^4 ohm-cm when the bath temperature increases as shown in Table 4.2. This reduction in the resistivity with the increasing grain size of films probably is due to the enhancements of the crystallinity of the films. The resistivity decreases hence conductivity increases. To explain the differences observed in the electrical conductivities, it must be remembered that in polycrystalline films, transport mechanism of charge carriers is

strongly influenced by grain size and the characteristics of grain boundaries. The grain sizes depend on the deposition parameters.

Table 4.2 Structural and electrical properties of ZnS films deposited by CBD

Deposition Method	Bath temperature (°C)	Grain Size (nm)	Band gap (eV)	Carrier concentrations (cm ⁻³)	Resistivity (Ohm-cm)	Strain ϵ
Chemical bath deposition	70	92	3.75	6×10^{10}	385×10^4	47×10^4
	75	108	3.71	22×10^{10}	122×10^4	31×10^4
	80	195	3.68	43×10^{10}	95×10^4	16×10^4

In general, the electron transport properties are affected by the presence of a number of defects such as structural disorders, dislocations and surface imperfections, and the variation of the grain size could also influence the activation energy. Since a polycrystalline film has crystallites joined at their surfaces via grain boundaries, the boundaries between crystallites play an important role in determining the conductivity of polycrystalline film. In the other words, the larger crystallite size results in a lower density of grain boundaries, which behave as traps for free carriers and barriers for carrier transport in the film. Hence, an increase in the grain size can cause a decrease in grain boundary scattering, which leads to an increase in the conductivity. It is observed that the resistivity decreases with increase in temperature, indicating semiconducting nature of film. The order of resistivity in the present work is in the range $\sim 10^4$ ohm-cm, which is suitable for solar cells [103]. Carrier concentrations increases with decreasing resistivity; it shows better crystallinity of the films. Increase in grain size results a decrease in grain boundaries and boundary height. Smaller boundary heights allow an increase in carrier mobility, and also this provides an increase in conductivity.

4.3.2 Analysis of the SP ZnS Films

Spray pyrolysis is a technique mentioned before which the solution is sprayed directly onto the substrate. A stream of gas (compressed air) is used for atomization of the solution through the nozzle. The main factors in determining the final physical and chemical properties of the films are the initial solution, the nozzle pressure, and the substrate temperature, among other parameters. In this part of the present study it reports on the effect of the substrate temperature on dependence on structure, optical properties and electrical properties of ZnS thin films.

4.3.2.1 Structural Properties of the SP ZnS Films

The ZnS films were deposited on glass substrates at different substrate temperature. The deposition time and the deposition rate were fixed. The structural characterization of deposited films was carried out by X-ray diffraction (XRD) technique on Bruker AXS D5005 diffractometer (monochromatic $\text{CuK}\alpha$ radiation, $\lambda=1.54056 \text{ \AA}$). The XRD patterns were recorded in 2θ interval from 20° up to 40° with the step 0.05° . The deposited films are homogenous, strong adherent, and have a bright white colour. X-ray diffraction profiles of ZnS thin films prepared at various substrate temperatures ($T_s=350\text{-}500^\circ\text{C}$) are shown in Figure 4.6.

The films prepared at substrate temperature $T_s=350^\circ\text{C}$ is amorphous. It is concluded that the ZnS films prepared at substrate temperatures $T_s\leq 350^\circ\text{C}$ do not have crystallinity. The diffractograms of ZnS films prepared at $T_s=350^\circ\text{C}$ show no peaks indicating amorphous phase. The observed relative intensities imply that all films deposited at substrate temperatures $T_s>350^\circ\text{C}$ are polycrystalline. ZnS is known to exist in two crystallographic forms, cubic (sphalerite or $\beta\text{-ZnS}$) and hexagonal (wurtzite, $\alpha\text{-ZnS}$). From diffraction profiles the diffraction angles and intensity of lines are measured with great accuracy.

Only one main peak can be observed at the diffraction angle of 28.5° on the spectrum obtained on the ZnS films prepared at different substrate temperatures as shown in Fig

4.6. This peak is assigned to both cubic and hexagonal phases of the planes $(111)_\beta$ or $(002)_\alpha$. The same results for the diffraction angle of 28.5° was found by Tran et al.[57]. More recently, Lee et al. [155] and Hichou et al. [154] reported cubic and a combination of cubic and hexagonal phases, respectively, for ZnS films grown by the different deposition techniques.

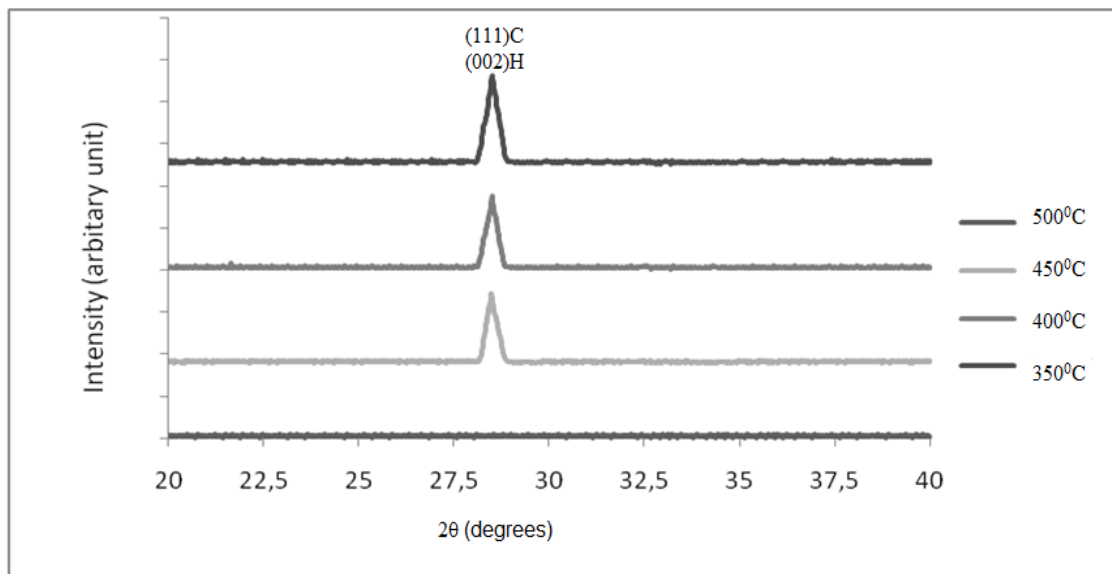


Figure 4.6 X-ray diffraction spectra for ZnS films deposited by SP at different substrate temperatures

As the substrate temperature increases the intensity of ZnS $(111)_\beta$ or $(002)_\alpha$ peak increases indicating an improvement of the crystallinity. The best crystallinity is obtained in the ZnS film prepared at substrate temperature 500°C .

It is clear that substrate temperature plays an important role in determining the structure of the ZnS films. From the XRD patterns given in Fig. 4.6, it was seen that all films deposited at different substrate temperatures ($T_s > 350^\circ\text{C}$) have a polycrystalline structure of cubic or hexagonal form as mentioned before, with a $(111)_\beta$ or $(002)_\alpha$ preferred orientation and no influence of substrate temperature on the preferential orientation of the films was seen. However, substrate temperature has a strong effect on the intensities of peaks. And also concluded that when the substrate temperatures increased the diffraction angles do not change; it shows that there is no change in crystallographic form. When peaks become sharper with increasing

substrate temperature, the grain size becomes larger. So it is concluded that at higher substrate temperature the crystallinity of the films are improved.

4.3.2.2 Optical Properties of the SP ZnS Films

In semiconductors, the relation connecting the absorption coefficient α , the incident photon energy $h\nu$ and optical band gap E_g takes the form [157],

$$\alpha h\nu = A(h\nu - E_g)^n \quad 4.2$$

where k is constant related to effective masses associated with the bands and $n=1/2$ for direct band gap material and 2 for indirect band gap material. To determine whether the films have direct or indirect band gap, the plots of $(\alpha h\nu)^2$ versus $h\nu$, and of $(\alpha h\nu)^{1/2}$ versus $h\nu$ were drawn. Better linearity was observed in the former case and it was determined that all films have direct band transition. The band gap energy was estimated from the plot of $(\alpha h\nu)^2$ versus $h\nu$. The optical band gap energies were found between 3.69 eV and 3.35 eV with increasing substrate temperatures as shown in Table 4.3. It was seen that the optical band gaps of the films slightly decreases with increasing substrate temperatures. This slight shift of the band gap with increasing substrate temperature is mainly related to the increase in carrier density. Another reason could be the improving crystallinity with increasing grain size.

4.3.2.3 Electrical Properties of the SP ZnS Films

The results for the films prepared at different substrate temperatures are tabulated in Table 4.3. As the table show, the grain size had grown with substrate temperature, and so the films prepared at higher substrate temperature have narrower grain boundaries, which result in smaller band gap energy and smaller resistivity. The resistivity had strongly decreased with increasing substrate temperature. The decrease in the resistivity is consistent with the XRD patterns, where the crystal growth was incomplete at $T_s=350^\circ\text{C}$, then it grows with the substrate temperature, where lines

became sharper which means larger grain size. Larger grains allow high mobility and higher carrier concentrations are obtained with increasing substrate temperature.

Table 4.3 Structural and electrical properties of ZnS films deposited by SP

Deposition Method	Substrate temperature (°C)	Grain Size (nm)	Band gap (eV)	Carrier concentrations (cm ⁻³)	Resistivity (Ohm-cm)	Strain ε
Spray Pyrolysis	350	45	3.69	8.2x10 ¹⁰	67x10 ⁴	76 x10 ⁴
	400	66	3.62	55 x10 ¹⁰	45 x10 ⁴	56 x10 ⁴
	450	82	3.40	80 x10 ¹⁰	18.45 x10 ⁴	45x10 ⁴
	500	88	3.35	98 x10 ¹⁰	10x10 ⁴	40 x10 ⁴

The better crystallinity level of the sample produced at T_s=500⁰C is probably the reason of this high conductivity. Similarly with CdS films, the order of resistivity in the present work is in the range ~10⁴ ohm-cm, which is suitable for solar cells [155].

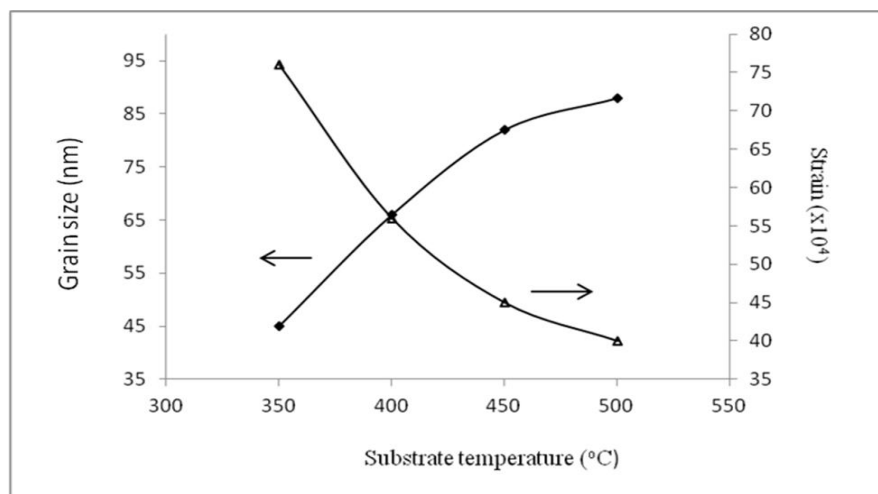


Figure 4.7 Variation of substrate temperature in the polycrystalline films with grain size and lattice strain of ZnS films deposited by spray pyrolysis method

When the substrate temperatures increased from 350⁰C to 500⁰C, the strain value is decreased from 76x10⁴ to 40x10⁴, consequently the crystallinity level of the ZnS films is growing. It is interesting to note that irrespective of the substrate temperature, the grain size improves and the defects like dislocation density and strain in the film

decrease with increased substrate temperature as shown in Figure 4.7. This may be due to the improvement in crystallinity in the films with increased substrate temperature.

4.4 Growth $Cd_xZn_{1-x}S$ Films

ZnS, CdS and their solid solutions are interesting optoelectronic materials. $Cd_{1-x}Zn_xS$ film is applicable to short-wavelength optical devices from visible to UV region because of various band gap that depend on the composition x . The films of $Cd_xZn_{1-x}S$ have also extensive applications in various electrical and optoelectronic devices. In this part firstly, the structural, electrical, optical and thermoluminescence properties of the $Cd_xZn_{1-x}S$ films deposited by spray pyrolysis with different substrate temperature with varying x compositions are reported and discussed. Secondly, the structural, electrical and optical properties of the $Cd_xZn_{1-x}S$ films deposited by chemical bath deposited at different bath temperatures with varying x compositions are provided and discussed.

4.4.1 Analysis of the CBD $Cd_xZn_{1-x}S$ Films

In this part, Polycrystalline zinc sulfide (ZnS) films and Cd-doped ZnS films have been deposited successfully by the chemical bath deposition method. The films have been characterized by x-ray diffraction method. Optical studies show that the band gap decreases with increasing the deposition temperatures and Cd content. The optical and structural properties of the films have been analyzed as a function of the deposition temperature and their Cd concentration, consisting in addition of a cadmium salt ($CdCl_2$) to the solution of ZnS. Structural, optical, and electrical analysis were done on $Cd_xZn_{1-x}S$ films with different composition (x) and different bath temperatures ($70^{\circ}C$, $75^{\circ}C$ and $80^{\circ}C$). For $x = 1.0$, it was observed that CdS film was obtained and also ZnS was investigated for $x=0$, also the other ones are $Cd_xZn_{1-x}S$ films.

4.4.1.1 Structural Properties of the CBD $\text{Cd}_x\text{Zn}_{1-x}\text{S}$ Films

The structural characterization of deposited films was carried out by X-ray diffraction (XRD) technique on Braker AXS D5005 diffractometer (monochromatic CuK_α radiation, $\lambda=1.54056\text{\AA}$). The XRD patterns were recorded in 2θ interval from 20° up to 35° . CdZnS films are produced by doping ZnS with 'Cd'. The doping causes changes in the structural properties of ZnS films.

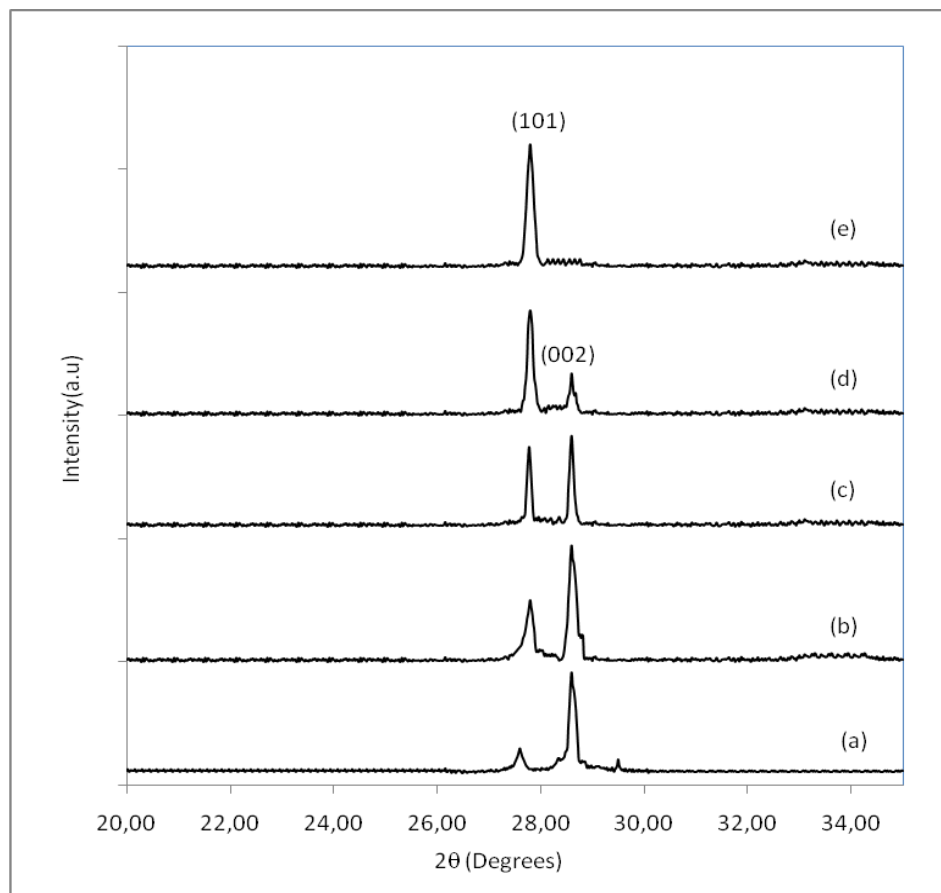


Figure 4.8 The transformation of preferred orientation in Cd addition to ZnS films, with increasing dopant content, (a) 0 %, (b) 5 %, (c) 10 %, (d) 15 %, (e) 20 %

A separate cadmium sulphide phase was not observed by XRD, since only peaks related to the hexagonal structure of ZnS are observed in the XRD spectra. In the case of Cd addition to ZnS films, only two main peaks, (002) and (101), are observed simultaneously (Fig.4.8). When the diffractogram for the undoped ZnS films is compared with the most appropriate XRD database, the peaks are indexed as in the

most appropriate card in the database and the ZnS-phase is confirmed to exist in the film with the (002) preferential orientation direction. According to the XRD reference card, the ZnS films have hexagonal crystal [156]. And Cd-doped ZnS films exhibit a polycrystalline structure in their as-grown forms, as seen in Fig. 4.8.

From the X-ray diffraction pattern given in Fig. 4.8, it is seen that the peak intensity of the (002) diffraction line decreases with increasing Cd content in the solution but the peak of (101) show an increasing trend. This different behavior from the undoped samples is thought as the contribution of Cd atoms into the ZnS structure by forcing the Zn and S atoms to form an ordered polycrystalline structure. The one additional peaks existent in the diffractogram of the Cd-doped films as being different from those of the undoped ones, is indexed as (101). This peak, after making a detailed analysis for possible compounds and elements, was defined to be the compound (CdS). This is an apparent indication of the existence of ZnS-phase and CdS microstructure together in the Cd-doped ZnS films.

The (101) reflection, having the highest intensity, is the preferred orientation for the structure which is indicating that cadmium content plays an important role in the formation of the doped samples [158,159]. And it is observed that the mutual intensity of these peaks is changing with increasing Cd content and the transformation from the (002) peak for Cd-poor ZnS to the (101) peak for Cd-rich ZnS is evident. The (002) peak is dominating for 5% Cd doped films and only a weak trace of the (101) orientation peak is observed. With increasing Cd content, the intensity of (002) peak is decreased, whereas the (101) peak becomes dominant.

Apparently, further increase in the Cd content is the reason for a complete change of the preferential orientations of the grains. Therefore, it can be inferred from the structural analysis that the evidence of excess sulphide in ZnS structure provides the possibility to construct CdS phase and results in a composite phase in the highly Cd-doped ZnS films. The same formation was observed in the Cd-doped InSe films deposited by flash evaporation [160]. Interestingly, with increasing dopant concentration, the intensity of the (101) peak increases dramatically while the (002) peak decreases and may be attributed to the preferential growth of films along the

(101) plane with the hexagonal phase. This increase in peak intensity with increasing dopant concentration indicates that Cd in all probability is substituting Zn in the ZnS lattice rather than occupying the interstitial sites, and is also supported by their comparable atomic sizes as discussed earlier [161,162]. Consequently, a considerable shift in the peak position of the (002) plane for ZnS films to the (101) plane is due to Cd addition to ZnS films for concentration of 20% to relative Zn.

4.4.1.2 Optical Properties of the CBD $\text{Cd}_x\text{Zn}_{1-x}\text{S}$ Films

The optical band gap of the ZnS films was estimated by extrapolation of the linear portion of α^2 versus $h\nu$ plots using the relation $\alpha h\nu = A(h\nu - E_g)^{1/2}$ where α is the absorption coefficient, $h\nu$ is the photon energy and E_g is the optical band gap. The value of the energy gap E_g is determined from the intercept of the extrapolation to zero absorption with the photon energy axis. Optical band of the ZnS film shows variations depending on its fabrication process. In general, polycrystalline films possess a higher band gap due to an electric field forming at the grain boundaries or imperfections caused by the potential barriers of free carrier concentration gradient [163].

It is observed that band-gap E_g decreases slightly when deposition temperature increases (3.71, 3.68, 3.63 eV for 70, 75, 80°, respectively). This decrease could be attributed to defects and impurities [164], such as interstitial zinc atoms. This abrupt energy gap extends to lower energies, due to the existence of structural defects and impurities within the material. The transitions via low-level impurities are responsible for this lower energy absorption region. Impurities in films are responsible for the low energy tail, called an impurity gap [165]. An energy band gap of 3.71 eV for ZnS films and 3.65 eV for Cd addition to ZnS films was obtained. This decrease in the band gap of ZnS after Cd addition can be related to the structural modification of ZnS films. It can also be supposed that the cadmium ions from the chemical bath deposition can replace either substitutional or interstitial zinc ions in the ZnS lattice creating the structural deformation. It is hypothesized that Cd introduces some additional energy levels in the ZnS band gap close to the valence band edge, with a consequent reduction of the energy associated with direct transition. Due to Cd

addition to the ZnS films, the optical transmission is reduced due to free hole absorption. And also the decrease of the band gap of ZnS by doping with Cd can be explained by the influence of near-band levels and the Fermi level shifted to lower energies since the transition levels shifts the absorption edge to higher energies and leads to the energy band broadening E_g . It is observed that the decrease in band gap with deposition temperature and Cd content is probably to increase in grain size, leading to reduction in density of grain boundary trapping centre and improved crystallinity of the film.

4.4.1.3 Electrical Properties of the CBD $\text{Cd}_x\text{Zn}_{1-x}\text{S}$ Films

The structural and electrical parameters such as grain size, strain, resistivity and carrier concentrations are given in Table 4.4 for bath temperatures 70, 75 and 80⁰ C with respect to the cadmium contents. It can be seen film's resistivity and carrier concentrations changes with grain size. And it is observed that the resistivity of $\text{Cd}_x\text{Zn}_{(1-x)}\text{S}$ films increases quadratically with increasing zinc content. These changes in the resistivity and carrier concentration might be partially attributed to the stoichiometric changes involving native defect concentrations at grain boundaries. This behavior can be explained as follows: when the grain and carrier density increases, the grain boundaries decrease and hence resistivity is reduced. The grain boundary is defined as region between two grains where crystal orientation changes. The grains tend to have the resistivity of the films; however, even if there is interconnectivity between two neighboring grains, this region will have high resistivity by purely geometry of narrowing. It can be observed that $\text{Cd}_x\text{Zn}_{(1-x)}\text{S}$ films taking place at oxygen sites in the $\text{Cd}_x\text{Zn}_{(1-x)}\text{S}$ are incorporated at the grain boundaries or at the film surface as its has been observed for other dopants. Meanwhile reduction in the crystal grain size could be due to the formation of other compounds and increase in resistivity and decrease in carrier density. From these results, it can be seen that the fundamental effect of the grain size is related to an increase in the grain and carrier concentrations of the crystallites and a decrease in the resistivity, energy band gap and the strain. This shows that the average grain size being not proportional to the film resistivity will have to be studied both as a function of energy band gap and grain size

to resolve the main contributor in scattering mechanism. In order to explain the drop in the resistivity with respect to grain size, it meant that a better packing of the $Cd_xZn_{(1-x)}S$ grains with a reduction of voids in it, is observed. Then, the resistivity should decrease in a monotonic way, as a function of the grain size, due to re-crystallization of the crystallites in the films, which induces the increase in the number of faults at the grain boundary.

Table 4.4 Structural and electrical properties of $Cd_xZn_{(1-x)}S$ films with various x composition deposited by CBD

$Cd_xZn_{1-x}S$	Bath Temperature	Carrier concentrations (cm^{-3})	Band gap (eV)	Grain Size (nm)	Resistivity (Ohm-cm)	Strain ϵ
x=1	70	7.5×10^{15}	2,65	92	3255	8.7×10^{-3}
	75	2.5×10^{16}	2,58	108	2895	8.2×10^{-3}
	80	8.4×10^{16}	2,50	195	2575	7.7×10^{-3}
0,8	70	7.5×10^{14}	2,81	91	13850	880
	75	25×10^{14}	2,72	105	12200	680
	80	84×10^{14}	2,68	181	11225	450
0,6	70	2.5×10^{13}	2,99	88	38500	12000
	75	15×10^{13}	2,82	101	36450	11500
	80	24×10^{13}	2,75	162	35250	9800
0,4	70	25×10^{12}	3,25	86	155000	85000
	75	35×10^{12}	3,20	97	135250	82000
	80	55×10^{12}	3,11	128	115450	79000
0,2	70	65×10^{11}	3,46	85	450250	225000
	75	77×10^{11}	3,39	93	445500	205000
	80	88×10^{11}	3,30	111	439000	185000
0	70	6×10^{10}	3.75	85	385×10^4	47×10^4
	75	22×10^{10}	3.71	91	122×10^4	31×10^4
	80	43×10^{10}	3.48	97	95×10^4	16×10^4

As a consequence, the quality factor of the film increases with increasing grain size. There are two possibilities to improve the crystallinity of the layers; the increase in the grain size to decrease the number of grain boundaries; the decrease in the barrier

height at the grain boundaries. Thus, it can be shown that the decrease in resistivity with increasing grain size of the films probably is due to the enhancement of the grain and crystallinity.

Table 4.4 shows the variation of grain size with energy band gap and strain. The energy band gap and strain of $\text{Cd}_x\text{Zn}_{(1-x)}\text{S}$ films increases quadratically with increasing zinc content. A dependence of band-gap energy shift on the grain size is attributed to a electron confinement effect related with the grain size in the films. It was observed that when the grain size was increased, the band-gap shifted to a lower energy value and the strain was decreased. Also, the shift observed at absorption edge toward lower photon energies for the films deposited on heated substrates could be attributed to the increase in crystallite size and change in the stoichiometry of the films, resulting in the formation of shallow acceptor levels in the forbidden band of $\text{Cd}_x\text{Zn}_{(1-x)}\text{S}$ films. The decrease in the energy gap by the grain size will be due to diminishing of the quantum size effect. This means that the size of the cluster of grains composing the as-deposited film is small enough to cause the quantum effects.

From the results of structure analysis, it is apparent that the optical band gap decreases with the decrease in defects and with the increase in grain size. Since strain is the manifestation of dislocation network in the films, the decrease in strain indicates a decrease in the concentration of lattice imperfections and the formation of high quality films with increasing grain size and improvement in the crystallinity with less defects. The change in energy band gap and lattice strain with grain size could infer that the lower the lattice strain, the lower the energy band gap. This implies that lattice strain in the films restricts the growth of grains. Ghosh *et al.*[166] have observed the similar results for the ZnO films grown by sol-gel process. It is found that although the data are scattered, there exists a trend of the crystallites to decrease the size with increasing strain. This may come from the retarded crystal growth due to the stretched lattice that can increase the lattice energy and diminish the driving force of the growth.

4.4.2 Analysis of the Sprayed $\text{Cd}_x\text{Zn}_{1-x}\text{S}$ Films

In this part, $\text{Cd}_x\text{Zn}_{1-x}\text{S}$ films were obtained with incorporation of Cd element into ZnS at different concentrations ($0 \leq x \leq 1$) by spray pyrolysis technique using aqueous solutions of CdCl_2 , ZnCl_2 and $(\text{CS}(\text{NH})_2)_2$, which were atomized with compressed air as carrier gas. The $\text{Cd}_x\text{Zn}_{1-x}\text{S}$ films were obtained on glass substrates at substrate temperatures of 350 °C, 400 °C and 450 °C. The structural, optical, and electrical properties of sprayed cadmium zinc sulfide (CdZnS) films were investigated.

4.4.2.1 Structural Properties of the Sprayed $\text{Cd}_x\text{Zn}_{1-x}\text{S}$ Films

Figure 4.9 shows the X-ray diffraction patterns of $\text{Cd}_x\text{Zn}_{1-x}\text{S}$ films deposited at a substrate temperature of 400 for different cadmium compositions, $x = 0.0, 0.2, 0.4, 0.6, 0.8$ and 1.0 , which indicates a clear dependence of film crystallinity on the ‘Cd’ composition, x .

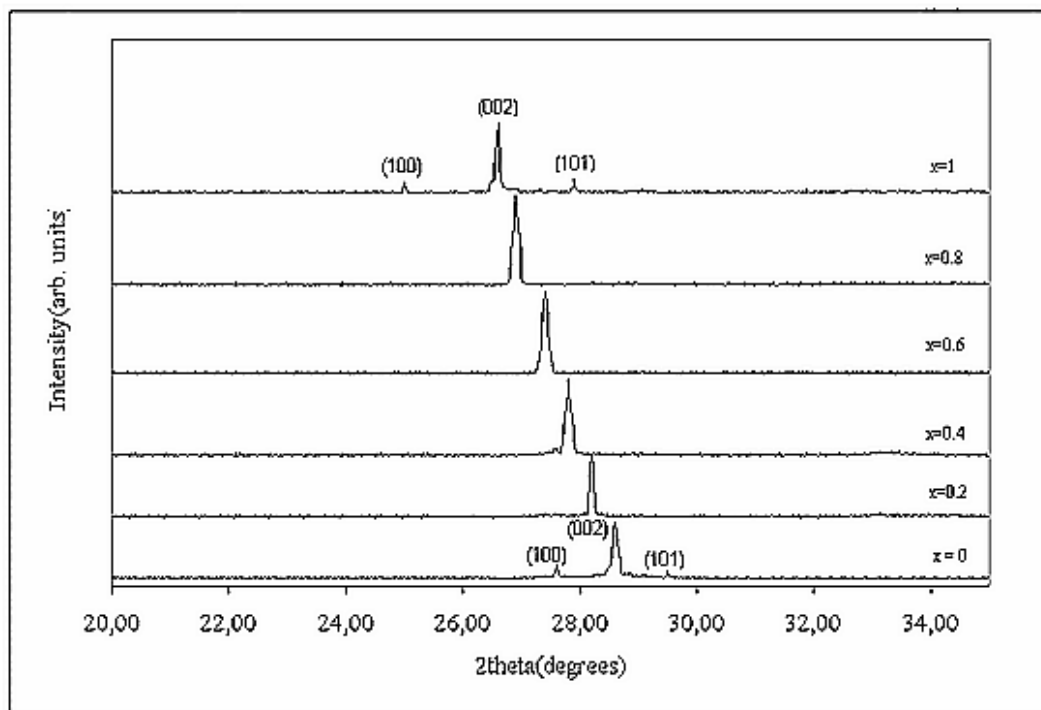


Figure 4.9 X-ray diffraction patterns of $\text{Cd}_x\text{Zn}_{1-x}\text{S}$ films with various x at $T_s=400^\circ\text{C}$

All the films were polycrystalline and showed the hexagonal wurtzite structure of ZnS. Cubic and hexagonal structures obtained by spray pyrolysis have been reported [167-169,65]. The layers exhibited the (002) crystal plane as the predominant orientation which were preferably oriented along the (002) plane in addition to the appearance of other peaks that correspond to the (100) and (101) orientations of ZnS for $x=0$.

Fig.4.9 also shows that the $Cd_xZn_{1-x}S$ films composed of mixed crystallite of both CdS and ZnS. In other words, the polycrystalline structure of $Cd_xZn_{1-x}S$ films is considered to be a mixture of wurtzite ZnS and CdS crystallite grains. For $x = 1.0$, it was observed that CdS film was obtained. The films of $x = 1.0$ were preferentially oriented along (0 0 2) plane for wurtzite hexagonal CdS film. Other low intensity peak of CdS film along (1 0 0) and (1 0 1) are also found. It was observed that the position of (002) peak shifted towards lower diffraction angles with the increase in Cd content in the layers, indicating the presence of tensile strain in the grown films. Also, this shows us the formation of a material with different phases due to the Cd amount. A similar phenomenon has also been reported [170]. The observed higher intensity of the (002) reflection for the layers grown at 400 °C might be due to the enhancement of horizontal mobility of ad-atoms and the condensation coefficient during the cluster formation with the increase in x composition that led to an improvement in the crystallinity, which is the usual phenomenon observed in the growth of thin films. It was concluded that the crystallinity levels of the ZnS films improved with Cd incorporation, which has a strong effect on the structural properties.

The grain size (D) values are calculated using the Scherrer formula [171],

$$D = \frac{0.9\lambda}{\beta \cos \theta} \quad (3.1)$$

where λ is the wavelength of the X-ray used (1.5406 Å), β is the full-width at half-maximum (FWHM) of the (002) peak which has maximum intensity and θ is the Bragg angle. The strains of the films were determined by the use of the following formula:

$$\varepsilon = \frac{\beta \cos \theta}{4} \quad (3.2)$$

It is seen that as the x composition increases, the (002) diffraction peaks shift to lower angles and the FWHM reduces, which indicates that grain growth has occurred, resulting in the partial relief of lattice strain within the films. From the FWHM and peak position of the (002) peak, the grain size and the lattice strain are calculated. It shows that the grain sizes and the lattice strain are influenced by the x composition as shown in Fig. 4.10 with the x composition increasing; both the grain sizes and the absolute peak intensities increase, while lattice strain decreases. The decrease in strain indicates a decrease in the concentration of lattice imperfections as the x composition increases. Thus, increasing the x composition decreases the density of nucleation center and, under these circumstances, a smaller number of centers start to grow, resulting in large grains. The small grain size is undesirable for most semiconductor applications because of the barrier effect of grain boundary on the mobility in planar direction [172]. Also, the increase in grain size with the x composition could be attributed to the enhanced reaction kinetics among the sprayed droplets as well as improvement in the ad-atom mobility on the substrate surface. It can be explained that the decreasing trend of grain size with the increase of strain due to the retarded crystal growth as the stretched lattice increases the lattice energy and diminishes the driving force for the grain growth.

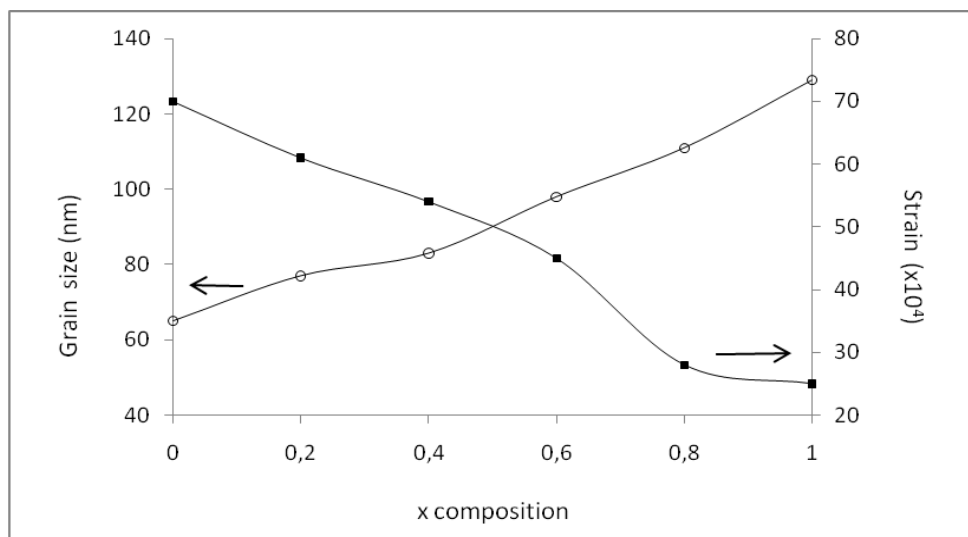


Figure 4.10 Variation of x composition in the polycrystalline films with grain size and lattice strain of $\text{Cd}_x\text{Zn}_{1-x}\text{S}$ films deposited by SP method at 400°C

The lattice strain provides a driving force for the grain growth during the increase in x composition. The lattice strain arises from a high atomic packing density and frozen-in crystallographic defects in the grains and grain boundaries [173]. Since the intragranular defects and grain boundaries contain more free energy than crystalline phase, the increase in the grain sizes in the films lowers free energy with increasing x composition. Moreover, the particle size and strain are manifestations of dislocation network in the films. The decrease in strain with an increase in the grain size indicates the formation of good quality films.

4.4.2.2 Optical Properties of the Sprayed $\text{Cd}_x\text{Zn}_{1-x}\text{S}$ Films

The dependence of the band gap of $\text{Cd}_x\text{Zn}_{1-x}\text{S}$ films on the x grain size is shown in Fig. 4.11. It can be seen that the band gap decreases from 3.20 to 2.40 eV as the grain size increases from 65 to 129 nm. This decrease in the band gap can be due to the influence of various factors such as grain size, structural parameters, carrier concentration, presence of impurities, deviation from stoichiometry of the film and lattice strain [174–176].

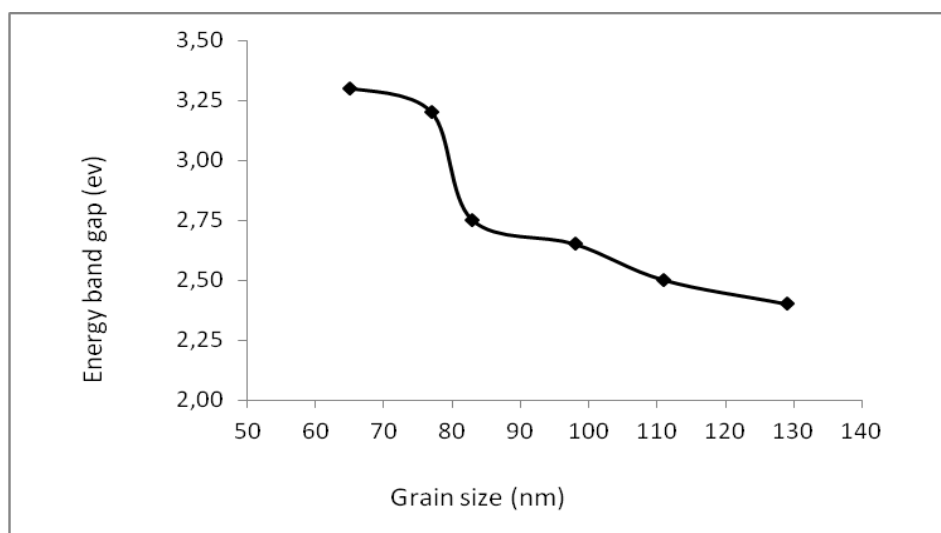


Figure 4.11 Variation of grain size in the polycrystalline films with energy band gap of $\text{Cd}_x\text{Zn}_{1-x}\text{S}$ films deposited by SP at 400°C

A detailed analysis is needed to bring out the effect of each of these parameters on the value of grain size. However, it is observed that the lattice parameters, grain size and

the strain have a direct dependence on the x composition of the films. Hence, it is considered that the observed decrease in E_g with increasing grain size is due to the decrease in lattice strain. From these results, it is clear that energy band gap decreases with increase in cadmium concentration. This shift of the band gap with the Cd incorporation resulted from the increase in carrier density or the improving crystallinity level. Earlier studies show that strain changes the interatomic spacing of semiconductors which affects the energy gap [177-179]. The effect of grain size depend on the band gap, as the result of electron confinement in grains [180] and also the effect of lattice strain is examined.

4.4.2.3 Electrical Properties of the Sprayed $Cd_xZn_{1-x}S$ Films

Figure 4.12 shows the variation of film's resistivity and carrier density with grain size. This behavior can be explained as follows: when the grain size increases, the grain boundaries decreases and hence resistivity is less. The decrease in the resistivity of the films as a function of the grain size is also due to re-crystallization of the crystallites in the films, which induces the increase in the number of faults at the grain boundary. As a consequence, the quality factor of the film increases with increasing grain size.

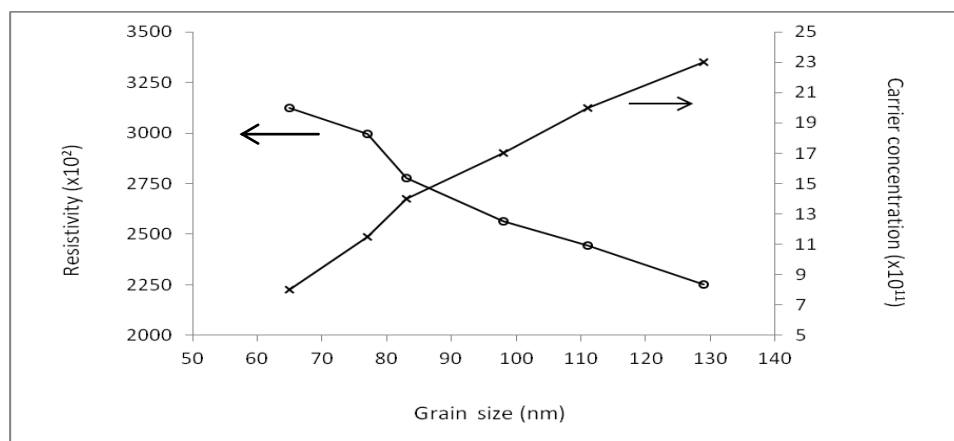


Figure 4.12 Variation of grain size in the polycrystalline films with resistivity and carrier density of $Cd_xZn_{1-x}S$ films deposited by SP at $400^{\circ}C$

It can be explained that the increase in the grain size results to decrease the number of grain boundaries, this means a decrease in the barrier height at the grain boundaries.

Thus, it can be shown in Table 4.5 that the decrease in resistivity with the increasing grain size of the films probably is due to the enhancement of the crystallinity of the films. This observation is attributed to the size effect observed in semiconductor films. This could also be supported by the variation of crystalline quality with the increase in film thickness as observed in the XRD analysis. A similar behavior was reported by several workers [181,182]. Also the increase in the carrier concentration as a function of the grain size can be attributed to grain boundary scattering and ionized impurity scattering in the case of spray deposited polycrystalline films [183].

Table 4.5 Structural and electrical properties of Sprayed $Cd_xZn_{1-x}S$ Films with various x at different substrate temperature

Substrate temperature	x composition	grain (nm)	resistivity ($\times 10^2$)	carrier concentration ($\times 10^{11}$)	strain ($\times 10^4$)	E_g (eV)
$T_s=350^\circ C$	1	121	4550	22	39	2,44
	0,8	102	4990	19	48	2,55
	0,6	88	5450	15	52	2,75
	0,4	72	5780	13	64	3,1
	0,2	59	7340	11	71	3,45
	0	45	6700	8,2	76	3,6
$T_s=400^\circ C$	1	129	2250	23	25	2,40
	0,8	111	2445	20	28	2,50
	0,6	98	2565	17	45	2,65
	0,4	83	2776	14	54	2,75
	0,2	77	2996	11,5	61	3,20
	0	65	3125	8	70	3,30
$T_s=450^\circ C$	1	138	1250	24	21	2,35
	0,8	128	1340	22	25	2,4
	0,6	123	1545	19	30	2,55
	0,4	115	1755	15	35	2,8
	0,2	95	1825	12	41	3,1
	0	82	1845	8	45	3,4

4.4.2.4 Thermoluminescence Properties of the Sprayed $Cd_xZn_{1-x}S$ Films

TL is observed when, in the process of irradiating a material, part of the irradiation energy is used to transfer electrons to traps and holes to centers. This energy, stored in the form of the trapped electrons, is released by raising the temperature of the material,

and the released energy is converted to luminescence. This trapping process and the subsequent release of the stored energy find important application in ionizing radiation dosimetry and in the operation of long persistence phosphors. Much information about the trapping process and the release of trapped electrons is obtained from the TL spectrum after turning off the irradiating source.

The earlier investigations have indicated that the efficiency of solar cells is markedly influenced by the methods of preparation, i.e. by substrate temperature and x composition. On the other hand, no study has recorded the effect of film production conditions on the intensity of TL signal. Therefore, in the present work, the influence of concentration ratio of different starting materials used in the spray pyrolysis method was firstly investigated on the shape and intensity of glow curves of $Cd_xZn_{1-x}S$ films and it was observed that they are highly affected by the film production conditions. Then, the appropriate conditions under which the glow peak of ZnS films has high TL efficiency were investigated.

The typical glow curves obtained from some of CdZnS samples are shown in Fig 4.13. All of the samples were exposed to beta-rays for 5 min after an annealing at 400 °C for 10 min. A careful investigation of these glow curves indicates that the ZnS samples have a main glow peak at approximately 120 °C, which decreases to 100 °C with increasing x composition, although, the shape and especially the peak intensities of glow curves are considerably different from each other. The intensity of TL signal of produced samples via spray pyrolysis method strongly depends on film production conditions and concentration of starting materials used in the spray pyrolysis method. For example, when the concentration of $ZnCl_2$ impurities in the produced samples increases, the intensity of TL signal also increases.

The typical glow curves (GCs) obtained from CdZnS films are shown the Figure 4.13. The shape and intensity of the GCs are changed after the CdS film is doped with zinc. It is well known that the TL performance of CdZnS film is very sensitive to the structural changes of defects and the presence of shallow and deep trapping levels within the material. Therefore, the number of trap states and intensity of GCs of many

TL materials are strongly affected by the variation of defects, defect clusters, surface states and dislocations in the lattice.

It is also obvious that the zinc-doped CdS film strongly modifies the aggregation state of impurity in the host lattice along with the existing traps within the material. Thus, there is no peak for undoped CdS films. Consequently, the zinc ions can also form defect complexes with these vacancies in the CdS lattice which can create trapping levels within the band gap and they can act as electron and hole traps which are responsible for the glow peaks in Zn-doped CdS films.

As the x composition increases the intensity of (0 0 2) peak increases and this peak becomes narrower indicating an improvement of the crystallinity. This means that the grain size of the films increases with increasing x composition. Therefore, the TL sensitivity of produced samples must depend on both their crystal structure and grain size. Thereupon the intensity of TL signal increases with improving of crystallinity of produced samples. In addition to this, the peak temperature, which is one of the most important parameters, apparently depends on the production conditions.

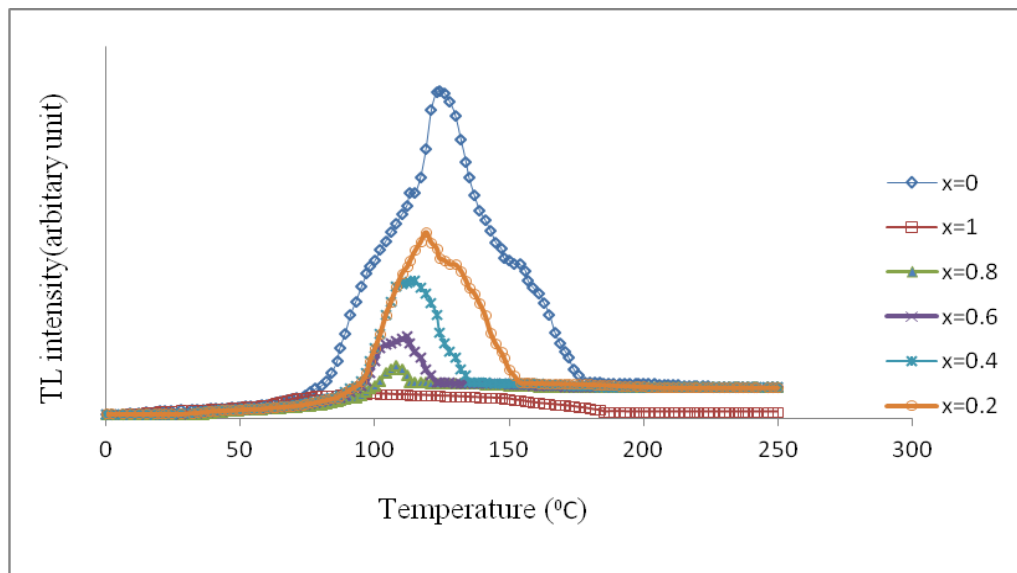


Figure 4.13 Selected glow curves of $\text{Cd}_x\text{Zn}_{1-x}\text{S}$ films produced by spray pyrolysis method at 400°C substrate temperature

In recent studies, it was found that the luminescence process in semiconductor particle size is very complex phenomena and it was attributed that the luminescence of

semiconductor particle size is generally arising from the deep traps of surface states whose energy levels lie within the band gap of semiconductor. It is seen that as the x composition decreases, the particle size decreases. Thus, the ions at the surface of samples quickly increase as the particle size is decreased. The excited electrons and holes from the surface ions are easily trapped at the surface states. So, the trapped carriers at the surface states are released by heating the sample and they recombine with each other and give out luminescence which is known as thermoluminescence. The number of surface ions and surface states increase due to the increase in the surface to volume ratio with decreasing size of the particles, so the number of trapped charged particles at surface state increases, thus TL efficiency is increased. Therefore, the TL of Zinc-doped CdS films may be related with the surface states. Another possible explanation of the increase in the TL efficiency is that the wave functions of electrons and holes are overlapped effectively with decreasing size of the particles, which may result in an increase in their recombination probability.

4.4.3 Analysis of Effect of Water Concentration on the Sprayed Cd_{0.5}Zn_{0.5}S Films

In this part, Cd_{0.5}Zn_{0.5}S films were deposited on heated clean glass (about 1 cm² of geometric area) substrates by spraying an aqueous solution in air atmosphere at various substrate temperatures in the range 300–450⁰C. The spray solutions are comprised CdCl₂ (0.5 M, Merck, ≥ 99%), ZnCl₂ (0.5 M, Merck, ≥ 99%) and SC(NH₂)₂ (0.5 M, Merck, ≥ 99%) in the deionized water. H₂O was used as the activator gas, which was carried out with air and gasified at 30⁰C. The spray flow rate was adjusted to about 0.3 ml/min and the distance between the nozzle (head of the sprayed source) and the substrate was kept at 20 cm in all cases.

4.4.3.1 Structural Properties of the Sprayed Cd_{0.5}Zn_{0.5}S Films

The structural properties of the films were studied by x-ray analysis with a Rigaku D/Max-IIIS model x-ray diffractometer ($\lambda = 1.5405 \text{ \AA}$). The film thicknesses were determined by an interferometric method (using multiple-beam Fizeau fringe method

at reflection of monochromatic light, $\lambda = 550 \text{ nm}$). The $\text{Cd}_{0.5}\text{Zn}_{0.5}\text{S}$ films deposited at various substrate temperatures were characterized by the x-ray diffraction (XRD) technique scanned in the 2θ range $20\text{--}35^\circ$. The diffractograms were obtained for the films grown on the amorphous glass plates (Fig. 4.14). The diffractograms depict that the deposits are polycrystalline and of hexagonal crystal structure for all the substrate temperatures [102]. The spectra clearly show that the films formed at substrate temperatures $300\text{--}450^\circ\text{C}$ exhibit a strong peak at around 27.40° corresponding to the (002) plane of polycrystalline $\text{Cd}_{0.5}\text{Zn}_{0.5}\text{S}$, whereas the intensity of its reflection increases with the substrate temperature. The intensity of the (002) peak and its narrowing with an increase in the substrate temperature up to 400°C indicates an improvement in the degree of crystallinity of the films. Hence, it can be assumed that the higher substrate temperature enables the atoms to move to the stable sites, which implies that films fabricated at these conditions are rather homogenous and that their crystalline state improves when the substrate temperature increases.

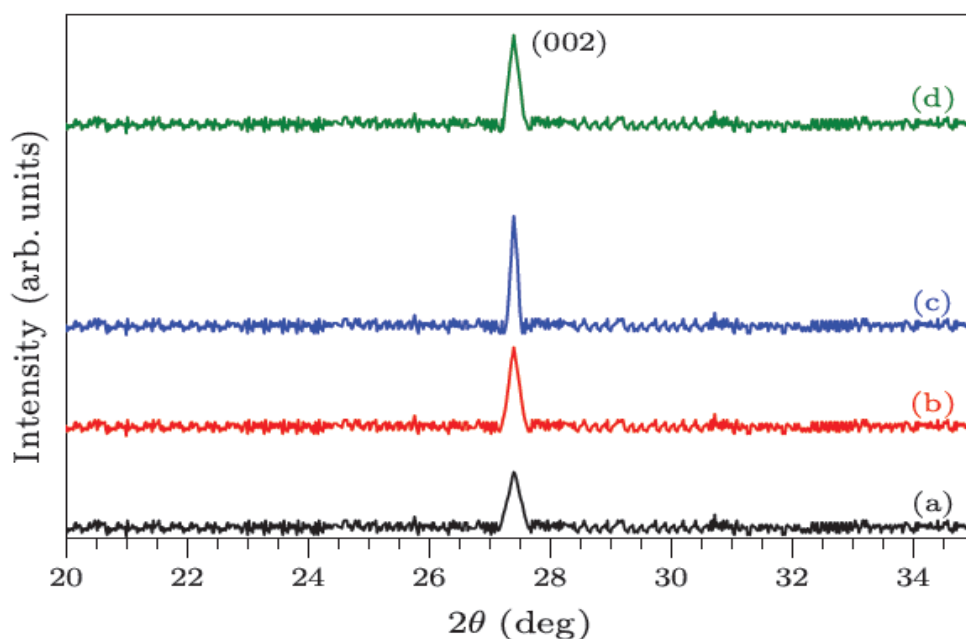


Figure 4.14 X-ray diffraction patterns of $\text{Cd}_{0.5}\text{Zn}_{0.5}\text{S}$ films with various substrate temperatures: (a) 300°C , (b) 350°C , (c) 400°C and (d) 450°C

It noticed that in these spectra that the intensity of the peak increases with temperature until 400°C , where it passes by a maximum and decreases with a further increase in substrate temperature. This evolution can be interpreted by the fact that increase in the

substrate temperature improves the crystallization of films of $\text{Cd}_{0.5}\text{Zn}_{0.5}\text{S}$. However, at higher temperatures, the temperature effect yields the formation of defects in the film and can also lead to the deterioration of the structural quality of films [184]. It is obvious that the growth of the $\text{Cd}_{0.5}\text{Zn}_{0.5}\text{S}$ film samples is strongly dependent on the substrate temperature. $\text{Cd}_{0.5}\text{Zn}_{0.5}\text{S}$ films were also prepared in the presence of 0%, 0.5%, 1.0% and 1.5% with activator H_2O content, which were examined by x-ray diffraction.

As shown in Fig. 4.15, their x-ray diffraction patterns show that all the films prepared with different concentrations of H_2O are composed of multicrystals, which have a similar structure to hexagonal wurtzite. The presence of water significantly enhances the growth rate of the samples over the H_2O content up to 1.0%. The increasing growth rate is coupled with some change in structure of the crystalline samples when in contact with water. It is observed that the diffraction peaks become sharper and stronger, indicating that the crystals in the $\text{Cd}_{0.5}\text{Zn}_{0.5}\text{S}$ film could grow larger with the increase of H_2O content. Further decrease in the (002)-peak intensity in the XRD for the concentration of water 1.0% may be attributed to the non-uniformity of the films.

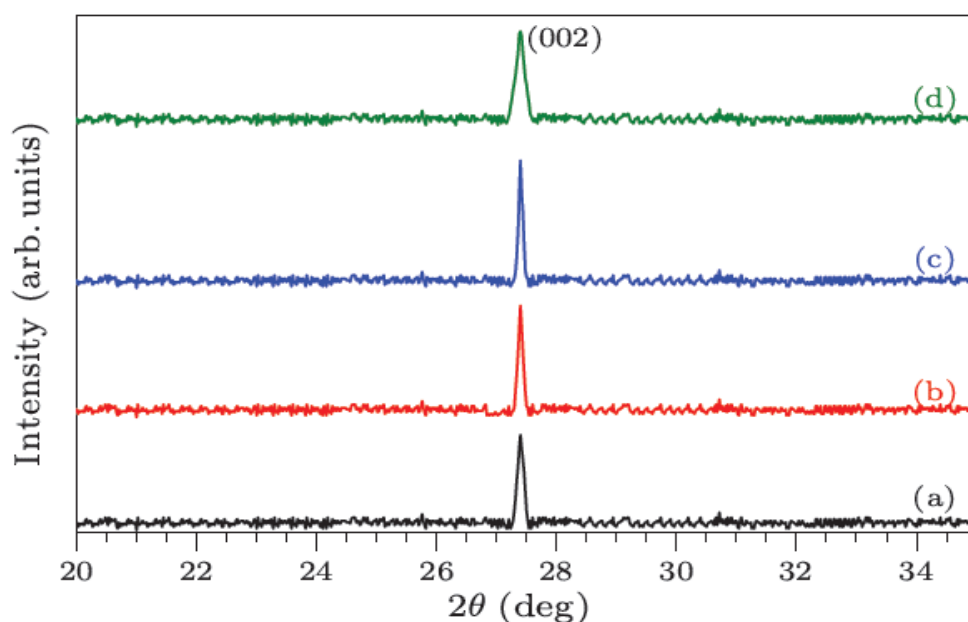


Figure 4.15 X-ray diffraction patterns of the $\text{Cd}_{0.5}\text{Zn}_{0.5}\text{S}$ film prepared by adding different concentrations of H_2O : (a)0%, (b) 0.5%, (c) 1.0%, (d) 1.5%

This effect can be explained if it is considered that the oxygen atoms of the water molecules substitute instead of sulphur atoms, and the water molecules are segregated at grain boundaries or at the film surface and, hence, the number of nucleation centers is reduced. It is observed that Cd_{0.5}Zn_{0.5}S films taking place at water molecules in the samples are incorporated at the grain boundaries or at the film surface;[185] meanwhile the reduction in the crystal grain size could be due to the formation of other compounds.

4.4.3.2 Electrical Properties of the Sprayed Cd_{0.5}Zn_{0.5}S Films

Table 4.6 summarizes the values of resistivity, transmittance and band gap according to the thickness and water concentrations. It is shown that thickness and water concentrations are the most important factors influencing film properties. The film thickness continuously increases as the quantity of water concentration up to 1.0% increases and then saturates. The expected reason for this is the supply of more number of ingredient ions with the increase in quantity of water concentrations. The results indicate that the film thickens with the increased H₂O content up to 1.0%. The growth rate of the film is faster at low H₂O concentrations and becomes lower when the H₂O concentration is higher than 1.0%. Without the activator H₂O, the crystal grains in the film are small and the film contains many holes and crystal interfaces.

Table 4.6 Electrical and optical properties of Cd_{0.5}Zn_{0.5}S films with different H₂O concentrations

Substrate temperature (°C)	Water (%)	Thickness (µm)	Grain size (nm)	Resistivity *10 ⁴ (Ω.cm)	Band gap (eV)	Transmittance (%)
400	0	155.0	45	150	2.90	78
	0.5	175.0	49	125	2.86	74
	1	188.0	55	98	2.80	70
	1.5	170.0	50	118	2.85	75

Therefore, the resistivity of the samples is high. With the increase of H₂O concentration, the crystal grains grow large. This signifies that the dislocations and

density of grain boundaries decrease. Therefore, it could be related to an improvement of the crystallinity leading to a decrease of donor sites trapped at the dislocations and grain boundaries [186]. From Table 4.6 it is clear that the crystallite size of $\text{Cd}_{0.5}\text{Zn}_{0.5}\text{S}$ films increases with an increase in the film thickness and water concentrations. This indicates that the film thickness contributes to the improvement in crystallinity with film thickness up to 188.0 μm . Also the trend of the increase in crystallite size may be interpreted in terms of a columnar grain growth in the structure. This observation is attributed to the size-dependent effect in semiconductor films and fine grain size of crystallites. It is observed that the resistivity of the films prepared at the same substrate temperature decreases with the increase in H_2O content. However, it increases when the H_2O concentration is higher than 1.0%. Thus it can be said that as the films get poor crystallinity, the resistivity is markedly increased, which is primarily due to the decrease in carrier concentration. The poor crystallinity of films indicates that the films consist of a few atomic layers of disordered atoms. Since the atoms in the poor crystallized area are disordered, there are a large number of defects due to incomplete atomic bonding. After trapping the mobile carriers, the traps become electrically charged, creating a potential energy barrier which impedes the motion of carriers from one crystallite to another, thereby reducing their carrier concentration. The poor crystallinity of the films is mainly due to low carrier concentration. The smaller grain size increases the grain boundary surface area, which is responsible for the decrease in carrier mobility. This can be attributed to the increase in randomly oriented crystallites. It is also noticed that the inter-grain barrier height increases with increasing water concentration, which is caused by the reduction in grain size. This increases grain boundary scattering so that electrical resistivity increases. The decrease in resistivity with the increase in H_2O content can also be explained by the fact that the grain size increases significantly, thus reducing grain boundary scattering, the crystal interfaces, transmittance and oxygen incorporation at grain boundaries. The number of free electrons restricted by the crystal interface decreases and the potential barrier to the carriers is lowered. On the other hand, the reduction in the resistivity can be also due to O_2 desorption from the films [187].

4.4.3.3 Optical Properties of the Sprayed Cd_{0.5}Zn_{0.5}S Films

As seen from Table 4.6, the transmittance of the films decreases as film thickness and water concentration (1.0%) increase. This is attributed to the increase in the crystallite size of the samples, which subsequently increases the absorption. These crystallites cause the diffusion of the incident light in the material. This yields the reduction in transmitted light. With an increase in the size of crystallites, light scattering is reduced, which results in transmittance improvement. Moreover, in the films, the onset of the absorption edge becomes less sharp. This is due to the fact that bigger crystalline sizes are deposited; and the scattered radiation becomes remarkable due to the surface roughness [188]. With increasing the thickness, the fundamental absorption can be observed to shift towards the shorter wavelength [189]. It is believed that the addition of water content produces many highly activated oxidizing species in the plasma thereby enhancing the reactivity of the incident particles due to improvement of the crystallinity of Cd_{0.5}Zn_{0.5}S films. In this study, the films have good crystalline qualities with film thickness and H₂O content increasing up to 1.0%. It is suggested that the increase in film thickness is caused by optical absorption on the film interior and surface. From these observations, the influence of the H₂O content on the E_g values is clearly evident. As the H₂O content increases up to 1.0%, the value of E_g decreases, which indicates that crystallization would cause the E_g narrowing due to the quantum size effect observed in the films of semiconductors. For the films deposited at relatively high water concentrations (> 1.0%) due to the lower grain size of Cd_{0.5}Zn_{0.5}S films, scattering at the grain boundaries results in the higher resistivity of the films. Also, the band gap can be observed to increase with an increase in the water concentration in the deposits. The nature of this variation in the band gap energy may be useful in the design of a suitable window material in the fabrication of solar cells. Moreover, with increasing water concentrations due to an applied oxygen vacancy in the films, the carrier concentration decreases and the resistivity increase. This is because the oxygen vacancies generating the free electrons decrease by diffusing the oxygen in films.

CHAPTER FIVE

CONCLUSIONS

In this work, semiconducting CdS, ZnS and $Cd_xZn_{1-x}S$ films were fabricated at different deposition conditions by spray pyrolysis and chemical bath deposition method. The influence of the preparation technique on the structural, electrical and optical properties of the polycrystalline CdS, ZnS and $Cd_xZn_{1-x}S$ films was investigated using by X-ray diffraction (XRD), Van der Pauw method and optical transmission.

CdS films were deposited by chemical bath deposition and spray pyrolysis method. CdS films were deposited on highly clean glass substrates at substrate temperatures 250, 275 and 300 °C, by using spray pyrolysis technique. The bath temperatures were adjusted as 70, 75 and 80 °C when CdS were produced by chemical bath deposition method. The crystal structure depended strongly on the deposition technique. The chemical bath deposition promoted the formation of the hexagonal phase, and the spray pyrolysis technique produced films with mixed structure of the hexagonal and cubic phase. The band gap energy measured in sprayed CdS films was lower than that of CBD-films. This decrease in the band gap can be attributed to the increase in grain size, cubic-hexagonal phase transition and the effect of impurities during the process. The decrease in FWHM of the sprayed CdS film indicates an improvement in the crystallinity of the sprayed CdS films according to the other deposition method CBD. The sprayed CdS sample appears to be more crystalline with larger grain size as compared to CBD samples. It is also found that the bath and substrate temperature had obvious effect on the electrical, structural, and optical properties. The increase in the bath and substrate temperature improves the crystallinity of the CdS films. When the bath and substrate temperature is increased, a shift in E_g toward the higher wavelength region attributing to the improvement of crystallinity is noticed. The optimum bath and substrate temperature are 80 °C and 300 °C, respectively. It is

observed that the substrate temperature and bath temperature affect the resistivity of the films and other properties. As the substrate temperature and bath temperature increases, the resistivity decreases. This behavior may be due to increase in the crystallite size and carrier concentration. Thus it can be said that the films had poor crystallinity and the resistivity markedly increased, which was primarily due to the decrease in the carrier concentration. These results indicate that CdS films with low resistivity and high transmittance can be produced by the spray pyrolysis method. The electrical resistivity of sprayed films is found to be about one hundredth of the resistivity of a CBD film. It is clear that the resistivity of sprayed films is smaller than that of the CBD film. The poor crystallinity resulted in lower carrier concentration in this study. Therefore, the resistivity was affected by the carrier concentration and temperature in this study. It can be inferred from the structural data that the value of the carrier concentration of the sprayed CdS films has higher value as the compared with CBD CdS films.

The ZnS films were deposited on glass substrates at different substrate temperature by spray pyrolysis method and different bath temperatures by chemical bath deposition method. The ZnS films were obtained on glass substrates at substrate temperatures of 350 °C, 400 °C, 450 °C and 500 °C by spray pyrolysis. The films prepared at substrate temperature $T_s=350^{\circ}\text{C}$ is amorphous. It is concluded that the ZnS films prepared at substrate temperatures $T_s\leq 350^{\circ}\text{C}$ do not have crystallinity. The observed relative intensities from structural analysis imply that all films deposited at substrate temperatures $T_s>350^{\circ}\text{C}$ are polycrystalline. It is clear that substrate temperature plays an important role in determining the structure of the ZnS films. From diffraction profiles the diffraction angles and intensity of lines are measured with great accuracy. Only one main peak can be observed at the diffraction angle of 28.5° on the spectrum obtained on the ZnS films prepared at different substrate temperatures. This peak is assigned to both cubic and hexagonal phases. It is suggested that if the bandgap of the ZnS films is $\leq 3,6$ eV, the films are cubic. Thus it can be said that the produced ZnS films are cubic except the film produced at $T_s=500$, because the film produced at $T_s=500$ has a bandgap value 3.69 eV. The substrate temperature has a strong effect on the intensities of peaks. When the substrate temperatures increased the diffraction angles do not change; it shows that there is no change in crystallographic form. However, when peaks become sharper

with increasing substrate temperature, the grain size becomes larger. So it is concluded that at higher substrate temperature the crystallinity of the films are improved. The better crystallinity level of the sample produced at $T_s=500^{\circ}\text{C}$. The optical band gaps of the films slightly decreases with increasing substrate temperatures. This slight shift in the band gap with increasing substrate temperature is mainly related to the increase in carrier density. Another reason could be the improvement in crystallinity with increasing grain size. The grain size had grown with substrate temperature, and so the films prepared at higher substrate temperature have narrower grain boundaries, which result in smaller band gap energy and smaller resistivity. The resistivity is strongly decreased with increasing substrate temperature. The better crystallinity level of the sample produced at $T_s=500^{\circ}\text{C}$ is probably the reason for this high conductivity. Larger grains allow high mobility. Higher carrier concentrations are obtained with increasing substrate temperature.

The influences of different bath temperatures (70, 75 and 80 $^{\circ}\text{C}$) on the structural, optical and electrical properties of the chemical bath deposited ZnS films are investigated. The same effects of temperature on growth of the films were found with sprayed ZnS films. The XRD patterns for CBD ZnS films at different deposition temperatures were investigated and it is shown that as the deposition temperature increases the intensity of peak increases and this peak becomes narrower indicating an improvement in the crystallinity. This shows that the grain size of the films increases with increase in the deposition temperature. Band gap information was obtained from transmission spectra and all films exhibit a sharp edge in absorption in the wave length range of 300 to 900 nm. Both films sprayed and chemical bath deposited have direct band gaps which are decreased with increasing substrate temperatures and deposition bath temperatures, respectively. The resistivity of the ZnS films was found to vary considerably with the bath temperature. The resistivity of the films reduced when the bath temperature increases. This reduction in the resistivity with increasing grain size of films probably is due to the enhancements of the crystallinity of the films. The resistivity decreases hence conductivity increases. It is observed that the resistivity decreases with increase in temperature, indicating semiconducting nature of film. Carrier concentrations increases with decreasing resistivity; it shows better crystallinity of the films. Increase in grain size results a

decrease in grain boundaries and boundary height. Smaller boundary heights allow an increasing in carrier mobility, and also this provides an increase in conductivity.

The semiconducting $\text{Cd}_x\text{Zn}_{1-x}\text{S}$ films were obtained with incorporation of Cd element into ZnS at different concentrations ($0 \leq x \leq 1$) by spray pyrolysis technique and chemical bath deposition. The $\text{Cd}_x\text{Zn}_{1-x}\text{S}$ films were obtained on glass substrates at substrate temperatures of 350, 400 and 450 °C. The $\text{Cd}_x\text{Zn}_{1-x}\text{S}$ films were deposited on glass substrates at different bath temperatures such as 70, 75 and 80 °C. Effects of the x composition and substrate temperatures/bath temperatures on structural, electrical, optical and thermoluminescence properties of sprayed cadmium zinc sulfide (CdZnS) films were investigated using X-ray diffraction (XRD), Van der Pauw method, optical transmission, and thermoluminescence dosimetry (TLD). The polycrystalline structure of $\text{Cd}_x\text{Zn}_{1-x}\text{S}$ films is considered to be a mixture of wurtzite ZnS and CdS crystallite grains. For $x = 1.0$, CdS film was observed and also for $x = 0$, ZnS film was observed. CdZnS films are produced by doping ZnS with 'Cd'. The doping causes changes in the structural properties of ZnS films. A separate cadmium sulphide phase was not observed by XRD, since only the peaks related to the hexagonal structure of ZnS are observed in the XRD spectra. For the Cd addition to ZnS films only two main peaks, (002) and (101), are observed simultaneously. From the X-ray diffraction pattern, it is observed that with increasing Cd content, the intensity of (002) peak is decreased, whereas the (101) peak becomes dominant. It was concluded that the crystallinity levels of the ZnS films improved with Cd incorporation, which has a strong effect on the structural properties. From the X-ray diffraction pattern, it is seen that as the x composition increases, the (002) diffraction peaks shift to lower angles and the FWHM reduces which indicates that grain growth has occurred, resulting in the partial relief of lattice strain within the films. From the FWHM and peak position of the (002) peak, the grain size and the lattice strain are calculated. It shows that the grain sizes and the lattice strain are influenced by the x composition. The strain is decreased that indicates a decrease in the concentration of lattice imperfections as the x composition increases. The decrease in strain with an increase in the grain size indicates the formation of good quality films. It was observed that band-gap E_g decreases slightly when substrate temperature/bath temperatures increases with increasing Cd content. This decrease in the band gap of ZnS after Cd addition can be related to the structural modification of ZnS films. This

shift in the band gap with the Cd incorporation resulted from the increase in carrier density or the improvement crystallinity level. It is observed that the decrease in band gap with deposition temperature and Cd content is probably due to the increase in grain size, leading to reduction in density of grain boundary trapping centre and improvement in crystallinity of the film. The observed decrease in E_g and strain with increasing grain size are due to the decrease in resistivity and the increase in carrier concentration and also the increasing in x compositions. The thermoluminescence properties of sprayed $Cd_xZn_{1-x}S$ films are investigated. The influence of concentration ratio of different starting materials used in the spray pyrolysis method was firstly investigated on the shape and intensity of glow curves of $Cd_xZn_{1-x}S$ films and it was observed that they are highly affected by the film production conditions. The intensity of TL signal of produced samples via spray pyrolysis method strongly depends on film production conditions and concentration of starting materials used in the spray pyrolysis method.

It is concluded that the usage different water concentrations influences the $Cd_{0.5}Zn_{0.5}S$ films prepared by the spray pyrolysis method on glass substrates heated the range 300-450 °C. X-ray diffraction studies revealed that all the films were strongly oriented along the (002) orientation that correspond to the hexagonal wurtzite structure. It was found that the structures and properties of the films were greatly affected by the H_2O content. Water in a certain range of concentrations promoted the formation of $Cd_{0.5}Zn_{0.5}S$ film and improved the properties of the films.

Finally in this work, chemical bath deposition method and spray pyrolysis method are found to be very suitable methods for high quality and low cost semiconducting film growth. These methods do not require complex systems and sophisticated equipments.

REFERENCES

- [1] Wilson, J. I. N., Woods, J. (1973). The electrical properties of evaporated film of cadmium sulphide. *J.Phys. Chem. Solids*, **30**, 171-181
- [2] Benramdane, N., Murad, W.A., Misho, R.H., Ziane, M., Kebbab, Z., (1997). A chemical method for the preparation of thin films of CdO and ZnO. *Materials Chemistry and Physics*, **48**, 119-123
- [3] Woggon, U., Hild, K., Gindele, F., Langbein, W., Hetterich, M., Grun, M., Klingshirn, C. (2000). Huge binding energy of localized biexcitons in CdS/ZnS quantum structures. *Phys. Rev. B*, **61**, 12632
- [4] Deulkara, S.H., Bhosalea, C.H., Sharonb, M. (2004). A comparative study of structural, compositional, thermal and optical properties of non stoichiometric (Zn,Fe)S chalcogenide pellets and thin films. *J. Phys. Chem. Solids*, **65**, 1879-1885
- [5] J. Vidal, O. De Melo, O. Vigil, N. Lopez, G. Contreras-Puente, O. Zelaya-Angel, O. (2002). Influence of magnetic field and type of substrate on the growth of ZnS films by chemical bath. *Thin Solid Films*. **419**, 118-123
- [6] Saitoh, T., Yokogawa, T., Narusawa, T. (1991). Single-Crystalline Epitaxial ZnS Waveguides for Phase Matched Second Harmonic Generation Devices. *Jpn. J. Appl. Phys.* **30**, 667-671
- [7] Khan, Z.R., Zulfequar, M., Khan, M.S. (2010). Optical and structural properties of thermally evaporated cadmium sulphide thin films on silicon (1 0 0) wafers. *Material Science And Engineering B*, **174**, 145-149
- [8] Das, N.S., Ghosh, P.K., Mitra, M.K., Chattopadhyay, K.K. (2010). Effect of film thickness on the energy band gap of nanocrystalline CsS thin film analyzed by spectroscopic ellipsometry. *Physica E*, **42**, 2097-2102
- [9] Acharya, K.P., Mahalingam, K., Ullrich, B. (2010). Structural, compositional, and optoelectronic properties of thin-film CdS on p-GaAs prepared by pulsed-laser deposition. *Thin Solids Films*, **518**, 1784-1787
- [10] Taneja, P., Vasa, P., Ayyub, P. (2002). Chemical passivation of sputter-deposited nanocrystalline CdS thin films. *Materials Letters*, **54**, 343-347

- [11] Su, B., Choy, K.L. (2000). Electrostatic assisted aerosol jet deposition of CdS, CdSe and ZnS thin films. *Thin Solids Films*, **361-362**, 102-106
- [12] Tejos. M., G. Rolon, B., Rio, R.D., Cabello, G. (2008). CdS amorphous thin films photochemical synthesis and optical characterization. *Material Science In Semiconductor Processing*, **11**, 94-99
- [13] Morales-Acevedo, A., Vigil-Galan, O., Contreras-Puente, G., Vidal-Larremendi, J., Arriaga-Mejia, G., Chavarria-Castaneda, M., Escamilla-Esquivel, A., Herhandez-Contreras, H., Arias-Carbajal, A., Cruz-Gandarilla, F. (2002). Physical properties of CdS thin films grown by different techniques: a comparative study. *Photovoltaic Specialists Conference, Conference Record of the Twenty-Ninth IEEE*, 624-627
- [14] Albin, D., Rose, D., Dhere, R., Levi, D., Woods, L., Swartzlander, A., Sheldon, P. (1997). Comparasion study of close-spaced sulimated and chemical bath deposited CdS films: Effects on CdTe solar cells. *Photovoltaic Specialists Conference, Conference Record of the Twenty-Sixth IEEE*, 367 – 370
- [15] Oliva, A.I., Castro-Rodriguez, R., Solis-Canto, O., Sosa, V., Quintana, P., Pena, J.L. (2003). Comparison of properties of CdS thin films grown by two technigues. *Applied Surface Science*, **205**, 56-64
- [16] Ravichandran, K., Philominathan, P. (2009). Comparative study on structural and optical properties of CdS films fabricated by three different low-cost techniques. *Applied Surface Science*, **255**, 5736-5741
- [17] Rami, M., Benamar, E., Fahoume, M., Chraibi, F., Ennaoui, A. (1999). Effect of the cadmium ion source on the structural and optical properties of chemical bath deposited CdS thin films. *Solid State Science*, **4**, 179-188
- [18] Khallaf, H., O. Oladeji, I., Chai, G., Chow, L. (2008). Characterization of CdS thin films grown by chemical bath deposition using four different cadmium sources. *Thin Solids Films*, **516**, 7306-7312
- [19] Prabahar, S., Dhanam, M. (2005). CdS thin films from two different chemical baths structural and optical analysis. *Journal of Crystal Growth*, **285**, 41-48
- [20] Liu, F., Lai, Y., Liu, J., Wang, B., Kuang, S., Zhang, Z., Li, J., Liu, Y. (2010). Characterization of chemical bath deposited CdS thin films at different deposition temperature. *Journal of Alloys And Compounds*, **493**, 305-308
- [21] Ikhmayies, J.S., N. Ahmad-Bitar, R. (2010). The influence of the substrate temperature on the photovoltaic properties of spray-deposited CdS:In thin films. *Applied Surface Science*, **256**, 3541-3545

- [22] Ramirez Bon, R., Sandoval-Inda, N.C., Espinoza-Beltran, F.J., Sotelo-Lerma, M., Zelaya-Angel, O., Falcony, C. (1997). Structural transition of chemically deposited CdS films on thermal annealing. *J. Phys. Condens. Matter*, **9**, 10051-10058
- [23] El Maliki, H., Bernede, J.C., Marsilac, S., Pinel, J., Castel, X., Pouzet, J. (2003). Study of the influence of annealing on the properties of CBD-CdS thin films. *Applied Surface Science*, **205**, 65-79
- [24] Chavez, H., Jordan, M., McClure, J.C., Lush, G., Singh, V.P. (1997). Physical and electrical characterization of CdS films deposited by vacuum evaporation, solution growth and spray pyrolysis. *Journal of Material Science*, **8**, 151-154
- [25] Rakhshani, A.E., Al-Azab, A.S. (2000). Characterization of CdS films prepared by chemical-bath deposition. *J. Phys. Condens. Matter*, **12**, 8745-8755
- [26] Roy, P., Srivastava, S.K. (2006). A new approach towards the growth of cadmium sulphide thin film by CBD method and its characterization. *Materials Chemistry And Physics*, **95**, 235-241
- [27] Hiie, J., Dedova, T., Valdna, V., Muska, K. (2006). Comparative study of nano-structured CdS thin films prepared by CBD and spray pyrolysis: Annealing effect. *Thin Solid Films*, **511**, 443-447
- [28] Cha, D., Kim, S., Huang, N.K. (2004). Study on electrical properties of CdS films prepared by chemical pyrolysis deposition. *Materials Science And Engineering B*, **106**, 63-68
- [29] Ramaiah, K.S., Pilkington, R.D., Hill, A.E., Tomlinson, R.D., Bhatnagar, A.K. (2001). Structural and optical investigations on CdS thin films grown by chemical bath technique. *Materials Chemistry And Physics*, **68**, 22-30
- [30] Metin, H., Esen, R. (2003). Annealing studies on CBD grown CdS thin films. *Journal Of Crystal Growth*, **258**, 141-148
- [31] Metin, H., Erat, S., Durmuş, S., Ari, M. (2010). Annealing effect on CdS/SnO₂ films grown by chemical bath deposition. *Applied Surface Science*, **256**, 5076-5081
- [32] Metin, H., Erat, S., Durmuş, S., Ari, M. (2010). Annealing effect on CdS/SnO₂ films grown by chemical bath deposition. *Applied Surface Science*, **256**, 5076-5081
- [33] Ashour, A. (2003). Physical properties of spray pyrolysed CdS thin films. *Turk J. Phys.*, **27**, 551-558

- [34] Raji, P., Sanjeeviraja, C., Ramachandran, K. (2005). Thermal and structural properties of spray pyrolysed CdS thin film. *Bull. Mater. Sci*, **28**, 233-238
- [35] Yadav, A.A., Barote, M.A., Masumdar, E.U. (2010). Studies on nanocrystalline cadmium sulphide (CdS) thin films deposited by spray pyrolysis. *Solid State Science*, **12**, 1173-1177
- [36] Martinez, M.A., Guillen, C., Herrero, J. (1998). Morphological and structural studies of CBD-CdS thin films by microscopy and diffraction techniques. *Applied Surface Science*, **136**, 8-16
- [37] Mazon-Montijo, D.A., Sotelo-Lerma, M., Rodriguez-Fernandez, L., Huerta, L. (2010). Afn, xps and rbs studies of the growth process of CdS thin films on ITO/glass substrates deposited using an ammonia-free chemical process. *Applied Surface Science*, **256**, 4280-4287
- [38] Kim, M., Min, B.K., Kim, C.D., Lee, S., Kim, H.T., Jung, S.K., Sohn, S. (2010). Study of the physical property of the cadmium sulfide thin film depending on the process condition. *Current Applied Physics*, **10**, S455-S458
- [39] Ximello-Quebras, J.N., Contreras-Puente, G., Aguilar-Hernandez, J., Santana-Rodriguez G., Arias-Carbajal Readigos, A. (2004). Physical properties of chemical bath deposited CdS thin films. *Solar Energy Materials & Solar Cells*, **82**, 263-268
- [40] Enriquez, J.P., Mathew, X. (2003). Influence of the thickness on structural, optical and electrical properties of chemical bath deposited CdS thin films. *Solar Energy Materials & Solar Cells*, **76**, 313-322
- [41] Gullien, C., Martinez, M.A., Herrero, J. (1998). Accurate control of thin film CdS growth process by adjusting the chemical bath deposition parameters. *Thin Solid Films*, **335**, 37-42
- [42] Moualkia, H., Hariach, S., Aida, M.S. (2009). Structural and optical properties of CdS thin films grown by chemical bath deposition. *Thin Solid Films*, **518**, 1259-1262
- [43] Khomane, A.S. (2010). Morphological and opto-electronic characterization of chemically deposited cadmium sulphide thin films. *Journal Alloys And Compounds*, **496**, 508-511
- [44] Petre, D., Pintilie, I., Pentia, E., Pintilie, I., Botila, T. (1999). The influence of Cu doping on opto-electronic properties of chemically deposited CdS. *Materials Science And Engineering B*, **58**, 238-243

- [45] Paulraj, M., Ramkumar, S., Varkey, K.P., Vijayakumar, K.P., Sudha Kartha, C., Nair, K.G.M. (2005). Characterizations of undoped and Cu doped CdS thin films using photothermal and other techniques. *Phys. Stat. Sol.*, **202**, 425-434
- [46] Acosta, D.R., Magana, C.R., Matinez, A.I., Maldonado, A. (2004). Structural evolution and optical characterization of indium doped cadmium sulfide thin films obtained by spray pyrolysis for different substrate temperatures. *Solar Energy Materials & Solar Cells*, **82**, 11-20
- [47] Cruz, J.S., Perez, R.C., Delgado, G.T., Angel, O.Z. (2010). CdS thin films doped with metal-organic salts using chemical bath deposition. *Thin Solid Films*, **518**, 1791-1795
- [48] Chandramohan, S., Strache, T., Sarangi, S.N., Sathyamoorthy, R., Som, T. (2010). Influence of implantation induced Ni-doping on structural, optical, and morphological properties of nanocrystalline CdS thin films. *Materials Science An Engineering B*, **171**, 16
- [49] Chun, S., Han, K.S., Lee, J.S., Lim, H.J., Lee, H., Kim, D. (2010). Fabrication CdS thin film and nanostructure grown on transparent ITO electrode for solar cells. *Current Applied Physics*, **10**, 196-200
- [50] Ochoa-Landin, R., Sastre-Hernandez, J., Vigil-Galan, O., Ramirez-Bon, R. (2010). Chemically deposited CdS by an ammonia-free process for solar cells window layers. *Solar Energy*, **84**, 208-214
- [50] Herrero, J., Gutierrez, M.T., Gullien, C., Dona, J.M., Martinez, M.A., Chaparro, A.M., Bayon, R. (2000). Photovoltaic windows by chemical bath deposition. *Thin Solid Films*, **361**, 28-33
- [51] Meth, J.S., Zane, S.G., sharp, K.G., Agrawal, S. (2003). Patterned thin film transistors incorporating chemical bath deposited cadmium sulfide as the active layer. *Thin Solid Films*, **444**, 227-234
- [52] Patil, S.B., Singh, A.K. (2009). Effect of complexing agent on the photoelectrochemical properties of bath deposited CdS thin films. *Applied Surface Science*, **256**, 2884-2889
- [53] Hankare, P.P., Chate, P.A., Sathe, D.J. (2009). CdS thin film: Synthesis and characterization. *Solid State Science*, **11**, 1226-1228
- [54] Khallaf, H., Olajedi, I.O., Chow, L. (2008). Optimization of chemical bath deposited CdS thin films using nitrilotriacetic acid as a complexing agent. *Thin Solid Films*, **516**, 5967-5973

- [55] Roy, P., Srivastava, S.K. (2006). A new approach towards the growth of cadmium sulphide thin film by CBD method and its characterization. *Materials Chemistry And Physics*, **95**, 235-241
- [56] Pike, R.D., Blanton, T.N., Wernberg, A.A. (1193). Preparation of zinc sulfid thin films by ultrasonic spray pyrolysis from bis(diethyldithiocarbamate) zinc (II). *Thin Solid Films*, **224**, 221-226
- [57] Tran, N.H., Lamb, R.N., Mar, G.L. (1999). Single source chemical vapour deposition of zinc sulphide thin films film composition and structure. *Colloids and Surfaces*. **155**, 93-100
- [58] Lee, J., Lee, S., Cho, S., Kim, S., Park, I.Y., Choi, Y.D. (2002). Role of Growth parameters on structural and optical properties of ZnS nanocluster thin films grown by solution growth technique. *Materials Chemistry And Physics*, **77**, 254-260
- [59] Yano, S., Schroeder, R., Ullrich, B., Sakai, H. (2003). Absorption and photocurrent properties of thin ZnS films formed by pulsed-laser deposition on quartz. *Thin Solid Films*, **423**, 273-276
- [60] Gunasekaran, M., Gopalakrishnan, R., Ramasamy, P. (2003). Deposition of thin films by photochemical deposition technique. *Materials Letters*, **58**, 67-70
- [61] Zhang, R., Wang, B., Zhang, H., Wei, L. (2005). The structure and optical properties of the nanocrystalline ZnS films prepared by sulfurizing the as-deposited ZnO films. *Applied Surface Science*, **241**, 435-441
- [62] Subbaiah, Y.P.V., Prathap, P., Reddy, K.T.R. (2006). Structural, electrical and optical properties of ZnS films deposited by close-spaced evaporation. *Applied Surface Science*, **253**, 2409-2415
- [63] Lopez, M.C., Espinos, J.P., Martin, F., Leinen, D., Ramos-Barrado, J.R. (2005). Growth of ZnS thin films obtained by chemical spray pyrolysis: The influence of precursors. *Journal of Crystal Growth*, **285**, 66-75
- [64] Nasrallah, T.B., Amlouk, M., Bernede, J.C., Belgacem, S. (2004). Structure and morphology of sprayed ZnS thin films. *Phys. Stat. Sol*, **201**, 3070-3076
- [65] Elidrissi, B., Addou, M., Regragui, M., Bougrine, A., Kachouane, A., Bernede, J.C. (2001). Structure, composition and optical properties of ZnS thin films prepared by spray pyrolysis. *Materials Chemistry And Physics*, **68**, 175-179
- [66] Öztaş, M., Bedir, M., Ocak, Ş., Yıldırım, R.G. (2006). The role of growth parameters on structural, morphology and optical properties of sprayed ZnS thin films. *Journal of Materials Science: Materials in Electronics*, **18**, 505-512

- [67] Yazıcı, A.N., Öztaş, M. and Bedir M. (2003). Effect of sample producing conditions on the thermoluminescence properties of ZnS thin films developed by spray pyrolysis method. *Journal of Luminescence*, **104**, 115-122
- [68] Roy, P., Ota, J.R., Srivatava, S.K. (2006). Crsytalline ZnS thin films by chemical bath deposition method and its characterization. *Thin Solid Films*, **515**, 1912-1917
- [69] Lee, H.J., Lee, S. (2007). Deposition and optical properties of nanocrystalline ZnS thin films by a chemical method. *Current Applied Physics*, **7**, 193-197
- [70] Ladar, M., Popovici, E., Baldea, I., Grecu, R., Indrea, E. (2007). Studies on chemical bath deposited zinc sulphide thin films with special optical properties. *Journal Alloys And Compounds*, **434**, 697-700
- [71] Nasr, T.B., Kamoun, N., Kanzari, M., Bennaceur, R. (2006). Effect of pH on the properties of ZnS thin films grown by chemical bath deposition. *Thin Solid Films*, **500**, 4-8
- [72] Göde, F., Gümüş, C., Zor, M. (2007). Investigations on the physical properties of the polycrystalline ZnS thin films deposited by the chemical bath deposition method. (2007) *Science Direct Journal of Crystal Growth*, **299**, 136-141
- [73] Liu, Q., Guobing, M., Jianping, A. (2008). Chemical bath-deposited ZnS thin films: Preparation and characterization. *Applied Surface Science*, **254**, 5711-5714
- [74] Johnston, D.A., Carletto, M.H., Reddy, K.T.R., Forbes, I., Miles, R.W. (2002). Chemical bath deposition of zinc sulfide based buffer layers using low toxicity materials. *Thin Solid Films*, **403-404**, 102-106
- [75] Kang, S.R., Shin, S.W., Choi, D.S., Moholkar, A.V., Moon, J., Kim, J.H. (2010). Effect of pH on the characteristics of nanocrystalline ZnS thin films prepared by CBD method in acidic medium. *Current Applied Physics*, **10**, S473-S477
- [76] Antony, A., Murali, K. V., Manoj, R., Jayaraj, M.K. (2005). The effect of the pH value on the growth and properties of chemical-bath-deposited ZnS thin films. *Materials Chemistry And Physics*, **90**, 106-110
- [77] Makhova, L.V., Konovalov, I., Szargan, R., Aschkenov, N. (2005). Composition and properties of ZnS thin films prepared by chemical bath deposition from acidic and basic solutions. *Phys. Stat. Sol*, **2**, 1206-1211
- [78] Dhanam, M., Kavitha, B., (2009). Influence of tea (complexing agent) on the structural properties of CBD ZnS thin films. *Chalcogenide letters*, **6**, 299-307

- [79] Fernandez, A.M., Sebastian, P.J. (1993). Conversion of chemically deposited ZnS films to photoconducting ZnO films. *J. Phys. D: Appl. Phys.* **26**, 2001-2005
- [80] Mu, J., Gu, D., Gu, X. (2005). A new approach to the fabrication of ZnO ultrathin films from annealing ZnS nanoparticulate films. *Materials Science And Engineering C*, **25**, 77-80
- [81] Wang, S., Xia, G., Shao, J., Fan, Z. (2006). Structure and UV emission of nanocrystal ZnO films by thermal oxidation of ZnS films. *Journal of Alloys and Compounds*, **424**, 304-306
- [82] Zhang, X. T., Liu, Y. C., Zhang, L. G., Zhang, J. Y., Lu, Y. M., Shen, D. Z., Xu, W., Zhong, G. Z., Fan, X. W., Kong, X. G. (2002). Structure and optically pumped lasing from nanocrystalline ZnO thin films prepared by thermal oxidation of ZnS thin films. *Journal of Applied Physics*, **92**, 3293-3298
- [83] Zhang, X.T., Liu, Y.C., Zhi, Z.Z., Zhang, J.Y., Lu, Y.M., Xu, W., Shen, D.Z., Zhong, G.Z., Fan, X.W., Kong, X.G. (2002). High intense UV-luminescence of nanocrystalline ZnO thin films prepared by thermal oxidation of ZnS thin films. *Journal of Crystal Growth*, **240**, 463-466
- [84] Zhang, R., Wang, B., Wan, D., Wei, L. (2004). Effects of the sulfidation temperature on the structure, composition and optical properties of ZnS films prepared by sulfurizing ZnO films. *Optical Materials*, **27**, 419-423
- [85] Zhang, R., Wang, B., Zhang, H., Wei, L. (2005). Influence of sulfidation ambience on the properties of nanocrystalline ZnS films prepared by sulfurizing the as-sputtered ZnO films. *Applied Surface Science*, **245**, 340-345
- [86] Yazıcı, N., Öztaş, M., Bedir, M., Kayalı, R. (2002). Determination of the Trapping Parameters of ZnS Thin Films Developed by Chemical Spraying Technique. *Turk J. Phys.*, **26**, 277-282
- [87] Öztaş, M., Yazıcı, A.N., (2004). The effect of pre-irradiation heat treatment on TL glow curves of ZnS thin film deposited by spray pyrolysis method. *Journal of Luminescence*, **110**, 31-37
- [88] Chen, W., Wang, Z., Lin, Z., Lin, L. (1997). Thermoluminescence of ZnS nanoparticles. *Applied Physics Letters*, **70**, 1465
- [89] Neumark, G.F. (1956). Electroluminescence and thermoluminescence of ZnS single crystals. *Physical Review*. **103**, 41-46
- [90] Öztaş, M., Bedir, M., Yazıcı, A.N., Kafadar, E.V., Toktamış, H. (2006). Characterization of copper-doped sprayed ZnS thin films. *Physica B*, **381**, 40-46

- [91] Eleruja, M.A., Adedeji, A.V., Ojo, I.A.O., Djebah, A., Osasona, O., Aladekomo, J.B., Ajayi, E.O.B. (1998). Optical characterization of pyrolytically deposited $Zn_xCd_{1-x}S$ thin film. *Optical materials*, **10**, 257-263
- [92] Valkonen, M.P., Lindross, S., Leskela, M. (1998). $Cd_xZn_{1-x}S$ solid solution thin films and CdS/ZnS multilayer thin films grown by SILAR technique. *Applied Surface Science*, **134**, 283-291
- [93] Sakai, H., Watanabe, M., Takiyama, K., Ullrich, B., (2003). Optical properties of $Zn_xCd_{1-x}S$ mixed crystal thin film produced by PLD. *Proc. of SPIE*, **4830**, 270-273
- [94] Shi, J., Yan, H., Wang, X., Feng, Z., Lei, Z., Li, C. (2008). Composition-dependent optical properties of $Zn_xCd_{1-x}S$ synthesized by precipitable-hydrothermal process. *Solid State Communications*, **146**, 249-252
- [95] Song, L., Zhang, S., Chen, B., Ge, J., Jia, X. (2010). Fabrication of ternary zinc cadmium sulfide photocatalysts with highly visible-light. *Catalysis Communications*, **11**, 387-390
- [96] Özer, T., Köse, S., (2009). Some physical properties of $Cd_{1-x}Sn_xS$ films used as window layer in heterojunction solar cells. *International Journal of Hydrogen Energy*, **34**, 5186-5190
- [97] Jia, G., Wang, N., Gong, L., Fei, X. (2009). Growth characterization of CdZnS thin film prepared by chemical bath deposition. *Chalcogenide Letters*, **6**, 463-467
- [98] Bedir, M., Kayalı, R., Öztaş, M. (2002). Effect of the Zn concentration on the characteristic parameters of $Zn_xCd_{1-x}S$ thin films developed by spraying pyrolysis method under the nitrogen atmosphere. *Turk J. Phys.* **26**, 121-126
- [99] Öztaş, M., Bedir, M. (2001). Some properties of $Zn_xCd_{(1-x)}S$ and $Zn_xCd_{(1-x)}S(In)$ thin films prepared by pyrolytic spray technique. *Pakistan Journal of Applied Sciences*, **4**, 534-537
- [100] Baykul, M.C., Orhan, (2010). Band alignment of $Cd_{(1-x)}Zn_xS$ produced by spray pyrolysis method. *Thin Solid Films*, **518**, 1925-1928
- [101] Raviprakash, Y., Bangera, K.V., Shivakumar, G.K. (2009). Preparation and characterization of $Cd_xZn_{1-x}S$ thin films by spray pyrolysis technique for photovoltaic applications. *Solar Energy*, **83**, 1645-1651
- [102] Raviprakash, Y., Bangera, K.V., Shivakumar, G.K. (2010). Growth, structural and optical properties of $Cd_xZn_{1-x}S$ thin films deposited using spray pyrolysis technique. *Current Applied Physics*, **10**, 193-198

- [103] Li, Sheng. (2006). *Semiconductor Physical Electronics* (2nd ed.). Springer. ISBN: 978-0-387-28893-2.
- [104] Callister, William D., (2007). *Materials science and engineering: An introduction* (7th ed.). John Wiley & Sons, Inc. ISBN-13: 978-0-471-73696-7
- [105] Razeghi, M., (2006). *Fundamentals of solid state engineering* (2nd ed.). Springer. ISBN 13: 978-0-387-28152-0
- [106] Kittel, Ch. (2004). *Introduction to Solid State Physics*. John Wiley and Sons. ISBN 0-471-41526-X.
- [107] Neamen, D.A. (2003). *Semiconductor Physics and Devices*. (3rd ed.). McGraw-Hill ISBN:0-07-232107-5.
- [108] Poole, Charles P., Ovens, Frank J. (2003). *Introduction to Nanotechnology*. John Wiley and Sons. ISBN 0-471-07935-9
- [109] A. A. Balandin and K. L. Wang (2006). *Handbook of Semiconductor Nanostructures and Nanodevices* (5-Volume Set), American Scientific Publishers. ISBN 1-58883-073-X.
- [110] Yu, Peter Y.; Cardona, Manuel (2004). *Fundamentals of Semiconductors: Physics and Materials Properties*. Springer. ISBN 3-540-41323-5.
- [112] Czichos, H., Saito, T., Smith, L. (2006). *Handbook of Materials Measurement Methods*. Springer. ISBN-10: 3-540-20785-6
- [113] Hummel, Rolf E.(2004). *Understand Material Science History, Properties, and Applications*. Springer. ISBN 0-387-20939-5
- [114] McKeevr, S.W.S. (1985). *Thermoluminescence of Solids*. Cambridge University Press. ISBN: 0-521-24520-6.
- [115] Poortmans, J., Arkhipov, V., (2006). *Thin Film Solar Cells Fabrication, Characterization and Applications*. John Wiley & Sons. ISBN-10: 0-470-09126-6
- [116] Bonnet, D. (2004). Proc. of 19th European PV Solar Energy Conf., WIP-Munich and ETA-Florence, **2**, 1657
- [117] Abu-Safe, H.H., Hossain, M., Naseem, H., Brown, W., Al-Dhafiri, A. (2004). Chlorine-doped CdS thin films from CdCl₂-mixed CdS powder. *Journal of Electronic Materials*, **33**, 128

- [118] Gruszecki, T., Holmström, B. (1993). Preparation of thin films of polycrystalline CdSe for solar energy conversion. *Solar Energy Materials and Solar Cells*, **31**, 227-234
- [119] Lel, J.H., Song, W.C., Yoo, S.Y. (2003). Characteristics of the CdZnS thin film doped by thermal diffusion of vacuum evaporated indium films. *Solar Energy Materials and Solar Cells*, **75**, 227-234
- [120] Albasam, A.A. (1999). Photoconductivity and defect levels in $Zn_xCd_{1-x}Se$ with ($x=0.5, 0.55$) crystals. *Solar Energy Materials and Solar Cells*, **57**, 323-329.
- [121] Rajebhosale, M.R., Pawar, S.H. (1982). Growth and Structural Properties of Cd-Zn S Films formed by Chemical Bath Deposition Technique. *Indian J. Pure Appl. Phys.*, **20**, 652
- [122] Deshmukh, L.P., Holikatti, S.G., More, B.M. (1995). Optical and structural properties of antimony-doped CdS thin films. *Materials Chemistry and Physics*, **39**, 278-283
- [123] Borse, S.V., Chavhan, S.D., Sharma, R. (2007). Growth, structural and optical properties of $Cd_{1-x}Zn_xS$ alloy thin films grown by solution growth technique (SGT). *Journal of Alloys and Compounds*, **436**, 407-414
- [124] Krunks, M., Madarasz, J., Leskela, T., Mere, A., Niinistö, L., Pokol, G. (2003). Thermoanalytical study of zinc thiocarbamide chloride, a single-source precursor for zinc sulfide thin films by spray pyrolysis. *J. Therm. Anal. Calorim.*, **72**, 497-506
- [125] Girtan M., Folcher G. (2003). Structural and optical properties of indium oxide thin films prepared by an ultrasonic spray CVD process. *Surf. Coat. Technol.* **172**, 242-250
- [126] EngineerDir. (2011). *Scientists have Shown that a Chunk of Hematite Can Conduct Electrons Under Certain Chemical Conditions*. United States: Kevin Rosso.
- [127] Xu, M., Chai, C., Luo, G., Yang, T., Mai, Z., Lai, W. (2000). Structural study of $Ni_{80}Fe_{20}/Cu$ multilayers by X-ray diffraction. *Thin Solid Films*. **375**. 205-209
- [128] Chaure, N.B., Bordas, S., Samantilleke, A.P., Chaure, S.N., Haigh, J., Dharmadasa, I.M. (2003). Investigation of electronic quality of chemical bath deposited cadmium sulphide layers used in thin film photovoltaic solar cells. *Thin Solid Films*, **437**, 10-17
- [129] Toyama, T., Oda, H., Nakamura, K., Fujihara, T., Shimizu, K., Okamoto, H. (2003). Improvement of CdS Window Layer for Large Open Circuit Voltages of

Low Environmental-Load CdS/CdTe Solar Cells *Mater. Res. Soc. Symp. Proc.*, **763**, 155–160

[130] Valdna, V. (1999). P-type doped CdTe. *Solid State Phenomena*, **67–68**, 309-314

[131] N. Romeo, N., Bosio, A., Canevari, V., Podestà, A., Mazzamuto, S., Guadalupi, G.M. (2004). High efficiency CdTe/CdS thin film solar cells with Sb₂Te₃ back contact by a thoroughly dry process. *19th European Photovoltaic Solar Energy Conf., Proceedings of the International Conf.*, 1718-1720

[132] Krunk, M., Madarasz, J., Hiltunen, L., Mannonen, R., Mellikov, E., Niinisto, L. (1997). Structure and thermal behaviour of dichlorobis(thiourea)cadmium(II), a single-source precursor for cds thin films. *Acta Chemica Scandinavica*, **51**, 294 – 301

[133] Oliva, A.I., Solis-Canto, O., Castro-Rodriguez, R., Quintana, P. (2001). Formation of the band gap energy on CdS thin films growth by two different techniques. *Thin Solid Films*, **391**, 28-35

[134] Laukaitis, G., Lindroos, S., Tamulevicius, S., Leskel, M. (2001). Stress and morphological development of CdS and ZnS thin films during SILAR on (100)GaAs. *Applied Surface Sciences*, **185**, 134-139

[135] S. Mathew, S., Mukerjee, P.S., Vijayakumar, K.P. (1995). Optical and surface properties of spray-pyrolysed CdS thin films. *Thin Solid Films*, **254**, 278-284

[136] Yazici, A. N., Oztas, M., Bedir, M. (2007). The thermoluminescence properties of copper doped ZnS nanophosphor. *Optical Materials*, **29**, 1091-1096

[137] Ajayi, O.B., Osuntola, O.K., Ojo I.A., Jeynes, C. (1994). Preparation and characterization of MOCVD thin films of cadmium sulphide. *Thin Solid Films*. **248**, 57-62.

[138] Rozati, S.M. (2006). The effect of substrate temperature on the structure of tin oxide thin films obtained by spray pyrolysis method. *Materials Characterization*, **57**, 150-153

[139] Berkat, L., Cattin, L., Reguig, A., Regragui, M., Bernede, J.C. (2005). Comparison of the physico-chemical properties of NiO thin films deposited by chemical bath deposition and by spray pyrolysis. *Materials Chemistry and Physics*, **89**, 11-20

- [140] Öztaş, M., Bedir, M., Öztürk, Z., Korkmaz, D., Sur, S. (2006). Structural and Optical Properties of Nanocrystal In_2O_3 Films by Thermal Oxidation of In_2S_3 Films. *Chinese Physics Letters*, **23** (6) 1610-1612
- [141] K.Y. Choi, K.Y., Kim, K.D., Yang, J.W., (2006). Optimization of the synthesis conditions of LiCoO_2 for lithium secondary battery by ultrasonic spray pyrolysis process. *J. Mater. Process. Technol.*, **171**, 118–124
- [142] Afify, H.H., El Zawawi, I.K., Battisha, I.K. (1999). Photoelectronic properties of (Cu, Fe, Al) incorporated CdS thin films. *J. Mater. Sci., Mater. Electron*, **10**, 497-502
- [143] Akyuz, I., Kose, S., Atay, F., Bilgin, V., (2007). Some physical properties of chemically sprayed $\text{Zn}_{1-x}\text{Cd}_x\text{S}$ semiconductor films. *Materials Science in Semiconductor Processing*, **10**, 103-111.
- [144] Sartale, S.D., Sankapal, B.R., Lux-Steiner, M.C., Ennaoui, A. (2005). Preparation of nanocrystalline ZnS by a new chemical bath deposition route. *Thin Solid Films*. **480-481**, 168-172
- [145] Bedir, M., Öztas, M., Yazici, A.N. (2001). Kimyasal Yöntemler Kullanılarak Elde Edilen ZnS ve CdS Ince Filimlerin Elektriksel ve Optiksel Özelliklerinin İncelenmesi. *Firat Üniversitesi Fen ve Mühendislik Bilimleri Dergisi*, **13**, 21-26
- [146] Lee, J.H., Park, B.O. (2004). Transparent conducting In_2O_3 thin films prepared by ultrasonic spray pyrolysis. *Surface and Coatings Technology*, **184**, 102-107
- [147] Öztaş, M., Bedir, M., Kayalı, R., Aksoy, F. (2006). Effect of the annealing conditions on the properties of InP thin films. *Materials Science and Engineering B*, **131**, 94-99
- [148] Öztaş, M. (2006). Characteristics of annealed ZnO:Cu nanoparticles prepared by spray pyrolysis. *Journal of Materials Science: Materials in Electronics*, **17**, 937-941
- [149] Yamaga, S., Yoshokawa, A., Kasain, H. (1990). Electrical and optical properties of donor doped ZnS films grown by low-pressure MOCVD. *Journal of Crystal Growth*, **86**, 252-256
- [150] Ruffner, J.A. Hilmel, M.D., Mizrahi, V. Stegeman, G.I., Gibson, U. (1989). Effects of low substrate temperature and ion assisted deposition on composition, optical properties, and stress of ZnS thin films. *Journal of Applied Optics*, **28**, 5209-5214

- [151] Ledger, A.M. (1979). Inhomogeneous interface laser mirror coatings. *Applied Optics*, **18**, 2979-2989
- [152] Brien, P.O., McAleese, J., (1998). Developing an understanding of the processes controlling the chemical bath deposition of ZnS and CdS. *Journal of Materials Chemistry*, **8**, 2309-2314
- [153] Cheng, J., Fan, D.B., Wang, H., Liu, B.W., Zhang, Y.C., Yan, H. (2003). Chemical bath deposition of crystalline ZnS thin films. *Semicond. Sci. Technol.* **18**, 676-679
- [154] A.El. Hichou, M. Addou, J.L. Bubendorff, J. Ebothe, B.El. Idrissi, M.Troyon, M. (2004). Microstructure and cathodoluminescence study of sprayed Al and Sn doped ZnS thin films. *Semiconduct. Sci. Technol.* **19**, 230-235
- [155] Lee, E.Y.M., Tran, N.H., Lamb, R.N. (2005). Growth of ZnS films by chemical vapor deposition of Zn[S₂CN(CH₃)₂]₂ precursor. *Applied Surface Science.* **241**, 493-496
- [156] Powder Diffraction File, (2000). *Joint Committee on Powder Diffraction Standards, ASTM*, Philadelphia, PA, Card 29-628.
- [157] Baykul, M.C., Balcioglu, A. (2000). AFM and SEM studies of CdS thin films produced by an ultrasonic spray pyrolysis method. *Microelectronic Engineering*, **51-52**, 703-713
- [158] Ohyama, M., Fujita, Y. (2003). Electrical and optical properties in sputtered GaSe thin films. *Surf. Coat. Technol.* **169-170**, 620-623
- [159] Thomas, M.B., (1971). Structural properties of vacuum deposited GaSe thin films. *Thin Solid Films*, **8**, 273-280
- [160] M. Benramdane, M., Guesdon, J.P., Julien, C. (1994). Growth and characterizations of Cd-doped InSe films. *Phys. Status Solidi, A Appl.Res.*, **146**, 675-683
- [161] Hankare, P.P., Yadhav, A.D., Bhuse, V.M., Khomane, A.S., Garadhar, K.M. (2003). Chemical deposition of thallium doped cadmium selenide thin films and their characterization. *Materials Chemistry and Physics*, **80**, 102-107
- [162] Wang, X.B., Li, D.M., Zeng, F., Pan, F. (2005). Microstructure and properties of Cu-doped ZnO films prepared by dc reactive magnetron sputtering. *J. Phys. D: Appl. Phys.*, **38**, 4104-4108

- [163] Jager, S., Szyszka, B., Szczyrbowski, J., Brauer, G. (1998). Comparison of transparent conductive oxide thin films prepared by a.c. and d.c. reactive magnetron sputtering. *Surf. Coat. Technol.*, **98**, 1304-1314
- [164] Demiryont, H., Nietering, K.E. (1989). Structure and optical properties of tin oxide films. *Sol. Energy Mater.*, **9**, 79-94
- [165] Zernani, H., Demiryont, H., Collins, G.J. (1986). Optical properties of UV laser photolytic deposition of hydrogenated amorphous silicon (a-Si:H). *Journal Applied Physics*, **60**, 2523-2529
- [166] Ghosh, T., Bandopadhyay, S., Roy, K.K., Maiti, A.K., Goswami, K. (2009). Optical studies on ZnO films prepared by sol-gel method. *Crystal Research and Technology*, **44**, 879-882
- [167] Lahtien, J.L., Lu, A., Tuomi, T. (1985). Effect of growth temperature on the electronic energy band and crystal structure of ZnS thin films grown using atomic layer epitaxy. *Journal Applied Physics*, **58**, 1851-1853
- [168] Tonouchi, M., Yong, S., Tarsuro, M., Hirosh, S., Masaki, O. (1990). Room-Temperature Synthesis of ZnS:Mn Films by H₂ Plasma Chemical Sputtering. *Journal Applied Physics*, **2**, L2453-L2456
- [169] Ashour, A., Afif, H., Mahmoud, S.A. (1994). Effect of some spray pyrolysis parameters on electrical and optical properties of ZnS films. *Thin Solid Films*, **248**, 253-256
- [170] Chavhan, S., Sharma, R.P. (2005). Growth, structural and optical transport properties of nanocrystal Zn_{1-x}CdS thin films deposited by solution growth technique (SGT) for photosensor applications. *Journal of Physics and Chemistry of Solids*, **66**, 1721-1726
- [171] Atay, F., Bilgin, V., Akyuz, I., Kose, S. (2003). The effect of In doping on some physical properties of CdS films. *Mater. Sci. Semicond. Proc.*, **6**, 197-203
- [172] Ma, Y.Y., Bube, R.H. (1977). Properties of CdS Films Prepared by Spray Pyrolysis. *Journal Electrochem. Sci.* **124**, 1430-1435
- [173] Puchert, M.K., Timbrell, P.Y., Lamb, R.N. (1996). Postdeposition annealing of radio frequency magnetron sputtered ZnO films. *J. Vac. Sci. Technol.* **A14**, 2220-2231
- [174] Zelaya-Angel, O., Alvarado-Gil, J.J., Lozada-Morales, R., Vargas, H., Ferreira da Silva, A. (1994). Band-gap shift in CdS semiconductor by photoacoustic

spectroscopy: evidence of a cubic to hexagonal lattice transition. *Appl. Phys.Lett.* **64**, 291-293

[175] Chopra, K.L. (1969). *Thin Film Phenomena*, McGraw-Hill, New York, p. 266

[176] Pattabi, M., Uchil, J. (2000). Synthesis of cadmium sulphide nanoparticles. *Solar Energy Mater. Solar Cells*, **63**, 309-314

[177] Pankove, J.I. (1971). *Optical Processes in Semi.*, Dover Publi., New York, p.22 (Chapter 2)

[178] Ghosh, R., Basak, D., Fujihara, S. (2004). Effect of substrate-induced strain on the structural, electrical, and optical properties of polycrystalline ZnO thin films. *Journal Applied Physics*, **96**, 2689-2693

[179] Srikant, V., Clarke, D.R. (1997). Optical absorption edge of ZnO thin films: The effect of substrate. *Journal Applied Physics*, **81**, 6357-6365

[180] Mathieu, H., Richard, T., Allegre, J., Lefebvre, P., and Arnaud. (1995). Quantum confinement effects of CdS nanocrystals in a sodium borosilicate glass prepared by the sol-gel process. *Journal Applied Physics*, **77**, 287-293

[181] Kale, S.S., Jadhav, U.S. and Lokhande, C.D. (1996). Preparation and characterization of chemically deposited CdS films. *Indian Journal of Pure Applied Physics*, **34**, 324-327

[182] Öztas, M. (2008). Influence of Grain Size on Electrical and Optical Properties of InP Films. *Chinese Physics Letters*, **25**, 4090

[183] Chopra, K.L., Mayer, S. Pandya, D.K. (1983). Transparent conductors-A status review. *Thin Solid Films*, **102**, 1-46

[184] Van Heerden, J.L. and Swanepoe, L.R. (1997). XRD analysis of ZnO thin films prepared by spray pyrolysis. *Thin Solid Films*, **299**, 72-77

[185] Tiburcio-Silver, A., Joubert, J. C., and Labeau, M. (1991). *Thin Solid Films*, **197**, 195-214

[186] Shigesato, Y., Takaki, S., Haranoh, T. (1991). Crystallinity and electrical properties of tin-doped indium oxide films deposited by DC magnetron sputtering. *Appl. Surf. Sci.*, **48-49**, 269-275

- [187] Xing, G.Z., Yao, B., Cong, C. X., Yang, T., Xie, Y.P., Li, B.H. and Shen, D.Z. (2008). Effect of annealing on conductivity behavior of undoped zinc oxide prepared by rf magnetron sputtering. *J. Alloys Compd.*, **457**, 36-41
- [188] Mahmoud, S.A., Akl, A.A., Kamal, H. and Abdel-Hady, K. (2002). Opto-structural, electrical and electrochromic properties of crystalline nickel oxide thin films prepared by spray pyrolysis. *Physica B*, **311**, 366-375
- [189] Hong, R., Hung, J., He, H., Fang, Z. and Shao, J. (2005). - Influence of oxygen partial pressure on the structure and photoluminescence of direct current reactive magnetron sputtering ZnO thin films. *Thin Solid Films*, **473**, 58-62

CURRICULUM VITAE

PERSONAL INFORMATION

Surname, Name: SÜR ÇELİK, SERAP

Nationality: Turkish (TC)

Date and Place of Birth: 30 November 1977, Gaziantep

Marital Status: Married

Phone: +90 555 488 38 98

Fax: +90 342 3601106

e-mail: ssur@gantep.edu.tr

EDUCATION

Degree	Institution	Year of Graduation
MS	University of Gaziantep Engineering of Physics Department	2005
BS	University of Gaziantep Engineering of Physics Department	2002
High School	Tekerekoğlu Anatolian High School	1996

WORK EXPERIENCE

Year	Place	Enrollment
2002- Present	University of Gaziantep Engineering of Physics Department	Research Asistant
2002-2002	M.E.B	English Teacher

FOREIGN LANGUAGES

English

PUBLICATIONS

1. Sur, S., Öztürk, Z., Öztaş M., Bedir, M., Özdemir Y. (2011). Effect of Water Concentration on the Characterization of Sprayed $Cd_{0.5}Zn_{0.5}S$ Films. *Chinese Physics Letters*, **28**, 067103
2. Öztaş, M., Öztürk, Z., Bedir, M. and Sür, S. (2010). Effect of the Grain Size on the Structural and Optical Properties of the Sprayed $Cd_xZn_{1-x}S$ Films. *Proc. 27th International Conference On Microelectronics (MIEL 2010)*, NIS, Serbia, 185-187
3. Sur, S., Öztürk, Z., Öztaş M., Bedir, M., Özdemir Y. (2011). Studies on structural and electrical properties of MnO films prepared by the spray pyrolysis method. *Physica Scripta*, **84**, 015701
4. Öztürk, Z., Sür, S. (2004). A simple model for the tunneling probability for the alpha half-lives. *Türk Fizik Derneği 22. Fizik Kongresi. Bodrum*

5. Korkmaz, D., Bedir, M., Öztaş, M., Öztürk, Z., Sür, S. (2008). Structural and optical properties of In_2O_3 films prepared by spray pyrolysis method at different substrate temperatures. *6. International Student Conference of the Balkan Physical Union. ISCBPU-6. Bodrum*
6. Öztaş, M., Bedir, M., Öztürk, Z., Korkmaz, D., and Sür, S. (2006). Structural and Optical Properties of Nanocrystal In_2O_3 Films by Thermal Oxidation of In_2S_3 Films. *Chinese Physics Letters*, **23**, 6

HOBBIES

Reading, cooking